FINAL REPORT

Laboratory Experimentation In Wood Frame Wall Drying With Comparisons To WALLDRY (Modified 1986 Version)

Presented to:

Tom Hamlin

Research Division

Canada Mortgage and Housing Corp.

685 Montreal Road
Ottawa, Ontario
K1A 0P7

Report No. 39165.OR/4   September 25, 1991

EXECUTIVE SUMMARY

Morrison Hershfield Limited (MHL), has undertaken a project for Canada Mortgage and Housing Corporation (CMHC) to further develop the WALLDRY computer program, a program which simulates moisture performance within residential wood frame walls. The purpose of this project was two fold: first, to conduct a laboratory experiment on selected types of residential wood frame walls to monitor moisture performance under known environmental conditions. Secondly, to modify WALLDRY to incorporate a mass air flow mechanism into the program's algorithms, and to allow the input of indoor and outdoor driving forces, as well as initial stud moisture contents into the model. This would allow a direct comparison of measured laboratory data with WALLDRY predictions.

The laboratory phase of the project incorporated the simulation of both winter and summer conditions on three pairs of test panels. Temperatures, humidities, and pressure differentials across the wall were set during testing for both conditions. While an attempt was made to maintain a steady environmental regime for the sequence of tests; temperatures, humidities and pressures varied due to mechanical systems effects, yielding some dynamical fluctuation in the environment during the experiment.

The result of the dynamic nature of the driving conditions has complicated the analysis of the data, but has resulted in some useful and interesting observations. Measured moisture content of the test studs reacted quickly and noticeably with indoor and outdoor temperature excursions. (It has not been determined if this is fully "real" phenomenon or perhaps a result of inaccurate temperature correction formula). Some differences between sealed and vented versions of each pair of panels are observed despite the small differences in the calculated air flow rates of the panels, (0.003 l/s/m^2 for the sealed versions, 0.012 l/s/m^2 for the vented at 10 Pa). Stud moisture drying rates do exhibit changes dependant on the air flow direction and magnitude.

The experimental data was input into the modified WALLDRY model and comparisons have been made of measured data and simulation results. While there is a general similarity in drying rates produced by the model and the experiment, there are a number of areas where differences occur, requiring further development.

The model lacks a mechanism to simulate the behavior of free or capillary water within the wood, which affects drying rates at moisture contents at or near fibre saturation. The model also deviates from the measured laboratory data during some simulations modes, such as infiltration in the vented panels. Further comparisons with other field monitored data is warranted before judgements can be made regarding the accuracy of the model.

The result of our modifications is a more "research oriented" version of WALLDRY. User input conditions include external and internal temperature and humidity, differential pressure across the wall, initial wood stud moisture content at nine nodes along the stud, and the position and relative magnitude of air leakage sites on either side of the stud space. This version of WALLDRY has the inputs of outdoor stimuli such as solar pumping, night sky radiation and wind temporarily disabled. This allows the researcher to concentrate on the internal mechanisms of moisture transportation without the complications inherent from the interaction of local and indeterminate outdoor weather phenomenon with the movement of energy and moisture in the wall system.

In this report we describe the laboratory experiment with a graphical synopsis of the experimental results. We also describe the modifications made to this version of the WALLDRY program, and then present comments on a comparison of the experimental results with the computer simulations.

RÉSUMÉ

Morrison Hershfield Limited (MHL) a entrepris une étude commandée par la Société canadienne d'hypothèques et de logement (SCHL) dans le but d'améliorer le logiciel WALLDRY, lequel simule les effets de l'humidité dans les murs à ossature de bois des habitations. Cette étude a pour objectif, d'une part, de mener un essai en laboratoire visant à contrôler les effets de l'humidité dans des conditions connues et, d'autre part, de modifier le logiciel WALLDRY pour ajouter à ses algorithmes un mécanisme de débit massique de l'air et permettre d'introduire, dans le modèle, des données relatives aux forces motrices de l'intérieur et de l'extérieur de même que la teneur en humidité initiale des poteaux. Ces améliorations permettraient de comparer directement les données obtenues en laboratoire avec les prédictions du programme WALLDRY.

Les essais en laboratoire ont simulé des conditions hivernales et estivales sur trois paires de panneaux témoins. La température, l'humidité et la différence de pression à l'intérieur des murs ont été établies durant les essais dans les deux types de conditions climatiques. Bien que les responsables des essais aient tenté de maintenir un milieu stable au cours des différents essais, la température, l'humidité et la pression ont varié à cause des installations mécaniques, occasionnant quelques fluctuations dynamiques du milieu.

L'analyse des données a donc été compliquée par ces écarts, mais a quand même permis de réaliser d'utiles et d'intéressantes observations. La teneur en humidité des poteaux à l'essai a réagi rapidement et de façon notable aux variations de la température extérieure et intérieure. (Nous n'avons pu déterminer s'il s'agissait d'un phénomène tout à fait «réel» ou plutôt le résultat d'une erreur dans la formule de correction de la température.) Quelques différences entre les versions étanches et ventilées de chaque paire de panneaux ont été relevées en dépit des faibles différences entre les débits d'air calculés des panneaux (0,003 L/s/m² pour les panneaux étanches, 0,012 L/s/m² pour les panneaux ventilés à 10 Pa). Les taux d'assèchement des poteaux ont varié selon la direction et l'ampleur du mouvement de l'air.

Les données des essais ont été introduites dans le modèle WALLDRY modifié et des comparaisons ont été faites entre les données enregistrées et les résultats des simulations. Il existe bien une similitude générale entre les taux d'assèchement produits par le modèle et ceux obtenus à l'essai, mais un certain nombre d'aspects comportent des différences, et des perfectionnements supplémentaires seront nécessaires.

Le modèle aurait besoin d'un mécanisme lui permettant de simuler le comportement de l'eau libre ou capillaire à l'intérieur du bois, car ces facteurs influent sur les taux d'assèchement lorsque la teneur en humidité atteint le point de saturation des fibres ou s'en approche. Les résultats obtenus avec le modèle diffèrent également des données de laboratoire enregistrées au cours de certains modes de simulation comme l'infiltration dans les panneaux ventilés. De plus amples comparaisons avec d'autres données obtenues sur le terrain sont requises avant de pouvoir porter des jugements sur la précision du modèle.

Les modifications que nous avons apportées à WALLDRY ont abouti à une version de ce logiciel plus axée sur la recherche. Les paramètres à introduire par l'utilisateur sont la température et l'humidité extérieures et intérieures, la différence de pression de part et d'autre du mur, la teneur en humidité initiale des poteaux de bois à la hauteur de neuf noeuds le long du poteau ainsi que la position et l'importance relative des zones d'infiltration d'air de chaque côté de la cavité formée par les poteaux. Cette version de WALLDRY neutralise temporairement les effets du vent, du pompage solaire et du rayonnement diffus nocturne. Les chercheurs peuvent ainsi mettre l'accent sur les mécanismes internes du transport de l'humidité sans avoir à se soucier des complications inhérentes à l'interaction entre les phénomènes climatiques locaux et indéterminés et le mouvement de l'énergie et de l'humidité dans l'ossature murale.

Ce rapport décrit les essais en laboratoire et présente un résumé graphique des résultats. Il explique en outre les modifications qui ont été apportées à l'actuelle version du logiciel WALLDRY et commente la comparaison des résultats expérimentaux avec ceux des simulations informatiques.

CMHC ✶ SCHL

Helping to house Canadians

National Office

700 Montreal Road
Ottawa, Ontario
K1A 0P7

Question habitation, comptez sur nous

Bureau National

700 chemin Montréal
Ottawa (Ontario)
K1A 0P7

Puisqu'on prévoit une demande restreinte pour ce document de recherche, seul le sommaire a été traduit.

La SCHL fera traduire le document si la demande le justifie.

Pour nous aider à déterminer si la demande justifie que ce rapport soit traduit en français, veuillez remplir la partie ci-dessous et la retourner à l'adresse suivante :

Le Centre canadien de documentation sur l'habitation
La Société canadienne d'hypothèques et de logement
700, chemin de Montréal, bureau C1-200
Ottawa (Ontario)
K1A 0P7

TITRE DU RAPPORT : _____

_____

Je préférerais que ce rapport soit disponible en français.

NOM _____

ADRESSE _____
    rue   app.

_____
    ville   province   code postal

No de téléphone   (   ) _____

TABLE OF CONTENTS

TABLE OF CONTENTS (CONTD.)

1. INTRODUCTION

The action of moisture, in the form of water vapour, liquid water or ice, has long been recognized as the leading cause of durability and performance degradation of building systems and components. The presence of moisture within residential wood frame walls is the leading cause of many problems, such as damage to finishes, wood rot, fungal growth and mold, (leading to possible health problems), thermal performance degradation, increased air leakage due to material degradation or component loosening, and eventual destruction of the wall system.

The mechanisms for moisture movement in wood frame wall systems are numerous and complex. Water vapour diffusion through materials, conduction by capillary action and/or surface films are just some of the mechanisms that can come into play. However, one of the most important mechanisms is the convection of air that carries moisture into or out of the wall system. Driving forces due to mechanical systems, solar pumping, and/or wind pressures and suctions all contribute to a highly complex interaction of moisture movement with air flow.

Canada Mortgage and Housing Corporation (CMHC) is developing a computer simulation program called WALLDRY as a tool to allow wall designers and researchers to predict the moisture performance of wood frame walls under selective climatic conditions.

In this study, Morrison Hershfield Ltd. has incorporated an air flow mechanism in the model, and performed a laboratory experiment to provide data for validation of the modified program. In the test program, six test walls, (vented and sealed pairs), were monitored while under going simulated winter and summer conditions. The results of the experiment were compared with predictions from the modified WALLDRY program. This report outlines the experimental procedure conducted, along with comparisons of the simulation predictions.

The modified WALLDRY program provides researchers with an important tool for investigating the behavior of moisture in wood frame wall systems, without the complications of micro-climatic influences. Wind effects, solar gains and night sky radiation have been temporarily removed in order to compare with monitored laboratory conditions. This has reduced the number of variables acting on the wall, providing a clearer look into internal mechanisms and effects. As an additional benefit, data can be imported from a common Lotus-type spreadsheet rather than the complex binary weather file as in the previous procedure.

2. PHASE 1: LABORATORY EXPERIMENT

2.1 Overview

In order to provide validation data for the WALLDRY model, a laboratory experiment was initiated to simulate winter and summer seasonal conditions on selected residential wood frame wall systems. Six 1.2m by 2.4m (4 ft x 8 ft) test panels, (three pairs), were tested in an environmental test chamber. One of each pair was sealed to limit air flow through the stud cavity, while the other had holes drilled in the sheathing and drywall to allow air flow into and through the wall.

The test panels were mounted in an environmental test chamber in which exterior and interior temperatures and humidity conditions could be simulated and recorded. Differential pressures, applied by a mechanical fan system, were measured across the wall panels as well as exterior sheathing. In each panel, stud moisture content, sheathing moisture content, stud cavity temperatures and humidity were recorded. In an effort to determine the relative gravimetric moisture loss or gain of each wall system, a periodic weighing of the test panels was performed by inserting a weigh scale cart under each panel. Initial and final weights of individual components of the panels were measured, along with the moisture content of the wood stud members. Finally, samples of the test studs were taken to Forintek Canada (Ottawa, Ontario), for species identification and oven drying calibration tests.

2.2 Description of Test Facility

The Morrison Hershfield Environmental Simulation Chamber consists of two parts, an inner "Chamber" for *outdoor* weather simulation, and an outer "Tent" area for simulating *indoor* conditions. (See Figures 1 and 2, Photos 1 and 2.) The chamber, 2.4m by 4.8m by 3.1m (8 ft x 14 ft x 10 ft) is constructed of 38mm by 89mm (2 in. x 4 in.) insulated wood stud walls, with 38mm by 300mm (2 in. x 8 in.) wood joist insulated floor and ceiling. Six openings, nominally 1.2m by 2.4m (4 ft x 8 ft), were made in the chamber wall for the insertion of the test panels. Cut outs in the floor below the test panel openings were made to accommodate the weigh scale cart. These were filled with Styrofoam inserts between weigh-ins.

Refrigeration in the chamber was provided by a 5 HP Tecumseh compressor combined with a 12000 BTU Blanchard condenser. Temperatures were set with a manual thermostat. Baffles were added in the ceiling of the chamber to prevent coil fan air flow from directly impinging on the test panels. (See Photo 3.) Heat was provided by two commercial fan heaters. Air flow for the differential pressure tests was supplied by a roof mounted squirrel cage fan, which was switched from infiltration (blowing into the chamber and through the exterior side of the test panels) to exfiltration (blowing out of the chamber, from the interior side of the panels). With this equipment, temperatures of -30°C to +50°C and pressures of +/-75 Pa could be generated.

The "tent" surrounding the chamber had dimensions of 6.1m by 7.9m (20 ft x 26 ft) and was composed of 38mm by 89mm (2 in. x 4 in.) wood frame covered with a polyethylene membrane. Air conditioning in the tent was supplied by a commercial unit. Humidity was set by an atomizer humidifier and a commercial dehumidifier. Air was circulated throughout the tent area by fans and the air conditioning unit.

2.3   Description of Instrumentation

The data acquisition, signal conditioning and A/D conversions were handled by a Sciemetrics (Nepean, Ont.) 8082A Data Acquisition System, (DAS). (See Photo 7, and Figures 3A and 3B). Data logging and scanning control was provided by an AT & T 6300 computer. Data acquisition and control software was custom written. The following is a list of the instrumentation employed: (See Photo 6 for illustration of instrumentation on test stud, and Figures 3A and 3B for schematics of the instrumentation layout).

1)	**Temperature:**	K type thermocouples
2)	**Diff. Pressure:**	Air Ltd. Model MP6KD Micromanometer
3)	**Pressure Scanning:**	24 channel Scanivalve
4)	**Moisture Content:**	Delmhorst Model RC2M Moisture Meter
5)	**Moisture Pins:**	Coe Engineering, green coat insulated
6)	**Cavity Humidity:**	Panametrics MiniCap 2 capacitive sensor
7)	**Humidity:**	ACR XT-102 Stickon Data Loggers
8)	**Weight:**	A&D Model FV150KA1 300lb cap. platform scale

The ACR XT-102 Stickon Data Loggers (Young Environmental Services, Vancouver B.C.) independently measured chamber and tent humidity in half hour increments. Periodically, temperature and humidity readings were also obtained with a Solomat MPM 2000 Thermo-hygrometer. All humidity measuring devices were calibrated in a range of salt solution jars prior to testing. Calibration results are given in Appendix L (RH Sensor Calibrations).

Data was collected in half hour increments with the Siemetric DAS. Data from both the Sciemetric DAS and ACR units were periodically downloaded on to floppy diskette, to be archived and analyzed on other computers. Data was subsequently split into files for the individual test panels, and averaged into hourly readings. The data was then imported into spreadsheets for analysis.

2.4   Description of Test Panels

Each test panel was constructed in accordance with standard residential construction practises. (See Figures 5 to 7, Photo 4.) There were three pairs of panels tested: a sealed and a vented version of each pair. All test panels were constructed in a similar way except for the external cladding system. The panels are identified as:

1)   **Panel A:** Wood (cedar) siding, no furring, Sealed

2)   **Panel B:** Wood (cedar) siding, no furring, Vented

3)   **Panel C:** Vinyl Siding, no furring, Sealed

4)   **Panel D:** Vinyl Siding, no furring, Vented

5)   **Panel E:** Vinyl Siding, with furring, Sealed

6)   **Panel F:** Vinyl Siding, with furring, Vented

The balance of the construction was (from interior):

1)   1/2" (12.7mm) drywall (unpainted)

2)   6mil polyethylene vapour barrier membrane

3)   38mm by 89mm (2"x4") studs (400mm o/c)

4)   38mm by 89mm bottom and two top wall plates

5)   RSI 2.1 fiberglass batt insulation

6)   11mm waferboard sheathing

7)   perforated asphalt impregnated building paper

Each panel had a 22 gauge galvanized steel sheet mounted on the panel side, top and bottom edges to prevent moisture transfer through the sides. The sheet steel was caulked at both faces of the panel to limit air leakage at the panel edge.

The vented panels were perforated by drilling both the sheathing and drywall. The waferboard sheathing was drilled with 21 3mm (1/8 in.) holes. These holes were arranged in three columns (7 holes per stud cavity), spaced 300mm (12 in.) vertically. This gave a total hole area of approximately $1.7cm^2$ (0.26 in^2) in the exterior sheathing. The vented area was based on Forintek studies on the leakage area of joints in exterior sheathing.

For the interior side of the vented panels, cutouts 13mm square, 300mm from the top of the bottom plate, were made in the polyethylene vapour barrier before installation of the drywall to permit air flow past the vapour barrier. Three 5mm (3/16 in.) holes were drilled through the drywall 300mm (12 in.) from the bottom, coinciding with the cutout locations. These holes resulted in a total hole area of $0.59cm^2$ (0.09 in^2). The leakage area was thought to be representative of walls without major perforations such as unsealed electrical outlet boxes. (See Figure 4 for hole locations).

2.5   **Description of Test Panel Assembly Process**

Wood studs were hand selected construction grade SPF obtained from a local lumber yard during early spring. Each stud was wrapped in polyethylene for approximately two months before being processed. Surface moisture content (MC), measured with a hand held Delmhorst MC meter, gave initial, uncorrected stud moisture contents (surface average) in the order of 25% to 30%.

All materials for the test panels were precut before the assembly process. Six studs with generally consistent moisture content on all four faces were selected for instrumentation. During assembly, initial moisture contents of the wood, and initial

weights of all test panel materials were recorded. (See Photo 5.) The stud frame, exterior sheathing, building paper and outer cladding was then constructed for each test panel and installed in the chamber. Each panel was wrapped in polyethylene to await the instrumentation and final assembly. Moisture pins, humidity sensors, pressure tubing and thermocouples were then installed in each panel. The data acquisition system was setup to monitor the instrumentation during the assembly process. Tent conditions were kept at an average of 20°C, 70% RH during the assembly operations to minimize wood drying.

Moisture pins were placed in the inner face of the selected test stud at three locations: 300mm from the top surface of the bottom plate, 300mm from the bottom surface of the top plate, and at the mid height of the stud. The pins were placed at a depth of 10mm (3/8 in.) into the wood, each pair of pins were set 25mm (1 in.) apart. The pins were placed along the grain, generally at the midpoint of the side of the stud. Some variations to this location were necessary to avoid knots and other visible imperfections on the wood surface. In addition to the wood stud locations, a set of MC pins were placed into the waferboard sheathing mid height of the wall in the center stud cavity, 25mm (1 in.) from the test stud.

Pressure tubing and K type thermocouples were placed close to the locations of the moisture pins. A custom built humidity sensor, employing a Panametrics MiniCap 2 RH sensor, was placed at the center location of the stud beside the moisture pins. (See Figures 3A and 3B).

After the installation of the instrumentation the fiberglass batt insulation was carefully applied. All instrumentation wiring was brought through the top of the panel and sealed with silicone sealant. The polyethylene sheets were edge sealed with caulking and stapled into position. The drywall was screwed into place, and sealant was applied at the drywall-sheet metal junction. Metal foil patches were applied to all drywall screw heads to seal against any extraneous air leakage that might occur at these locations.

The panels were held in place in the chamber wall by means of wood spacers on the chamber side, and wooden slats on the tent side. The wooden slats applied pressure to the panels when screwed in tight. These slats were loosened for the panel weighing process described below. Air sealing was accomplished by means of

polyethylene sheet connecting the inside (chamber) wall and the panel edges. The sheets hung loosely to allow panel movement during the weighing process. Closed cell foam was stapled to the wooden slat surface to provide a thermal break.

2.6 Description of Test Sequence

Two climatic conditions were simulated, first winter, then summer. Average conditions are illustrated in Table 1:

TABLE 1
AVERAGE CLIMATIC CONDITIONS

Condition	Winter	Summer
External (chamber) temperature:	-15°C	38°C
External (chamber) relative humidity:	50% to 70%	60% to 70%
Internal (tent) temperature:	20°C	20°C
Internal (tent) relative humidity:	40%	70%

The target differential pressure across the wall for infiltration and exfiltration modes was 10 Pa. Because of various mechanical effects the average differential pressures varied from this value. Recorded average values were:

1) Neutral differential pressure: (Blower fan off)

    Average neutral (winter):   -0.74 Pa

    Average neutral (summer):   0.41 Pa

2) Infiltration: (Air forced through the walls from the chamber (exterior))

    Average infiltration (winter): -8.43 Pa

    Average infiltration (summer): -4.06 Pa

3) Exfiltration: (Air drawn in through the walls from the tent (interior))

    Average exfiltration (winter): 11.50 Pa

    Average exfiltration (summer): 14.14 Pa

Each of the above differential pressure conditions were maintained for periods that allowed enough time for stud moisture content drying rates to be determined. Test sequences and duration times are given in Table 2 below:

TABLE 2

WALLDRY TEST SEQUENCE

No.	Run		Dates	Duration
1	Winter	Neutral Pressure	05/25 to 06/15	22 days
2	Winter	Infiltration	06/15 to 07/03	18 days
3	Winter	Exfiltration	07/03 to 07/19	16 days
4	Summer	Neutral Pressure	07/19 to 08/09	21 days
5	Summer	Infiltration	08/09 to 08/30	21 days
6	Summer	Exfiltration	08/30 to 09/17	18 days

The data acquisition system (DAS) and ACR units were set for half hour increment scanning and recording. For each scanning cycle, thermocouple temperatures were scanned. Next, the Scanivalve with mechanical switcher was activated. The Scanivalve scanned pressure taps, moisture content pin resistance (through the Delmhorst meter), and the stud cavity humidity sensor voltages in a scan rate of approximately 2 seconds. All readings were appended to the data collection file, as well as displayed on the screen.

To determine the weight loss or gain of moisture from the panel system, periodic weighing of the panels were attempted. This was done by first loosening the holding slats to free the panels. The Styrofoam blocks below the test panels were removed and the weigh scale cart was positioned under the panel. The panel was jacked up to allow the positioning of setting blocks under the scale. The scale was then let down on the blocks for stability. The test panel was balanced vertically on the scale and a reading was recorded. The balancing of the panel on the scale proved to be a sensitive operation, therefore a minimum of three readings were recorded for each weighing, and the average was taken as the result. The experience with this testing

approach was less than satisfactory. Ice accumulation in particular caused errors in the measurement.

After the conclusion of the last run, the test panels were disassembled and removed from the chamber while the data acquisition system monitored the remaining panels. (See Photo 8.) Each piece was weighed and the moisture content was recorded. Sections of the instrumented test studs were taken to the laboratory at Forintek Canada (Ottawa, Ontario), for species identification and oven dry calibration tests.

3. EXPERIMENTAL RESULTS

3.1 Presentation of Results

Data derived from the laboratory phase of the study are presented in a series of graphs which allow a visual analysis of trends. This data is available in Lotus 123 spreadsheets.

For the sake of brevity and to avoid confusion due to the large amount of data, the graphs from one pair of panels used in the analysis are presented here. The two test panels are:

> **Panel A**: "Sealed", Wood (cedar) siding
> **Panel B**: "Vented", Wood (cedar) siding

Measurement data for the other panels is included in this report. The other panel designations are repeated here:

> **Panel C**: "Sealed", Vinyl siding, no furring
> **Panel D**: "Vented", Vinyl siding, no furring
>
> **Panel E**: "Sealed", Vinyl siding, with furring
> **Panel F**: "Vented", Vinyl siding, with furring

3.2 General Observations: Laboratory Phase

While the intent of the experiment was to create and maintain a stable environment, variable conditions such as refrigeration defrost cycles, equipment power outages, etc., resulted in significant variations in temperatures, relative humidities, and driving pressures.

Notable changes in interior and exterior conditions include:

1)   During the winter infiltration sequence, temperatures increased when warm, more humid air was blown into the chamber to create infiltration pressures. This caused ice buildup on the refrigeration coils and hence warmer temperatures in the chamber and stud cavities. The defrost cycle was

manually adjusted in the middle of the infiltration run from twice a day to four times a day to compensate.

2) At the beginning of the winter exfiltration run, the air conditioning unit in the tent failed for several hours. This caused a dramatic rise in the interior and cavity temperatures.

3) During the winter exfiltration run, the applied differential pressure steadily increased over time. This was noted and the fan volume was manually set lower to compensate. The result was a noticeable drop in differential pressure.

4) At the start of the summer run, the thermostat was accidentally set too high, causing chamber (external) temperatures to rise to 50°C over a weekend period.

5) Tent (internal), relative humidity was difficult to control during the summer runs which were conducted in late summer of 1990. During this time, the air conditioning unit in the tent was working continuously during the day to maintain 20°C. This action resulted in dryer air, which had to be constantly humidified to maintain the desired 70% RH. RH dropped during the day and increased during the night.

3.3 Data Review: Introduction

The laboratory phase of this project was to produce data under controlled and monitored conditions which could be used for future analysis and development of the WALLDRY model. Complete analysis of the data is beyond the scope of this project, but a number of data analysis and validation procedures were undertaken. The results of this analysis and a visual review of the graphical data provides some insight into moisture transport processes which will require further evaluation.

3.4 Temperature

There were significant variations in environmental temperatures due to the equipment problems mentioned earlier. This has made it difficult to evaluate the resulting cavity temperature data to discern whether there was a significant difference between the

sealed and vented pairs of test panels. This was addressed by analyzing the temperature index developed from the measured data. Temperature index is obtained as follows:

$$T1 = \frac{(T_c - T_o)}{(T_i - T_o)}$$

where TI is the Temperature Index, T_c is stud cavity temperature, T_o is outdoor temperature, T_i is indoor temperature.

In a purely conductive heat flow situation, TI should be constant. If there is convective heat transfer through the wall TI will vary with the magnitude of air leakage. In winter conditions, exfiltration will warm the cavity and raise the temperature index asymptotically to a value of 1.0. Infiltration will lower the temperature index to an asymptote of zero.

The temperature index for each data point was calculated and plotted against pressure differential. These graphs are shown in Appendix C: (Temperature Index). The following points are noted:

1)   The consistency of the data groups indicate the measured temperatures are reasonable.

2)   There is slight variation of temperature index with pressure indicating heat transfer is not purely conductive.

3)   For the vinyl siding panels, (panels C, D, E, F), there is no significant difference between the vented and sealed panels. (The wood siding panels (panels A and B), do show a slight difference in magnitude). This indicates that the air flow must be of a small volume.

The volume of air leakage through the holes in the vented panels is calculated as approximately 0.012 l/s/m^2 at 10 Pa.

3.5 Cavity Humidity

Outdoor and indoor RH was measured with the ACR units, which were checked against the factory set calibration, (accuracy of +/-4% RH). The ACR units operated without incidence.

Relative humidity in the stud cavity was measured in the center of the cavity, next to the test stud, with a Panametrics sensor and circuit. The Panametric sensors themselves have an accuracy of +/-2% RH. Salt solution calibration values of the entire circuit are shown in Appendix L. During the experiment, some sensors experienced erratic behavior, (negative readings or values well over 100%), this has been attributed as water condensing on the surface of the sensor. After a period of several hours, it appears the sensors would settle and resume reasonable measurements. However, some periods of RH measurements in the stud cavities had to be discarded as unreliable.

Measured relative humidities in the stud cavities were very high (100%) at the beginning of the winter test cycle. This was confirmed by visual observation when one of the panels was taken apart before the actual experiment (only a day after assembly), to check the RH sensor. The insulation, studs, plates and vapour barrier were very wet with condensation. Cavity RH generally decreased during the winter runs, from highs of 100%, down to levels of approximately 60% to 70%.

During the summer runs, and subsequent to the high initial temperature, most stud cavities exhibited constant RH levels between 60% to 70%. At the end of testing, wet studs and insulation was observed in all panel stud cavities. Fungal growth had settled in the bottom areas of all panels (slightly less in Panel B, (wood siding, vented)).

To determine the effect of venting on cavity humidity, RH and temperature data was converted to humidity ratios (a measure of the moisture content of the air), then to a Humidity Index (HI). The humidity index is determined by:

$$HI = \frac{(W_c - W_o)}{(W_i - W_o)}$$

where W_c is the cavity humidity ratio, W_o is the outdoor humidity ratio, and W_i is the indoor humidity ratio. The graphs of humidity index are shown in Appendix E.

While water phase change and drying effects make this analysis technique less predictable and reliable than the temperature index analysis, one would expect that air leakage would cause the humidity index to increase in winter exfiltration mode, and reduce in infiltration. This was generally not the case. Other factors may be involved and should be explored in more detail.

3.6 Differential Pressure

Differential pressures were obtained by means of plastic tubing connected to a Scanivalve switch. Pressures were measured with an Air Ltd. MP6KD differential micromanometer with a resolution of 1 Pa, and a range of 1999 Pa. The reference zero was placed in the chamber (outdoors), with a separate tap for instrumentation zero correction. All references to pressure differential, however, will be as noted as:

1)   Infiltration: Negative indoor pressure

2)   Exfiltration: Positive indoor pressure

In the experiment, each seasonal run, (winter and summer), consisted of three differential pressure configurations: neutral, (chamber fan off); infiltration, (fan blowing into chamber through exterior side of test walls); exfiltration, (fan drawing air from chamber through interior side of test walls). In the infiltration and exfiltration runs, the pressure differential was to be set at nominally 10 Pa. The pressure differential was set manually by a butterfly valve, based on a hand held manometer reading. Over time the pressure readings deviated from this setpoint, particularly during the winter exfiltration run.

All pressure values have been zero corrected. As can be seen in the graphs presented in Appendix D, there is a small pressure differential during the neutral conditions, which may be due to either an instrumentation offset, or temperature driven pressures. The values plotted in the graphs have not been corrected for this effect. The graphs show the average of the three cavity pressure taps versus the driving pressure differential. The cavity pressure values represent the proportion of the driving pressure taken up by the exterior sheathing.

We can assume that in both the sealed and vented panels the interior faces of the test panels were much more air tight than the exterior faces. We would therefore expect that most of the driving pressure difference would be carried by the interior surface and the pressure across the exterior sheathing would be a small percentage of the total driving pressure. (See Appendix D).

In general, the proportion of driving pressure carried by the exterior sheathing is small for the summer runs. In the winter runs, especially for the vented panels in exfiltration mode, the proportion carried by the exterior sheathing is larger than in other runs, and increases steadily with time. One possible explanation is that moisture accumulation and frost may have sealed the vent holes, essentially slowing air flow as the run progressed. The gradual increase in chamber pressure, (which was detected and compensated for, as shown in the graphs of pressure), may be attributed to this phenomenon as well.

3.7 Air Leakage

The primary difference between the sealed and vented experimental panels was the area of intentional leakage holes that were placed in the interior drywall sheathing and exterior waferboard sheathing. In the sealed panels careful attention was paid to providing uninterrupted surfaces on both of the interior faces. The exterior sheathing also contained no joints, the only known penetrations were the nail holes.

The holes drilled in the drywall provided a leakage area of approximately 0.18 cm²/m². The holes drilled in the exterior sheathing provided approximately 0.56 cm²/m² of intentional leakage area.

Since the interior surface of the leaky panels had a leakage area of less than $\frac{1}{3}$ of the exterior surface, it can be assumed that it would be the governing air leakage flow rate and this could be calculated by the orifice equation:

$$ Q = C_1 A \sqrt{\frac{2\Delta P}{\rho}} $$

where Q = flow (m³)
C_1 = flow (coefficient (0.61 for orifice)
ΔP = pressure difference across sheathing (Pa)
ρ = density of air (1.2 kg/m³)
A = leakage area (cm²)

To validate this assumption, an additional test panel was fabricated and tested to determine it's leakage characteristics. The test panel was identical in construction to the vinyl sided panels without furring (panels C and D). The exterior sheathing was provided with the 21 5mm holes used in the vented panels. The interior surface was initially left untouched.

Air leakage testing consisted of fabricating a wood and polyethylene enclosure over the outer face attached to the metal flashing edge. Air was removed from this enclosure by a vacuum system. The pressure difference across the test section was measured with an Air Ltd (Model MP6KD) micromanometer while the flow rate of air being drawn from the enclosure was measured with a Dwyer RCM-102 rotameter type flowmeter capable of measuring from 10 to 100 standard cubic feet per hour (0.079 to 0.787 l/s) with a stated accuracy of ±10%.

The test procedure consisted of:

- Masking off the inner face of the panel with a sheet of polyethylene.
- Measuring the flow required to create predetermined levels of pressure across the test section.

This flow was the incidental leakage from leaks in the test enclosure hoses and equipment. The polyethylene mask on the inner face was then removed and the section retested. The measured flow rate minus the incidental leakage measured at the same pressure can be assumed to be the panel's leakage in the sealed condition. Because of the limited measurement range the pressures at which flow rates could be measured was different for sealed and vented conditions. In the sealed panel, pressures and flows were measured at approximately 100, 200 and 400 Pa; with the vented panel, approximately 50, 75, 100 and 200 Pa.

Holes matching those used in all vented panels were then drilled through the drywall and vapour barrier. The sample was retested. The measured flow rate minus the incidental flow leakage was assumed to be the leakage of the vented panel.

The measured flow rate of the leaky panels at 100 Pascals was 0.075 l/s/m^2 which was approximately 4 times the pressure flow for the sealed panel at 0.017 l/sec/m^2.

The difference between the sealed and unsealed panel is 0.058 l/sec/m² which compares quite favorable with the expected flow rate using the equation above, which gives a calculated flow rate at 100 Pa of 0.051 l/sec/m².

WALLDRY accepts air leakage information in the form of coefficients for the flow equation:

$$Q = C \Delta P^n$$

The air leakage testing described above required measuring leakage at pressure differences which were much higher than the walls were subjected to during the laboratory testing and it was only possible to get a limited number of test points. The testing could not provide a reliable "n" value. However, "n" must be between 0.5 and 1.0 and assuming "n" = 0.75 is a reasonable estimate. Using this assumption the appropriate value for "C" for WALLDRY comparison runs can be calculated. "C" values of 0.00214 l/sec/m²/Pa^n and 0.00054 l/sec/m²/Pa^n for the vented and sealed panels, respectively, were used in the WALLDRY simulation runs.

3.8 Moisture Content (MC)

Moisture content was derived from moisture pins placed in three locations of the inside surface of the test stud, (top, middle, and bottom regions). Readings were obtained with a Delmhorst Model RC2M Moisture Meter. The millivolt readings were converted to uncorrected moisture content values by the formula:

$$MC = 5.556854 * \exp(0.024373 * mV)$$

where MC is the wood moisture content and mV is the original millivolt reading. (Note that this conversion formula is for readings under 80 mV, in which all readings were in this case. The MC values were then corrected for temperature and species by a formula devised by Garrahan, (see Ref. 2). The formula is:

$$MC_{corr} = \frac{\left[\dfrac{(MC + 0.567 - 0.0260T + 5.1E\text{-}05T^2)}{0.881 * (1.0056)^T} - b \right]}{a}$$

where T is the temperature in degrees Celsius, and "a" and "b" are wood species factors. In our case, we used:

Balsam Fir   a = 0.900
                        b = 0.35

Eastern White Spruce   a = 0.702
                        b = 0.818

Forintek Canada has identified the species of our instrumented test studs as follows:
1) Panel A: Fir
2) Panel B: Fir
3) Panel C: Spruce
4) Panel D: Fir
5) Panel E: Spruce
6) Panel F: Spruce

Oven dry calibrations were performed at the end of the experiment (See Table 3). Results show the calibrations of the spruce specimens were within 10% MC, while the fir specimen calibrations are scattered, with some specimens differing by greater than 20%. This might indicate that the correction factors for the fir specimens are in error, however, the scatter could be due to the fact that the over dry samples include the whole cross section, and could contain more knots or other imperfections than in the spruce specimens.

In examining the moisture content readings in which the experiment is based, no significant differences due to panel cladding type can be identified. A possible exception to this is the data for both Panel A and B, the wood siding panels, appears to be more "well behaved", (less variation, smoother curves, fewer unexplained peaks, etc.). This could be a coincidence, or possibly could have been a result of the high thermal mass or insulating value of the cedar siding smoothing temperature and moisture variations.

We found no consistent pattern between the drying rates exhibited by the different types of test panels, by the species, or when comparing the top, middle and bottom readings of an individual stud. All studs exhibited varying drying rates along their lengths. The dominance of local internal moisture distribution patterns or physical makeup is suggested for the cause of this phenomenon.

TABLE 3

MOISTURE CONTENT POST CALIBRATION

Panel Posit.	Post Cal MC (mV)	Post Cal MC (%)	Correct. MC (%)	Forintek Oven Dry MC (%)	Diff. Pins/ Oven Dry	Species
PANEL A						
Top	14.1	7.8	9.8	10.49	6.8%	FIR
Mid	13.1	7.6	7.9	10.61	25.1%	FIR
Bot	15	8.0	8.3	10.73	22.3%	FIR
PANEL B						
Top	16.2	8.2	8.6	10.48	17.9%	FIR
Mid	15.9	8.2	8.5	10.42	18.1%	FIR
Bot	21.4	9.4	9.8	10.32	4.8%	FIR
PANEL C						
Top	14.7	8.0	9.9	10.6	6.2%	SPRUCE
Mid	14.4	7.9	9.9	11.07	10.9%	SPRUCE
Bot	15.4	8.1	10.1	11.39	11.0%	SPRUCE
PANEL D						
Top	13.9	7.8	8.1	10.24	20.8%	FIR
Mid	13.5	7.7	8.0	10.24	21.6%	FIR
Bot	14.9	8.0	8.3	10.25	18.8%	FIR
PANEL E						
Top	14.5	7.9	9.9	10.38	4.7%	SPRUCE
Mid	14.8	8.0	10.0	10.64	6.3%	SPRUCE
Bot	15.1	8.0	10.1	11.09	9.3%	SPRUCE
PANEL F						
Top	14.9	7.99	10.0	10.49	4.7%	SPRUCE
Mid	14.7	7.95	9.9	10.89	8.7%	SPRUCE
Bot	14.2	7.85	9.8	10.67	8.1%	SPRUCE

Initial moisture contents of all wood studs were measured at the fibre saturation point (approximately 30%), or above. In general, MC of the studs followed a drying trend during the winter runs, dropping from fibre saturation levels to ranges of 15% to 20%. Two notable (apparently temperature related) anomalies are seen in the winter MC measurements. At the beginning of the winter infiltration run, MC readings initially increased then dropped over several days. At the beginning of the winter exfiltration run, when the indoor temperatures increased over the period of several hours, most moisture content readings dip in response. Note that the MC reaction is opposite in direction for increased temperatures coming from the outdoor or inside directions. The phenomenon exhibited by these responses have yet to be explained, however, several causes can be attributed, such as:

1) Capillary water being thermally driven through the wood when the cavity temperatures warmed, (the chamber refrigeration coils were not operating efficiently due to frost buildup, as noted earlier. Air conditioner shut down in the tent was also responsible for a rise in cavity temperatures during winter exfiltration). The direction may be across the stud or perhaps inwards, (surface to core or vice versa).

2) Equalization of moisture content from the high cavity RH; from connecting pieces such as the sheathing, top and bottom plates; or between local moisture pockets within the stud could result in the observed trends.

3) Inaccurate temperature correction factors in the MC correction formulas could cause enhanced peaks. (Note that the peaks and valleys are seen in the raw millivolt readings).

These and other explanations need further investigation.

The summer runs show a dramatic rise in MC at the beginning of the neutral mode, during the extreme "outdoor" temperatures of 50°C. This appears to be a temperature driven phenomenon as described above.

The summer neutral mode is characterized by fairly rapid drying rates which then level off at 11% to 18% MC levels. The MC during the summer infiltration runs remained fairly constant, while during the summer exfiltration run some MC readings dropped further. It has been noted that this drop seems to occur at the bottom of the studs for the vented panels, while it occurs at the top of the studs in the sealed panels. (Holes in drywall were near the bottom in the vented panels). No explanation for this observation has been derived, however, it may be the work of convection in the vented panels overriding the effects of gravity as exhibited in the sealed panel.

While the waferboard sheathing moisture content was measured in each panel, (at the center, near the test stud), we have not analyzed these measurements since the correction factors for these readings are still under development at Forintek Canada. A graph of sheathing MC for Panel A, uncorrected except for the Delmhorst millivolt to MC conversion, is presented in Appendix F. The readings for Panel B do not show any variation from 7% MC, which may be indicative of an unfortunate placement of the MC pins. However, the sheathing MC for Panel A shows many of the effects described for the stud MC.

3.9   Sorption Isotherms

Wood is a hygroscopic material, it holds moisture at an equilibrium with the surrounding atmospheric vapour pressure. When green wood is exposed to atmospheric conditions after felling, it loses moisture until the moisture content reaches an equilibrium point with the ambient atmosphere. This equilibrium moisture content, or EMC, is proportional to the atmospheric relative humidity, (or by inference, the relative vapour pressure). The curve relating EMC with RH at a constant temperature is called the sorption isotherm. The sorption isotherm is a hysteresis curve, moisture will not be re-absorbed at the same levels as the initial desorption, due to various changes in the wood structure and chemistry.

Sorption isotherms have been calculated empirically for many porous materials, including many types of wood. (See References 3 to 6. Formulas have been devised to calculate the sorption curves of many materials. The sorption curve for spruce at 20°C, derived empirically (Ref. 3, 4) is shown in Appendix G. The curves are plotted from the following formulas:

$$\text{Desorption:} \quad MC = 30.9 * \exp\left[\left(\frac{-1}{1.05}\right) * \ln\left(1-\frac{\ln(RH)}{0.383}\right)\right]$$

$$\text{Adsorption:} \quad MC = 33.7 * \exp\left[\left(\frac{-1}{1.95}\right) * \ln\left(1-\frac{\ln(RH)}{0.0626}\right)\right]$$

Calculated EMC is plotted with measured moisture content against time (see Appendix G). In general terms, the graphs visually illustrate the driving force for drying rates. The greater the difference between the EMC and the MC, the stronger

is the impetus from the MC to reach the value of the EMC. It must be noted that several factors affect the calculation of EMC, however, which can affect the certainty of this analysis. These factors are as follows:

1) Temperature: While the EMC for a particular specimen is mainly related to RH, higher temperatures reduce the EMC, while lower temperatures may increase the EMC, (a temporary, reversible function).

2) Difference between species: Several species have been measured by various sources. Many species appear to have similar sorption isotherms, but some differences exist. In the calculations presented here, values and equations for spruce have been used.

3) Structure of the specimen: Kinds and proportions of cell wall constituents and extractives, differences between sapwood and heartwood, fibre orientation, etc., all can affect the resulting sorption rates.

4) Accuracy of measurements: Potential errors exist because of the accuracy of the RH sensor and MC pin data. The depth of MC measurements also affect the comparisons between MC and EMC.

3.10   Gravimetric

Weight measurements during the experiment were obtained with an A&D Model FV150KA1 platform scale. This scale has a capacity of 150 kg and a resolution of 0.05 kg. The scale was placed under each test panel after the panel was loosened from the chamber walls.

The weight measurements taken throughout the test were complicated by the sensitivity of the weigh scale to the positioning and balance of the test panels. (The panels hung over the side of the platform). Several readings were taken at each panel over an extended time period to obtain an average reading to be used in analysis. Errors of the order of 4 to 5% (5kg) can be expected. (See Table 4). A further complication resulted when ice began to form on the top surfaces of the test panels during the winter infiltration run. Ice was removed periodically, however, it is uncertain if other ice, forming on the inside surfaces or edges could have affected the results. The resulting additive errors (and hence accuracy) from these factors places a doubt on the results.

An inspection of the gravimetric graphs reveals test panel weights (See Appendix H), generally increased quickly at the beginning of the winter run, then levelled off throughout the winter. Weights dramatically dropped off after the summer runs were begun, indicating the weight of ice is a probable factor in the winter readings. Hills and valleys shown in the graphs in APPENDIX H are probably due to the difficulty of maintaining a balance of the wall on the scale rather than a real weight change. Caution is urged in attempting to derive an analysis of trends in this data.

Each part of the test panels were weighed both prior to assembly and at disassembly. These pieces included the four studs, two top headers, bottom plate, as well as the waferboard sheathing and gypsum board. (See Table 5). Some general observations can be made concerning these measurements. Please note that the test panels were subjected to drying conditions in the winter and slightly wetting conditions in the summer, (generally speaking). Overall, it was expected that most test panel components would have lost weight over the course of the experiment.

In all panels, the four stud members lost weight. The average loss of weight for each panel's studs were on the order of 18% to 23%, (except Panel A at 30%). In the vinyl siding panels, the vented panels of each pair lost slightly more than the sealed pairs. In all except Panel B, the bottom plate gained weight (5% to 20%). Note that Panel B exhibited less mold and was drier in appearance than the others. In all panels, the sheathing gained a small percentage of weight (5% on average), as did the gypsum board (average 0.5%, except for Panel E which lost 2.4%).

TABLE 4: TEST PANEL WEIGHT MEASUREMENTS

DATES	DAYS AFTER BEGIN	PANEL A AVERAGE (kg)	MAXIMUM (kg)	MINIMUM (kg)	HIGH/LOW DIFF(%)	PANEL B AVERAGE (kg)	MAXIMUM (kg)	MINIMUM (kg)	HIGH/LOW DIFF(%)	NOTES
MAY 10	0	111.34	111.45	111.20	0.22%	105.71	106.20	105.20	0.95%	Install End
MAY 25	15	112.80	113.05	112.55	0.44%	105.29	105.40	105.20	0.19%	Win(Neut) Begin
MAY 28	18	119.46	119.50	119.40	0.08%	108.38	109.30	107.35	1.80%	
MAY 30	20	118.88	119.25	118.40	0.71%	108.56	109.75	107.25	2.30%	
JUNE 1	22	118.81	120.40	117.15	2.74%	110.15	112.40	108.25	3.77%	
JUNE 5	26	119.04	119.95	118.10	1.55%	108.41	108.75	108.00	0.69%	
June 8	29	117.81	118.85	116.95	1.61%	109.50	109.75	109.15	0.55%	
June 11	32	116.51	117.40	115.60	1.54%	109.03	109.70	108.30	1.28%	
June 13	34	118.44	119.00	117.95	0.89%	107.54	107.90	107.05	0.79%	Win(Inf) June 15
June 18	39	116.90	117.50	116.05	1.24%	106.57	106.80	106.30	0.47%	
July 3	54	117.51	117.65	117.20	0.38%	105.74	106.60	104.95	1.56%	Win(Exf) July 3
July 19	70	117.46	118.30	116.40	1.62%	110.06	110.30	109.70	0.55%	End Winter
July 20	71	111.50	112.10	111.05	0.94%	104.25	104.55	103.95	0.58%	Sum(Neut) Begin
Aug 8	90	96.05	97.00	94.95	2.13%	101.96	102.20	101.65	0.54%	Sum(Inf) Aug 10
Aug 29	111	98.06	99.00	97.15	1.89%	100.17	100.50	99.90	0.60%	Sum(Exf) Aug 30
Sept 17	130	103.85	103.95	103.70	0.24%	99.88	100.15	99.70	0.45%	End Test

TABLE 5: PANEL WEIGHTS (INDIVIDUAL PIECES)
WALLDRY PRETEST AND POST-TEST

PANEL ITEM	SEALED PANELS				VENTED PANELS			
	PRE-WEIGHT (kg)	POST-WEIGHT (kg)	WEIGHT DIFF (kg)	PERCENT GAIN OR LOSS	PRE-WEIGHT (kg)	POST-WEIGHT (kg)	WEIGHT DIFF (kg)	PERCENT GAIN OR LOSS
PANELS A AND B	**PANEL A: WOOD SIDING**				**PANEL B: WOOD SIDING**			
Left stud	4.85	4.30	-0.55	-11.3%	3.60	2.95	-0.65	-18.1%
Center left	5.70	3.60	-2.10	-36.8%	4.00	2.90	-1.10	-27.5%
Center right	4.50	2.95	-1.55	-34.4%	5.00	4.55	-0.45	-9.0%
Right stud	5.70	3.50	-2.20	-38.6%	4.90	4.10	-0.80	-16.3%
Top header (outside)	2.95	2.20	-0.75	-25.4%	3.35	2.10	-1.25	-37.3%
Top header (inside)	3.05	2.05	-1.00	-32.8%	2.55	2.10	-0.45	-17.6%
Bottom plate	2.80	3.35	0.55	19.6%	2.90	2.45	-0.45	-15.5%
Sheathing	22.90	23.05	0.15	0.7%	21.60	22.75	1.15	5.3%
Gypsum panel	24.85	24.95	0.10	0.4%	24.90	25.00	0.10	0.4%
PANELS C and D	**PANEL C: VINYL SIDING**				**PANEL D: VINYL SIDING**			
Left stud	5.00	4.40	-0.60	-12.0%	4.65	3.30	-1.35	-29.0%
Center left	4.00	3.30	-0.70	-17.5%	4.45	3.35	-1.10	-24.7%
Center right	5.95	4.25	-1.70	-28.6%	4.60	3.35	-1.25	-27.22%
Right stud	4.35	3.30	-1.05	-24.1%	4.75	2.95	-1.80	-37.9%
Top header (outside)	2.20	1.90	-0.30	-13.6%	2.20	2.00	-0.20	-9.1%
Top header (inside)	2.95	2.30	-0.65	-22.0%	2.20	1.95	-0.25	-11.4%
Bottom plate	2.05	2.35	0.30	14.6%	2.15	2.40	0.25	11.6%
Sheathing	21.50	22.70	1.20	5.6%	21.60	22.75	1.15	5.3%
Gypsum panel	24.70	24.85	0.15	0.6%	25.15	25.25	0.10	0.4%
PANELS E and F	**PANEL E: VINYL/FURRING**				**PANEL F: VINYL/FURRING**			
Left stud	4.65	4.25	-0.40	-8.6%	5.00	3.40	-1.60	-32.0%
Center left	5.55	3.55	-2.00	-36.0%	5.80	4.40	-1.40	-24.1%
Center right	4.40	3.60	-0.80	-18.2%	4.35	3.90	-0.45	-10.3%
Right stud	4.45	4.05	-0.40	-9.0%	4.90	4.20	-0.70	-14.3%
Top header (outside)	2.35	2.10	-0.25	-10.6%	3.20	2.10	-1.10	-34.4%
Top header (inside)	3.00	2.30	-0.70	-23.3%	2.35	1.85	-0.50	-21.3%
Bottom plate	2.40	2.80	0.40	16.7%	3.00	3.15	0.15	5.0%
Sheathing	21.40	22.40	1.00	4.7%	21.25	22.25	1.00	4.7%
Gypsum panel	25.15	24.55	-0.60	-2.4%	25.15	25.35	0.20	0.8%

4. PHASE II: ALGORITHM MODIFICATIONS

4.1 Background

In order to compare the laboratory data with WALLDRY simulation output, the present version of WALLDRY had to be modified to accept indoor and outdoor environmental data, as well as differential pressure gradients across the wall. Before this study, outdoor weather was input from a binary file of Environment Canada weather data. Indoor conditions could only be specified through four set variables: winter temperature and RH, and summer temperature and RH. The first task was to allow the input of laboratory test data, or idealized conditions if desired.

The present version of WALLDRY also lacked an algorithm for describing the transport of water vapour by mass air flow through air leakage into the cavity, which can be a major mechanism for vapour transport. The program has been modified to accept a user specified air leakage characteristics (using the formula $Q=C \Delta P^n$), and a "field of influence" of air leakage for the vertical nodes from 1, (bottom) to 9, (top).

4.2 Approach

Three sets of modifications were undertaken. These were:

1) An easily implemented system of data handling was developed for the specification of:
   - airtightness characteristics of the panels, including the field of influence of any leaks.
   - initial moisture contents of the studs;
   - test duration in hours;
   - mean hourly exterior temperatures and RH;
   - mean hourly interior temperatures and RH; and
   - mean hourly pressure difference across the wall panel.

2) Heat and mass balance algorithms were developed and programmed to account for gross effects of air flow through the cavity. (See below.)

3) Input, output, and other routines were modified in the program to handle the new inputs, the lab generated data, and the new algorithms.

4.3   Input Modifications

Changes have been made to the data handling system that inputs the environmental driving forces into the program. The binary data file for outdoor temperature and RH was replaced for the purposes of handling lab generated data (the advantages of the compressed binary format for handling large weather data files were not needed for the lab data). A simple LOTUS 1-2-3 spreadsheet was set up to input lab generated indoor and outdoor conditions for each hour. The rationale for the approach is that spreadsheets are a common means of handling large volumes of data throughout the research community. Generating a complete set of initial conditions, set up characteristics, and the hour-by-hour lab conditions, all in the same spreadsheet should take a matter of minutes with this approach, and minimizes the risk of error. All input data can be reviewed graphically with LOTUS style graphs, to visualize the large number of inputs involved.

A number of initial conditions such as stud moisture contents was not previously read by WALLDRY. This data is now included in the same spreadsheet that contains the hourly lab conditions described above.

See Appendix J for a sample of the new spreadsheet format for input specifications and hourly lab conditions. This spreadsheet is labelled "LABINPUT.WK1" on the submitted disk. A file readable by WALLDRY is produced by printing this file, (with chosen filename) to disk in an ASCII format. (Note: select a dot matrix printer, setup without page breaks). Just before executing the simulation, WALLDRY prompts the user for this file name for input. (**NOTE**: at present this version of WALLDRY requires **positive** values for infiltration pressures, opposite of what is used in this report. This was done because of an earlier undetected sign error in the pressure measurements, which has subsequently been corrected in the raw data spreadsheets. This sign difference does not affect the results of the WALLDRY simulation, but must be noted).

A new master spreadsheet was also formatted to receive the data generated by the simulation. This file is called "MASTER.WK1", (as previously). Appropriate headings are provided, and two graphs show the moisture content histories for the surfaces of the sheathing and studs. **NOTE**: It is an option in WALLDRY as to what MC layer (1-22), and elements (1-9), are saved in the output. (WALLDRY Screen 1.4.2). The headings related to these elements must be adjusted in MASTER.WK1. (See Appendix J).

4.4   **Algorithm Modifications: Condensation Efficiency**

(NOTE: There are currently disagreements regarding the concept of condensation efficiency as outlined below, (from M. Swinton, IRC, see Ref 7). The concept has been incorporated into the model and is awaiting further developments at IRC for refinement).

When interior or exterior air leaks through an insulated wall cavity, the water vapour concentration of the air stream entering the cavity can be different than the water vapour concentration of the air leaving the cavity. The difference in moisture flow rates entering and leaving via the air stream is the amount of moisture left in (or picked up from) the cavity.

Detailed modelling of this phenomenon is beyond the scope of this work and of the WALLDRY modelling framework in general. Nevertheless, a simplified heat and mass balance model can be set up, based on the results of the detailed heat, air and moisture research currently underway at IRC, VTT in Finland, and the Solar Energy Research Center in Florida.

From this body of work, the concept of "condensation efficiency" has emerged. It expresses the results of detailed interactions of heat, air and moisture within the cavity in terms of an overall result: the ratio of the actual quantity of moisture deposited to a theoretical potential for moisture deposition under specific conditions. This concept was used to incorporate the effects of air leakage into the WALLDRY model. Condensation efficiency is a function of leakage rate and flow path.

A condensation efficiency of 20% has been proposed to run the model. It should be noted however, that the simulation runs in this report have been run with the condensation efficiency variables set at 100%. (A sensitivity analysis of these variables has not been done at this time).

4.5   **Algorithm Modifications: Mass Air Flow**

The following unknowns need to be determined to solve for the quantity of moisture condensed or picked up from the cavity for a known set of indoor and outdoor temperatures and RH's:

1)   the overall leakage rate through each wall panel

2)   the vertical distribution of the leakage rate into and out of the cavity

3)   the water vapour concentration of air entering the cavity (assumed uniform vertically)

4)   the water vapour concentration of air leaving the cavity (the vertical distribution of which needs to be determined)

5)   the net moisture deposited or picked-up, as determined by a mass balance of the moisture in the air streams.

The distribution of condensation deposition vertically is also unknown. It is proposed that the vertical distribution be assigned judgmentally at this stage, based on the location of leaks planned into the test walls. Again with guidance from the more detailed models and experimental results, we can specify a "field of influence" of a leak. Current research shows that this field is concentrated near the entrance of the leak, on the cold side of the cavity. Provision has been made to allow the user to specify the "field of influence" as an input, for both infiltration and exfiltration. Based on the distribution of planned leaks in the test panel, the user can specify a focussed leak in one or more locations or a distributed leak (all elements) vertically.

The water vapour concentrations of indoor, outdoor and cavity air are already calculated by WALLDRY, and thus can be used directly with the new algorithm.

The new algorithm solves for the quantity of condensed/evaporated water at each element vertically by multiplying the following factors:

1)   the index of the "field of influence" for each element (typically 1 or 0, depending on the proximity of the element to the leak location - can also be a fraction). This tells the model how the total moisture deposited in the cavity is distributed locally.

2)   the total air flow rate through the wall.

3)   the difference between the water vapour density of air entering the cavity and the theoretical water vapour density of air leaving the cavity.

4)   the condensation of air leaving the cavity.

5)   the condensation efficiency.

WALLDRY already calculates the temperatures and vapour pressures of the cavity surfaces. Therefore, these quantities are used directly with the "condensation efficiency" concept to estimate actual moisture condensation/evaporation.

The normalized leakage characteristic of the wall panels can be determined through a standard leakage test, and expressed in the standard way:

$$Q = C\Delta P^n$$

where Q = flow rate, L/s
C = normalized flow coefficient, $(L/s/m^2)/Pa^n$
ΔdP = pressure difference across the wall, Pa
n = flow exponent (varies between 0.5 and 1.0)

4.6 Modifications to Selected Routines

Modifications to existing subroutines of the WALLCALC.BAS file were made to incorporate the new algorithm for air leakage, and to account for new input routines. These modifications are listed in Appendix K, and described briefly below.

The initial stud moisture contents, panel leakage characteristics, and number of hours to be simulated are read in a new routine in sub-routine "OpenWeather". This routine is executed just before the simulation begins, so that previously specified information such as the simulation time (WALLDRY Screen 1.3), and initial moisture contents (WALLDRY Screen 1.1.7), are over-ridden by the data in the new input file.

The hour-by-hour lab conditions are read into the program through a new INPUT line in sub-routine "GetWeather". The input lines relating to the transfer of climatic data to the program have been "commented out". No climatic data need be present in the directory to run the modified program, (WALLDRY Screen 1.2).

Equations were set up in the "NetMoisture" sub-routine to account for the moisture mass balance resulting from air leakage. The hourly quantity of condensed or evaporated moisture is stored in a shared array named MSOURCE - an existing array originally set up in the program for moisture transfer occurring through mechanisms other than vapour diffusion. The condensation/evaporation rates stored in

MSOURCE are used to update the moisture contents of wood elements at the cavity surfaces on an hourly basis. This update is done in sub-routine "UpdateMoisture". The quantity of moisture condensed/evaporated is also used to calculate latent heat effects in sub-routine "HeatEffects".

The sensible heat transfer equations relating to the transport of different temperature air through the cavity were set up in the "HeatEffects" sub-routine. The sensible heat transfer equations are analogous to the moisture transfer equations. As well, a "heat transfer efficiency" is used in exactly the same way as the "condensation efficiency", to account for the fact that the leakage stream may not have time to cool to cavity surface temperatures as it passes through the cavity.

The CALL statement that invokes the calculation of night sky radiation has been "commented out", since there is no night sky effect in the laboratory experiment.

5. SIMULATION RESULTS

5.1   Introduction

The phenomenon of moisture transport in a wall system is a complex interaction of several driving phenomenon: vapour pressure; differential pressures due to wind; stack effect; mechanical systems; thermal gradients; capillary action; and weather phenomenon such as solar pumping, or night sky radiation. Moisture can enter the wall system through many interrelated sources as well: through wind driven rain, snow, or ice; from water vapour in the air; or from internal vapour sources such as from occupants, ventilation systems or building materials.

An individual wall design may exhibit different behavior in various climate regimes due to the variations of seasonal humidities and temperatures and effects from local micro-climatic influences. Internal room conditions will also influence moisture related behavior for any particular wall design.

WALLDRY was written with the idea of helping wall designers, builders, and researchers predict the moisture related behavior of wood frame wall systems in various climatic regimes. The original WALLDRY version (1986) lacked the mechanism to account for air flow into and out of the wall stud cavity, an important factor since most wall panels are not perfectly air tight, and the introduction of moisture laden air can account for a significant portion of water vapour entering, or leaving the wall cavities.

In order to account for the effects of mass air transport in the wall system, an algorithm has been introduced into the model to account for the amount and location of air leakage, the driving force of the pressure differential across the wall, and for the relative efficiency of condensation within the wall. The laboratory experiment on six selected wall systems was carried out to validate the modified program and to highlight any deficiencies in the model. Experimental data, specifically the outdoor and indoor temperatures, relative humidities, and the differential pressures across the wall, has been used as input into the WALLDRY computer program. Results for a pair of these panels, (Panels A and B, the wood siding panels), are plotted comparing the experimental data with the WALLDRY simulation results. (See Appendix I)

5.2 Comparison of Results: General

Simulation runs using the WALLDRY program were performed in order to evaluate the effectiveness of the model in predicting the performance monitored in the laboratory experiment. Indoor and outdoor temperatures and humidities, and differential pressures across the wall, were obtained from the experiment for use in the simulation. Initial moisture contents of the studs for each run were also obtained from the experiment for input into the program. The moisture content readings were used as input for vertical elements 2, 5, and 8, (second from bottom, middle and second from top, respectively). WALLDRY has nine vertical elements, 1 thru 9, (bottom to top). The initial moisture content for the other elements were interpolated from the measured laboratory values. (See Tables 6A and 6B).

The WALLDRY simulations presented here were accomplished by running each pressure regime, (neutral pressure, infiltration, and exfiltration) separately, then graphing the results together. The results of the runs are illustrated in Appendix I: (Laboratory/Simulation Comparison Graphs). The graphs for one pair of panels are presented here, Panels A and B, (wood siding). Graphs are shown comparing the top, middle, and bottom MC measurements, with their corresponding simulation values.

Some general observations can be made regarding the comparisons. First, while the experimental MC data is dynamic and shows relatively rapid responses to temperature (and/or RH) changes, the WALLDRY simulation data is smooth and straight. WALLDRY is not predicting the MC responses to the changing inputs as seen in the experimental data. It should be noted (as mentioned previously), that the response of MC to temperature and/or RH in the laboratory data could be the result of free capillary water movement, water storage and release from the sheathing, or perhaps temperature correction factors.

Aside from the high moisture content differences, WALLDRY also shows a pronounced drying rate for both the winter and summer infiltration runs for the vented (Panel B) bottom stud. This is not borne out in the experimental data. The bottom stud MC location is opposite the holes placed in the drywall, (the location of the greatest field of influence for the holes in the simulation). It is assumed WALLDRY is reacting to the air flow mechanism here, however inaccurately.

A combination of runs performed on Panels A and B with different values for air flow coefficients illustrate favorable sensitivity of WALLDRY to the magnitude of air flow. Changes in relative slope and end moisture content with changes in the air flow coefficient "C" are observed. (See Appendix I (Air Flow Sensitivity Graphs).

TABLE 6A: Winter
INITIAL MOISTURE CONTENTS FOR
WALLDRY SIMULATION RUNS

RUN CODE	BOTTOM J1	MH BOTTOM J2	J3	J4	MH MIDDLE J5	J6	J7	MH TOP J8	TOP J9
PANEL_RUN					WINTER				
A_NT	32.62	33.33	34.04	34.75	35.46	35.63	35.80	35.97	36.14
A_IN	25.84	26.88	27.92	28.97	30.01	27.05	24.08	21.12	18.16
A_EX	17.75	19.22	20.69	22.16	23.63	21.84	20.05	18.26	16.47
B_NT	31.28	30.83	30.38	29.94	29.49	30.67	31.85	33.03	34.21
B_IN	14.39	14.85	15.31	15.78	16.24	19.68	23.13	26.57	30.01
B_EX	13.15	13.31	13.47	13.62	13.78	15.48	17.18	18.88	20.58
C_NT	35.06	34.99	34.92	34.84	34.77	34.16	33.55	32.94	32.33
C_IN	16.91	16.87	16.83	16.79	16.75	18.90	21.04	23.19	25.34
C_EX	12.72	12.60	12.48	12.36	12.24	14.18	16.11	18.05	19.99
D_NT	35.76	33.35	30.94	28.54	26.13	25.11	24.08	23.06	22.04
D_IN	25.73	25.15	24.57	24.00	23.42	21.10	18.78	16.46	14.14
D_EX	20.15	21.47	22.79	24.12	25.44	21.79	18.14	14.49	10.84
E_NT	39.32	39.31	39.30	39.29	39.28	35.91	32.54	29.17	25.80
E_IN	25.90	25.83	25.76	25.70	25.63	24.10	22.57	21.04	19.51
E_EX	19.58	19.46	19.34	19.21	19.09	17.73	16.38	15.02	13.66
F_NT	36.89	36.40	35.91	35.41	34.92	35.75	36.59	37.42	38.25
F_IN	26.57	27.21	27.85	28.50	29.14	29.01	28.89	28.76	28.63
F_EX	17.18	20.23	23.28	26.34	29.39	27.74	26.08	24.43	22.78

TABLE 6B: Summer
INITIAL MOISTURE CONTENTS FOR
WALLDRY SIMULATION RUNS

			WALLDRY MOISTURE CONTENT ELEMENT						
RUN CODE	BOTTOM J1	MH BOTTOM J2	J3	J4	MH MIDDLE J5	J6	J7	MH TOP J8	TOP J9
PANEL_RUN					**SUMMER**				
A_NT	13.25	13.82	14.39	14.97	15.54	15.12	14.71	14.29	13.87
A_IN	13.04	12.93	12.82	12.70	12.59	13.67	14.75	15.83	16.91
A_EX	12.88	12.79	12.70	12.62	12.53	13.74	14.96	16.17	17.38
B_NT	13.59	12.87	12.15	11.42	10.70	12.45	14.20	15.95	17.70
B_IN	17.61	17.02	16.43	15.83	15.24	14.48	13.73	12.97	12.21
B_EX	17.02	16.58	16.14	15.70	15.26	14.59	13.92	13.25	12.58
C_NT	12.79	12.70	12.61	12.51	12.42	13.98	15.55	17.11	18.67
C_IN	20.22	19.52	18.82	18.11	17.41	16.46	15.50	14.55	13.60
C_EX	20.86	20.08	19.30	18.51	17.73	16.75	15.76	14.78	13.80
D_NT	20.60	19.88	19.16	18.45	17.73	16.49	15.26	14.02	12.78
D_IN	13.64	13.61	13.58	13.55	13.52	13.01	12.49	11.98	11.47
D_EX	13.19	13.28	13.37	13.47	13.56	12.89	12.21	11.54	10.87
E_NT	17.33	17.14	16.95	16.75	16.56	15.66	14.75	13.85	12.95
E_IN	18.16	17.70	17.24	16.79	16.33	15.76	15.19	14.62	14.05
E_EX	17.14	16.94	16.74	16.54	16.34	15.99	15.65	15.30	14.95
F_NT	14.22	16.99	19.76	22.52	25.29	23.86	22.42	20.99	19.56
F_IN	19.11	18.14	17.17	16.20	15.23	15.12	15.00	14.89	14.78
F_EX	19.29	18.14	16.99	15.84	14.69	14.82	14.96	15.09	15.22

As can be seen in the graphs, some of drying rates for laboratory measured stud moisture content and WALLDRY simulation stud moisture content are quite comparable, while others are not. Table 7 summarizes the general level of agreement for Panels A and B. The following sections include comments on the trends noted.

5.3   Winter

In the winter neutral pressure runs, experimental moisture contents started out at or above the fibre saturation level. At the beginning of the experiment, MCs rapidly increased over the first few hours, in response to changing temperatures. Moisture contents then declined along a gentle exponential decay curve. Since WALLDRY does not take free, or capillary water, into account, and we can assume it is present in the studs during this run, the resulting simulation curves generally do not agree well with the experimental data. In many cases, the WALLDRY slope of the simulation results are comparable to the experimental ones, yet the absolute values are quite far apart.

WALLDRY also does not respond to the increase in MC as shown by the experimental stud MC curves during the winter infiltration run, and the "dip" in MC at the beginning of the exfiltration run. As noted previously, these phenomena might be associated with factors WALLDRY cannot model.

5.4   Summer

When the summer run began, experimental moisture contents increased dramatically, (from levels of around 15% MC), then decreased almost as rapidly. It is assumed that this is in reaction to the high heat experienced by the panels (50°C) at this time. While WALLDRY does show a general increase in MC, it does not predict the peaks. (Note: the experimental peaks could be a result of inaccurate temperature corrections or assumptions, though in all probability they represent "real" events). In all cases, WALLDRY predicts MC increases over the course of the neutral run, while the experiment shows a decrease or levelling off of MC.

In the summer infiltration runs, WALLDRY does come into close agreement with the experimental results, except for the noted discrepancy in the bottom stud of the vented panel, (WALLDRY predicts a faster drying rate for the bottom of the stud in vented panels).

TABLE 7
WALLDRY LAB/SIM COMPARISON

COMPARISON MATRIX:

A: Good agreement, (slope and end point)
B: Generally good slope agreement
C: Not good correlation

PANEL A: SEALED		WINTER				SUMMER		
		Neutral	Infiltration	Exfiltration		Neutral	Infiltration	Exfiltration
TOP		C	A	B		B	B	C
MID		A	B	A		C	C	C
BOT		A	B	A		C	B	A
PANEL B: VENTED								
TOP		B	B	A		C	A	C
MID		C	A	A		C	A	B
BOT		C	C	A		C	C	A

MH

In the summer exfiltration runs, experimental results showed an increased drying rate for the top of the stud in the sealed panels, and in the bottom of the stud of the vented panels. (convection in the vented panels is suspected as the cause of the effect). WALLDRY does predict that the top of the studs in the sealed panels should increase in drying rate, (the middle and bottom of the studs should actually decrease in drying rate), while for the vented panels, WALLDRY predicts the bottom of the stud should increase in drying rate. This mirrors the effect observed in the experimental data, leading to a conclusion that the phenomenon observed is perhaps "real" and that the model can accurately predict it.

5.5   Discussion of Results

Local variations in wood moisture content readings and their respective drying rates complicate comparative analysis. However, the similarity in many slopes between experimental and simulation results should be construed as encouraging. Perhaps the greatest drawback in the model is a lack of a mechanism for taking capillary water into account. It would certainly add to the complexity of the model, but as seen here, it is important if one wishes to model moisture content data properly.

Experimental results show that moisture content reacts quickly to external changes in environmental conditions. WALLDRY does not model temperature and/or RH variations that occur in short time frames. It remains to be seen if WALLDRY could have the capabilities to model short time constant factors, or (more importantly) if these effects are significant to wall performance evaluation.

The comparisons made between experimental data and simulations using various air flow rates would suggest that WALLDRY is relatively sensitive to the magnitude of air leakage through the wall. The fact that WALLDRY had predicted the phenomenon observed in the summer exfiltration runs (noted above) would indicate some degree of accuracy of the model. This is encouraging but should be explored using other measured data as input.

Further work should be undertaken to investigate the sensitivity of variables such as condensation efficiency. Simulation runs using data gathered from other sources and input into WALLDRY are required in order to properly assess the relative effectiveness of this variable.

6. CONCLUSIONS

The outcome from the laboratory experiment is a valuable set of data for the analysis of wood frame wall system performance under representative summer and winter conditions; in neutral, exfiltrating and infiltrating pressure regimes. The data includes a dynamic environment of driving temperatures, humidities and pressures which, while not planned, has actually proved to be useful in assessing the performance of the wall systems and the evaluation of the WALLDRY simulation model. A preliminary analysis of the data has been described in this report and is summarized here:

1) It has been noted that the measured wood moisture content, corrected for temperature, responded very quickly to changes in the indoor and outdoor temperatures to which the walls were exposed. While inaccurate temperature compensation is one explanation for this, the fact that these trends were noted in uncorrected data, and that the moisture content responded in opposite directions depending on whether the cavity was heated from the inside or outside leads one to believe that it is likely a real effect. The actual mechanism for the moisture transfer in these cases was not determined.

2) Over the course of the entire experiment the studs and top plates of the test walls dried. The bottom plates and exterior sheathing gained moisture and it was noted that fungal growth developed in all panels in the lower regions. Upon dismantling of the test panels, extremely wet insulation, wood and polyethylene was observed.

3) There was no discernable pattern in moisture content measurements with respect to the different cladding types, (wood or vinyl), whether or not furring was used, or the species of the wood used in construction, (spruce or fir). Exceptions: the two wood siding panels appeared to have a better behaved data set which could be either due to a coincidence or influence of the insulation, thermal mass, or water absorbing qualities of the cedar siding.

4) Moisture content drying rates appeared to be governed as much by local wood moisture conditions as the location within the wall assembly. For example, there was no discernible pattern as to whether the top, bottom or middle of a vertical stud member had the greater drying rate or highest ending moisture content.

5)   Even though air flows through the holes in the vented panels was small (expected flow at 10 Pa for the vented panels of 0.012 l/s/m^2 versus 0.003 l/s/m^2 for sealed panels), there were subtle patterns noticed in the wood stud drying rates. A particular example occurs in the exfiltration mode of the summer condition, where the bottom of the studs dried faster in the vented panels but the top of the studs dried faster in sealed panels. Since the WALLDRY model predicts this unexpected behavior, it is believed this is a real phenomenon and is likely to be related to convection.

6)   Temperature data behaved very much as one would expect when one examines how changes in driving pressure affected the temperature index of the wall system. When comparing the temperature index values of sealed and vented panels, the small volume of air flow appears not to have caused a significant difference in the cavity temperatures.

7)   In an equilibrium situation, one would expect air flow direction to affect the humidity index (the difference between air moisture content of the cavity to outside and from inside to outside). Exfiltration in cold weather should raise the humidity index, while infiltration should lower it. This was not found to be the case in the test panels indicating that cavity humidity ratios were governed primarily by the vapour pressure induced from the drying of building materials rather than air flow.

10)   The data indicated that in cold weather, moisture and/or frost was collecting on the exterior sheathing and was actually sealing off leakage areas. This resulted in a variable air flow rate, especially in the exfiltration mode.

The findings of the comparisons between the experimental data and the WALLDRY simulation results would indicate that WALLDRY has the ability to model certain aspects of the performance of moisture in residential wood frame walls. Some further modifications of the program are necessary to enhance the accuracy of the model. Comparisons of WALLDRY predictions with other field measured data is also warranted, before greater confidence in the model can be expressed. To summarize:

1)   Despite a relative small difference in air flow rates between vented and sealed panels, (0.009 l/s/m^2 at 10 Pa), and modest air flow rates as a whole (vented panels: 0.012 l/s/m^2 at 10 Pa), some subtle similarities are observed between the measured data and WALLDRY model results.

2)   Excursions in driving conditions, such as temperatures, has resulted in dynamic stud moisture content drying rates. WALLDRY does not predict this behavior, though in many cases the slopes of drying rates are similar between model and measured data.

3)   Initial stud moisture contents in the experiment were at or near fibre saturation (30%). The movement of free or capillary water is presumed in the experimental data, but is not evident in the model predictions. This version of WALLDRY does not model the behavior of capillary moisture, hence, as expected, the model results do not agree with the measured values at these levels of moisture content.

4)   Some interesting observations were noted in the measured data concerning stud moisture drying rates, which was also observed in the WALLDRY simulation results. Generally, a notable increase in drying rates are exhibited during exfiltration for the top of the stud in sealed panels, while this occurs for the bottom of the stud in the vented panels. WALLDRY does predict this drying rate anomaly.

5)   WALLDRY predicts a faster drying rate for the bottom of the studs in the vented panels in infiltration modes, which is not borne out in the experimental data.

6)   WALLDRY does not predict the same anomalies due to indoor and outdoor temperature fluctuations (rise in MC with outdoor rise in temperature, drop in MC with indoor rise in temperature) as evidenced in the experimental data.

7)   The sensitivity analysis performed by comparing WALLDRY predictions using various wall leakage rates shows that WALLDRY is capable of modelling effects due to convective flow. It also demonstrated that the calculated values for air flow rates of both the sealed and vented panels compare reasonably well with the actual measured data.

7. RECOMMENDATIONS

WALLDRY has been modified to model the effects of mass air flow through the wall assembly. A laboratory experiment on selected wall designs has been performed in order to provide data for simulation comparisons. These comparisons have been performed and the resulting similarities and differences have been noted. Further development work is suggested to further refine the model and to verify the model's accuracy in predicting the behavior of moisture in wood frame wall systems:
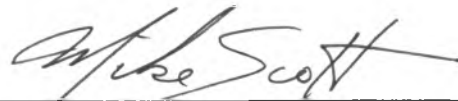
1) The movement of capillary water within wood studs is not currently modelled in WALLDRY. Our results illustrate the need to incorporate this mechanism to model the behavior of wood moisture more closely.

2) The WALLDRY model is insensitive to short time constant phenomena. In our comparisons, the model does not follow temperature and/or RH variations as shown in the experimental data. However, this may or may not be important for long duration analysis such as a complete season, or a year. Comparisons between the model and data produced by field studies is required in order to judge the requirements for short period modelling.

3) A close look at the various driving forces and their interactions acting on the wall system is warranted. WALLDRY uses the values for cavity temperature, humidity and differential pressures in it's intermediate calculations. Modifying WALLDRY to output these values will perhaps shed some insight into how these forces behave within the wall cavity.

4) The instrumenting of wood studs to obtain their moisture content is a problematic procedure; local wood properties can affect the output and cause significant differences in the results. As seen in our laboratory experiment, a single wood stud can have three different drying rates. It is difficult to separate the possible effects of local moisture structures and external driving conditions. It is believed the internal moisture structure of the wood stud can affect the local drying rate of the wood. The utilization of more moisture content measurement locations, (perhaps to correspond to WALLDRY's nine elements), to obtain a clearer picture of a particular stud's drying rate, is recommended in future work. MC measurement points at different depths

(including the immediate surface), will contribute to a better statistical understanding of the behavior of moisture in wood as well as the wall system itself. This holds true for measurement locations of RH, temperature and pressure as well.
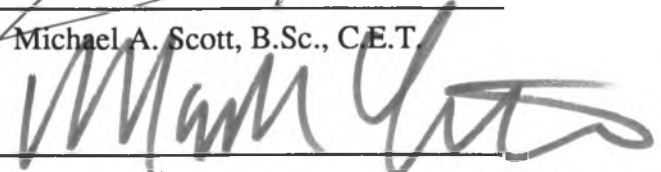
6)   The difference in leakage area or flow rates between leaky and vented panels in this experiment was not great. While the vented panels are representative of typical walls without major penetrations such as unsealed electrical outlets, testing panels with greater leakage areas is desirable. An experiment using identical test panels but with a variety of air leakage rates is suggested.

7)   This study incorporated measurements of moisture content pins in the exterior sheathing with the knowledge that correction factors for these measurements are under development. As the exterior sheathing is an important reservoir of moisture and affects the overall thermal performance of the wall system, it is recommended that future studies incorporate sheathing moisture pin readings as a matter of course. An examination of moisture transport between the studs and exterior sheathing, for example, should prove valuable in developing better models of moisture behavior.

8)   In the present study, we attempted to examine total wall system moisture loss or gain through measurements of the change in weight of the test panels during the experiment. However, the results were not positive because of problems in the mechanics of the measuring system. An examination of total system moisture performance would still be a valuable asset in understanding the flow of moisture to and from the wall.

9)   In this study, external weather phenomenon such as solar gains, wind effects and night sky radiation have been temporarily disabled. This was done to directly compare WALLDRY output with the laboratory data, and to eliminate some of the complicating variables. Some further work will be required to replace these variables, as introducing another vertical connection between nodes in the cladding cavity will complicate the algorithms. The addition of larger environmental data sets will cause micro-computer disk space and memory limitations that might have to be addressed.

10) The analysis of the behavior of moisture in wood should include an investigation into the driving force of internal moisture. A better understanding of how local internal moisture profiles affect wood drying rates is required. Local variations in wood moisture profiles are suspected of causing noted variations in drying rates in this experiment. Moisture pins inadvertently placed in anomalous wood structures such as internal limbs or knots could jeopardize accurate MC measurements. As an addendum to this study, we are evaluating the use of Magnetic Resonance Imaging (MRI) in discerning internal moisture profiles. The results of investigations into how the drying rate of wood studs is affected by internal mechanisms should assist in modelling how wood reacts to the complex interactions of driving forces.

MORRISON HERSHFIELD LIMITED

Michael A. Scott, B.Sc., C.E.T.

Mark Lawton, P.Eng.

REFERENCES CITED

[1] _____ "ASHRAE 1989 Fundamentals, Chapter 6: Psychrometrics" American Society of Heating, Refrigeration and Air Condition Engineers, Inc., Atlanta, Georgia.

[2] Garrahan, P. 1989 "Moisture Meter Correction Factors" Report 88-03-40-91K-501 Forintek Canada Corp., Ottawa, Ontario.

[3] Hansen, K.K. 1986, "Sorption Isotherms - A Catalog" Building Materials Laboratory, The Technical University of Denmark, Technical Report 162/86, Lyngby, Denmark.

[4] Hedlin, C.P., 1968 "Sorption Isotherms of Twelve Woods at Subfreezing Temperatures" National Research Council of Canada, Ottawa, Ontario.

[5] Siau, John F., 1984 "Transport Processes in Wood" Springer-Verlag, New York, New York.

[6] Skaar, Christen, 1988 "Wood-Water Relations" Springer-Verlag, New York, New York.

[7] Swinton, M.C. 1991 "Walldry Program Modifications to Simulate the Drying of Wall Panels Tested by Morrison Hershfield" Report No. CR6316.1, National Research Council of Canada, Ottawa, Ontario.

[8] Tveit, Annanias, 1966, "Measurements of Moisture Sorption and Moisture Permeability of Porous Materials" Norwegian Building Research Institute, Oslo, Norway.

APPENDIX A

Figures

TYPICAL PANEL OPENING 1220 MM X 2440 MM

TENT ENCLOSURE INTERIOR

TENT ENCLOSURE ENTRANCE

A/C UNIT

HUMIDIFER

2400 MM

PANEL OPENING

CHAMBER INTERIOR

PANEL OPENING

PANEL OPENING

REFRIGERATION COIL

UNIT HEATER

4300 MM

A

A

CHAMBER ENTRANCE

PANEL OPENING

PANEL OPENING

6700 MM

"OUTSIDE" CONDITIONS

PANEL OPENING

DATA ACQUISITION SYSTEM

"INSIDE" CONDITIONS

4900 MM
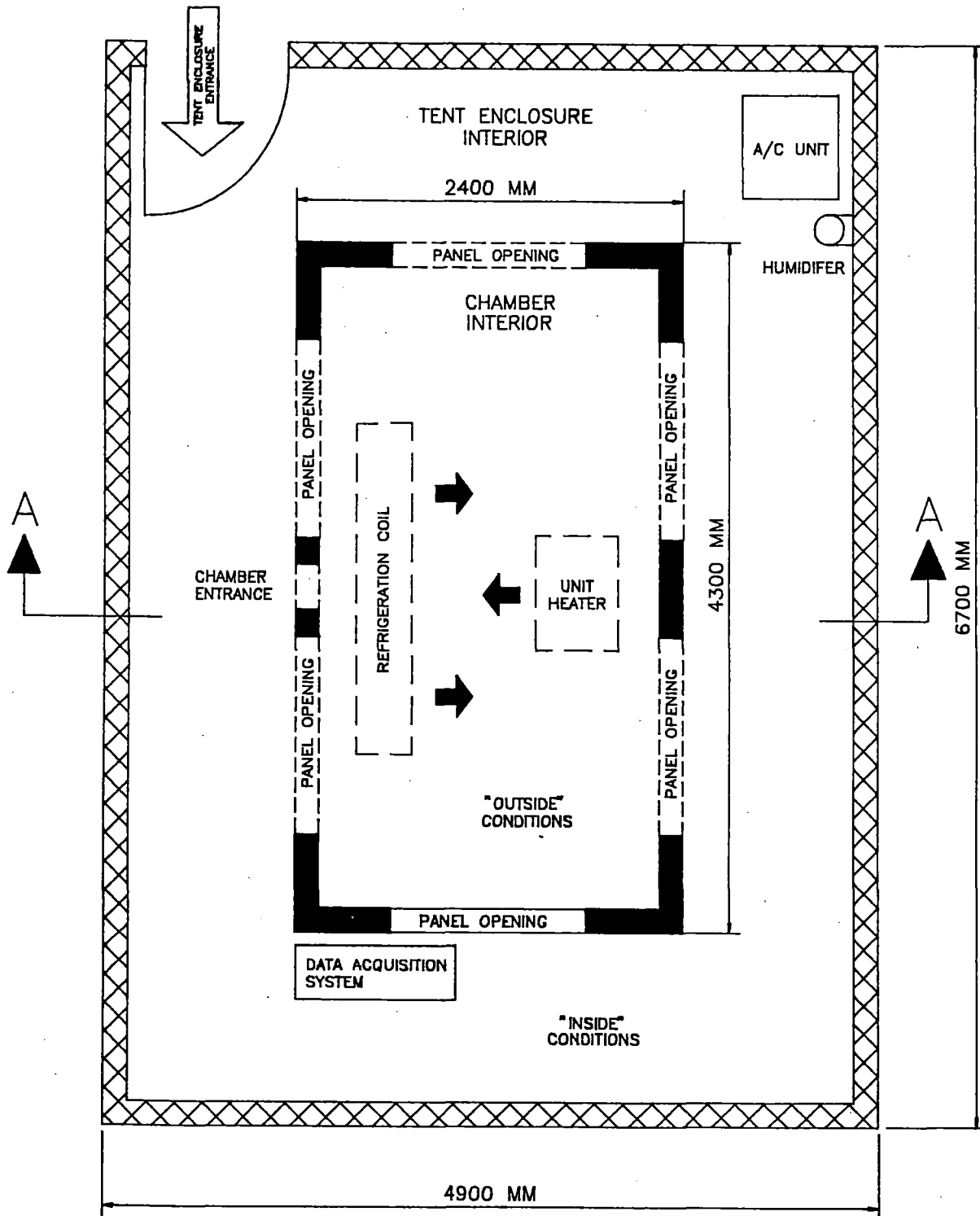
FIGURE 1

PLAN VIEW OF
WALLDRY TEST CHAMBER

REFRIGERATION
COMPRESSOR

REFRIGERATION
COIL

CHAMBER AREA
"OUTSIDE" CONDITIONS

UNIT
HEATER

1/2" PLYWOOD
FIBERGLASS BATT INSULATION
38 X 89 mm STUD WALL
1/2" PLYWOOD

TENT ENCLOSURE AREA
"INTERIOR" CONDITIONS

PANEL OPENING

38 X 89 mm WOOD STUD WALL
WITH POLY

CONCRETE FLOOR
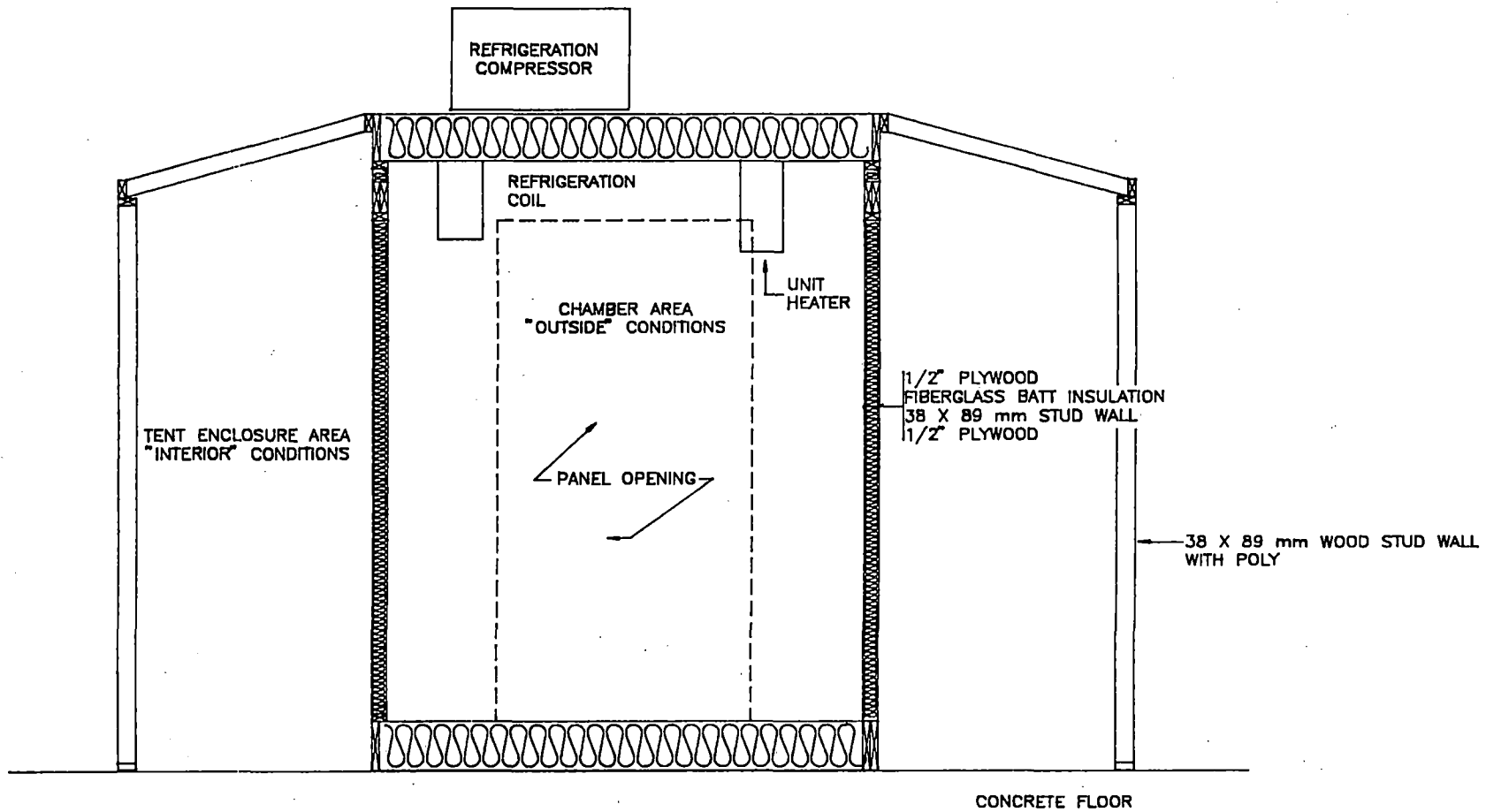
FIGURE 2

SECTION A—A
CROSS SECTION VIEW OF TEST CHAMBER

CHAMBER REFERENCE
1 TEMPERATURE
1 PRESSURE
1 RELATIVE HUMIDITY

TENT REFERENCE
2 TEMPERATURE
2 PRESSURE
1 RELATIVE HUMIDITY

TOP

300 MM TYPICAL

A B C

A — MOISTURE PIN
B — THERMOCOUPLE
C — PRESSURE TAP
D — HUMIDITY SENSOR

MIDDLE

A B C D

B B   B B

BOTTOM

A B C

300 MM TYPICAL

CHAMBER
SIDE
"OUTDOORS"

TENT
SIDE
"INDOORS"
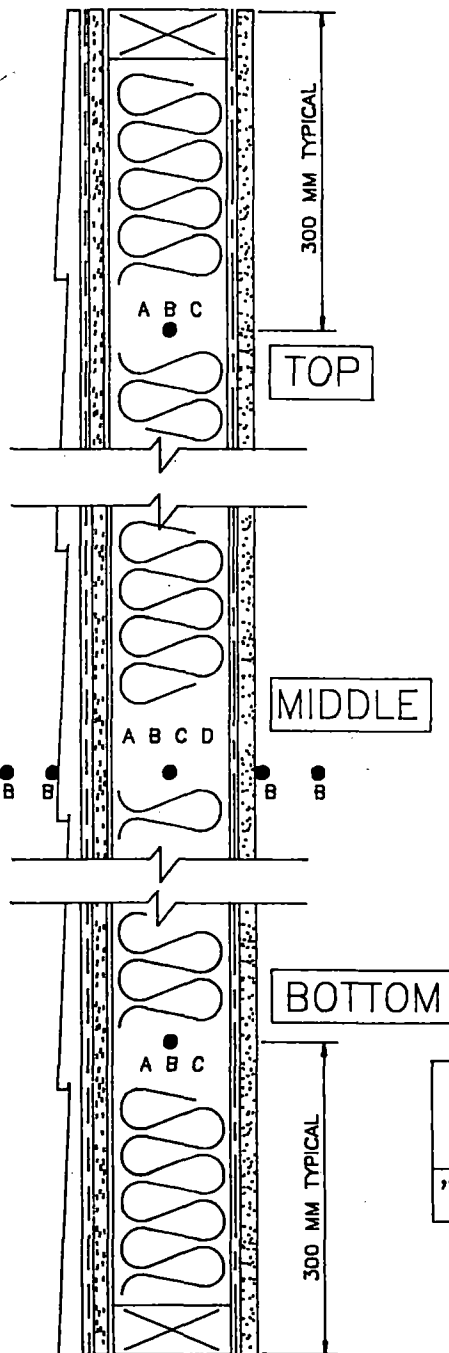
FIGURE 3A

LOCATION OF INSTRUMENTATION
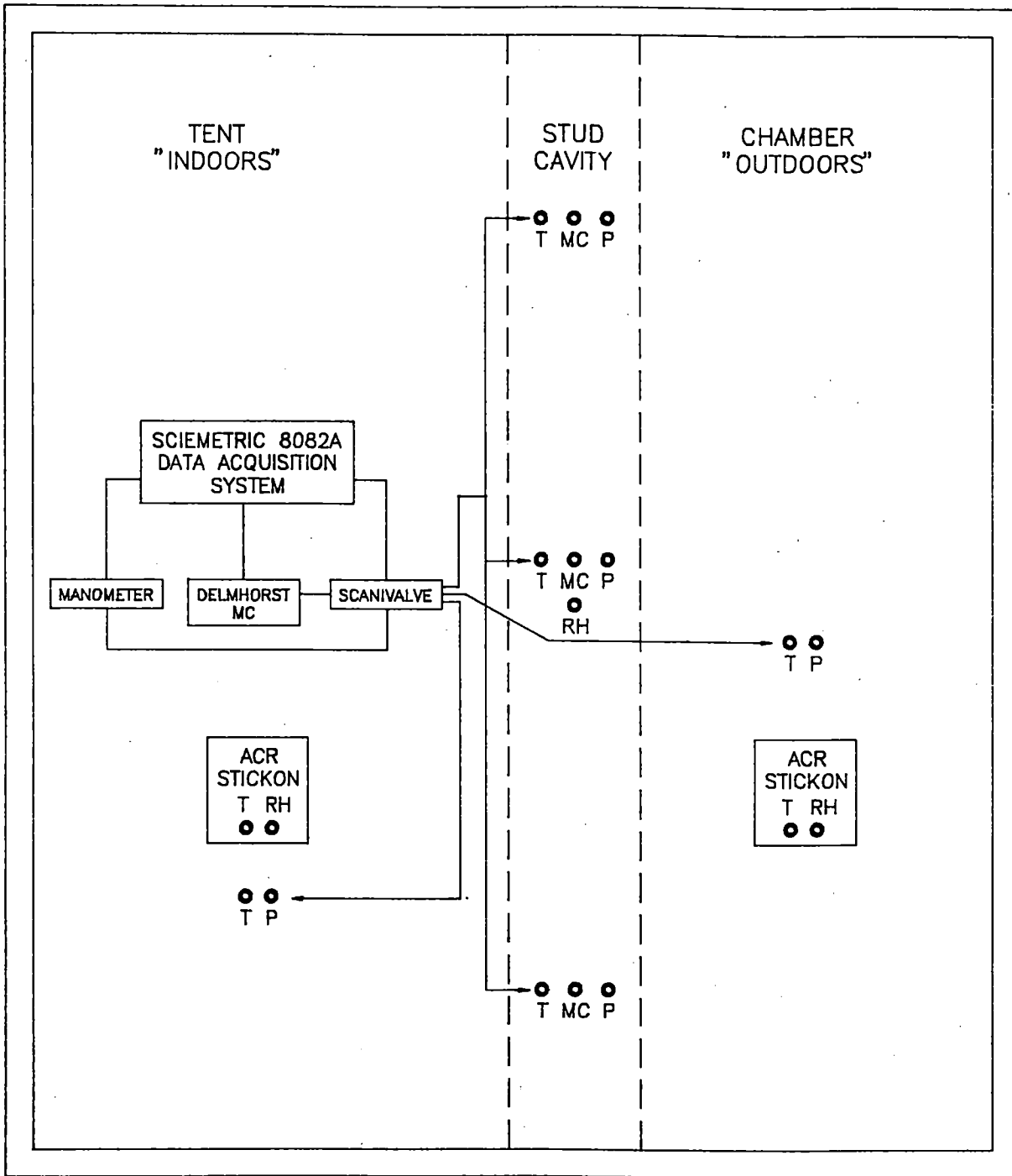
FIGURE 3B

SCHEMATIC OF INSTRUMENTATION

3mm (1/8")
DIA. HOLE
TYP.

5mm (3/16")
DIA. HOLE
TYP.

300mm
TYP.

300mm

300mm

200mm   400mm   400mm
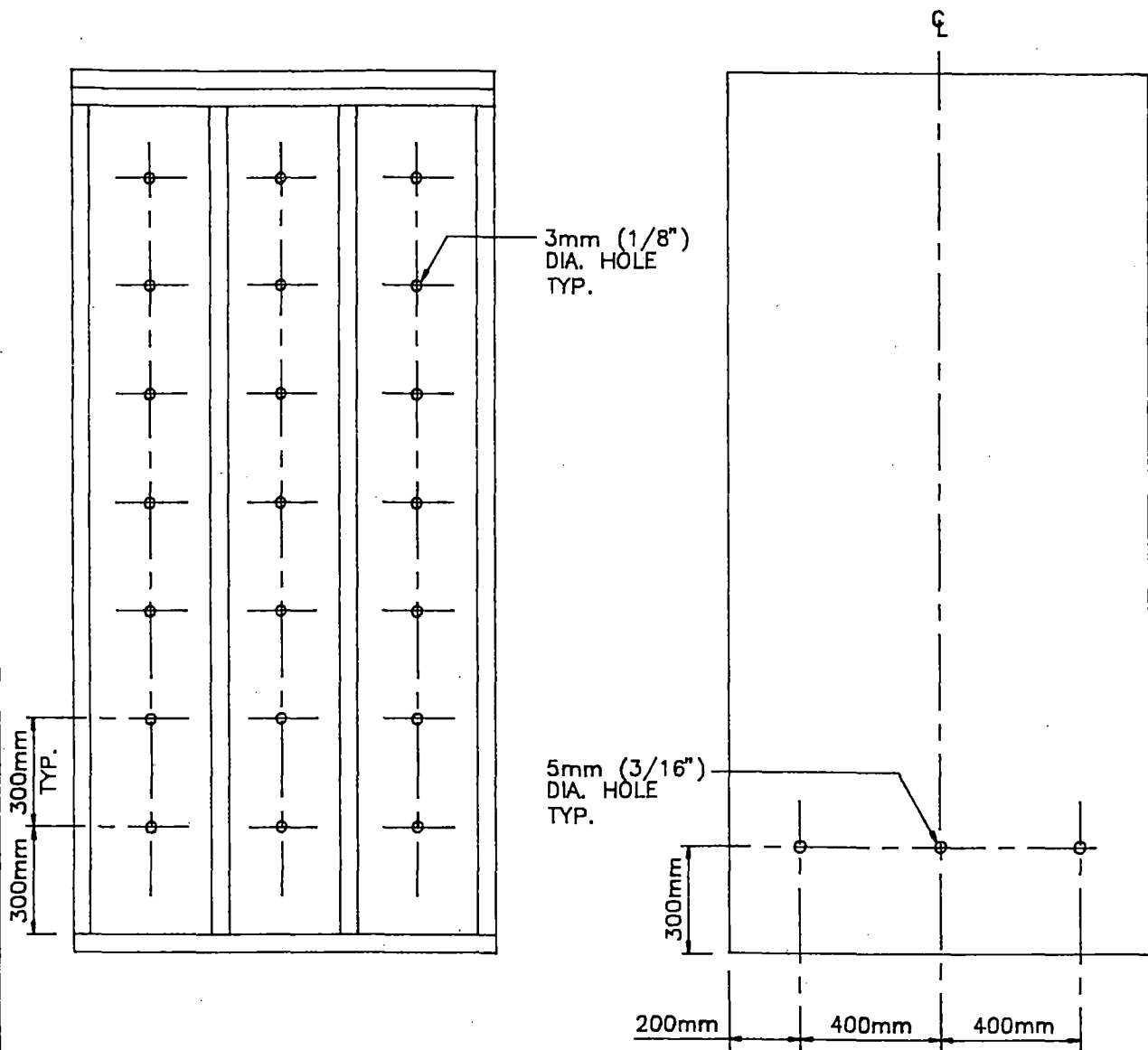
EXTERIOR
SHEATHING

INTERIOR
DRYWALL

FIGURE 4

LOCATION OF HOLES
DRILLED IN VENTED
PANELS "B","D" AND "F"
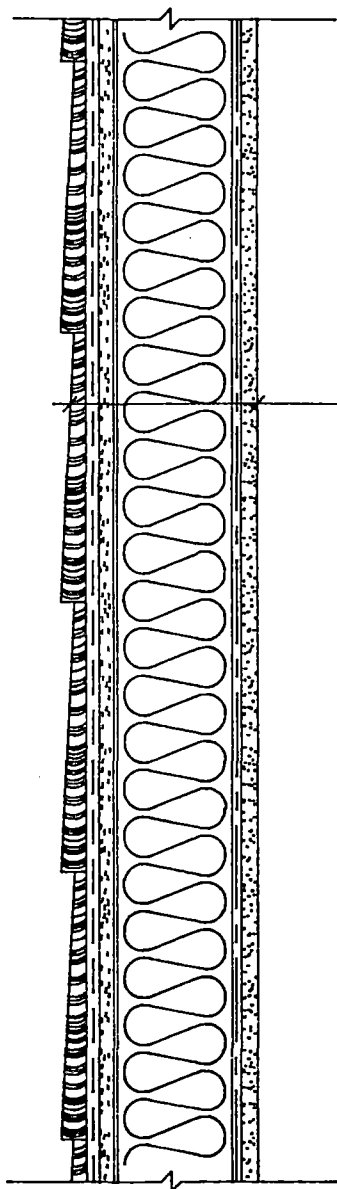
12.7 mm DRYWALL
6 MIL POLY. VAPOUR BARRIER
38 X 89 WOOD STUD @ 400 mm O/C
FIBERGLASS BATT INSULATION RSI 2.1
11 mm WOOD SHEATHING
ASPHALT IMPREGNATED BUILDING PAPER (PERFORATED)
WOOD SIDING

FIGURE 5

CROSS SECTION OF
TEST PANELS "A" AND "B"
WOOD SIDING
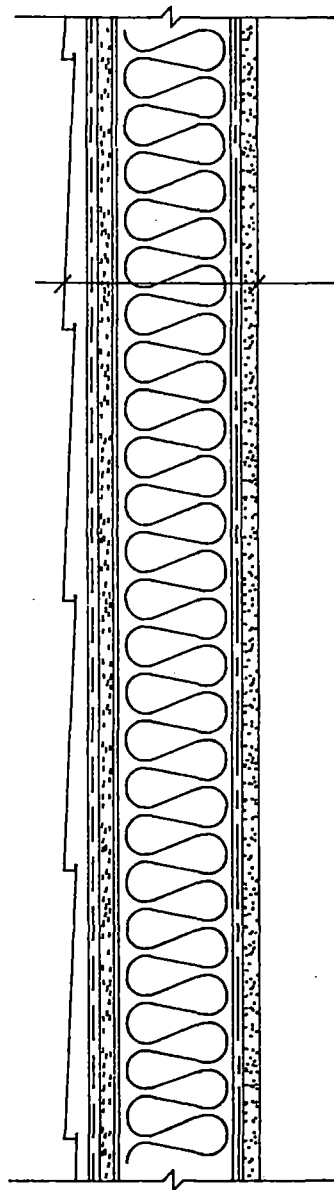
12.7 mm DRYWALL
6 MIL POLY. VAPOUR BARRIER
38 X 89 WOOD STUD @ 400 mm O/C
FIBERGLASS BATT INSULATION RSI 2.1
11 mm WOOD SHEATHING
ASPHALT IMPREGNATED BUILDING PAPER (PERFORATED)
"DOUBLE FOUR" VINYL SIDING

FIGURE 6

CROSS SECTION OF
TEST PANELS "C" AND "D"
VINYL ON SHEATHING
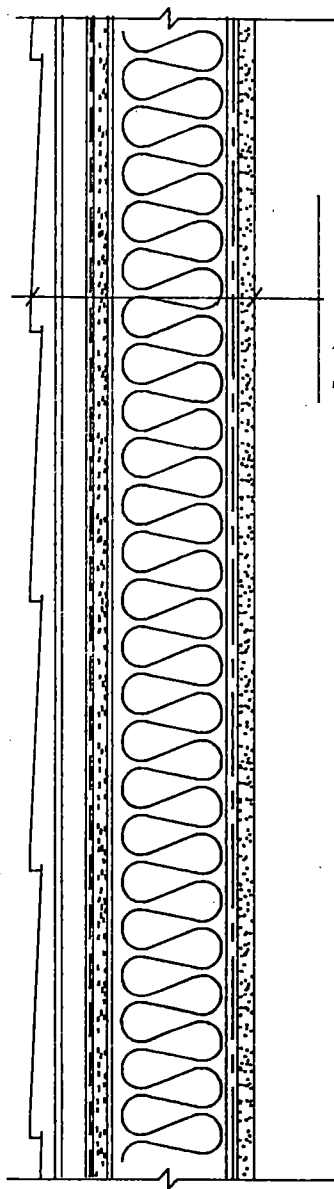
12.7 mm DRYWALL
6 MIL POLY. VAPOUR BARRIER
38 X 89 WOOD STUD @ 400 mm O/C
FIBERGLASS BATT INSULATION RSI 2.1
11 mm WOOD SHEATHING
ASPHALT IMPREGNATED BUILDING PAPER (PERFORATED)
19 X 89 WOOD FURRING
"DOUBLE FOUR" VINYL SIDING

FIGURE 7

CROSS SECTION OF
TEST PANELS "E" AND "F"
VINYL SIDING WITH WOOD FURRING

APPENDIX B
Photos

Photo 1
View of test chamber and tent under construction.
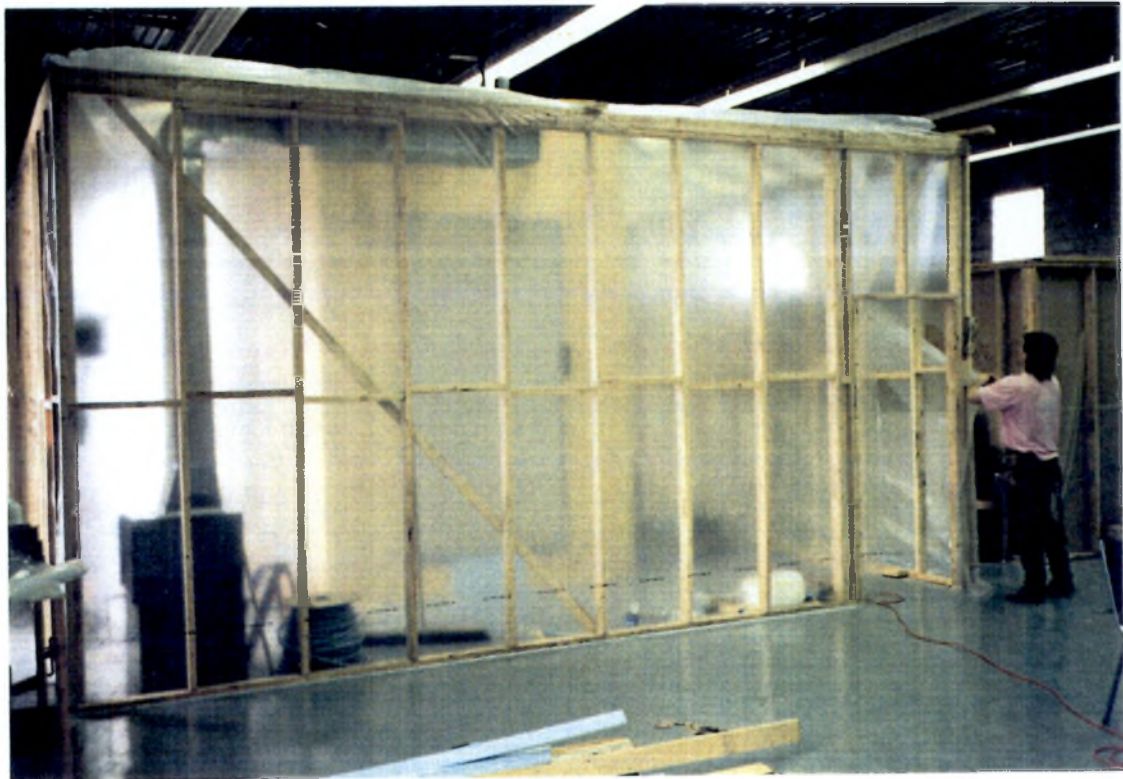
Photo 2
Polyethylene tent enclosure.

Photo 3
View of refrigeration coil with fan baffles in chamber

Photo 4
Construction of test panels.

Photo 5
Weighing of text panel components with weigh scale cart.

Photo 6
Close-up of instrumented test stud (centre)
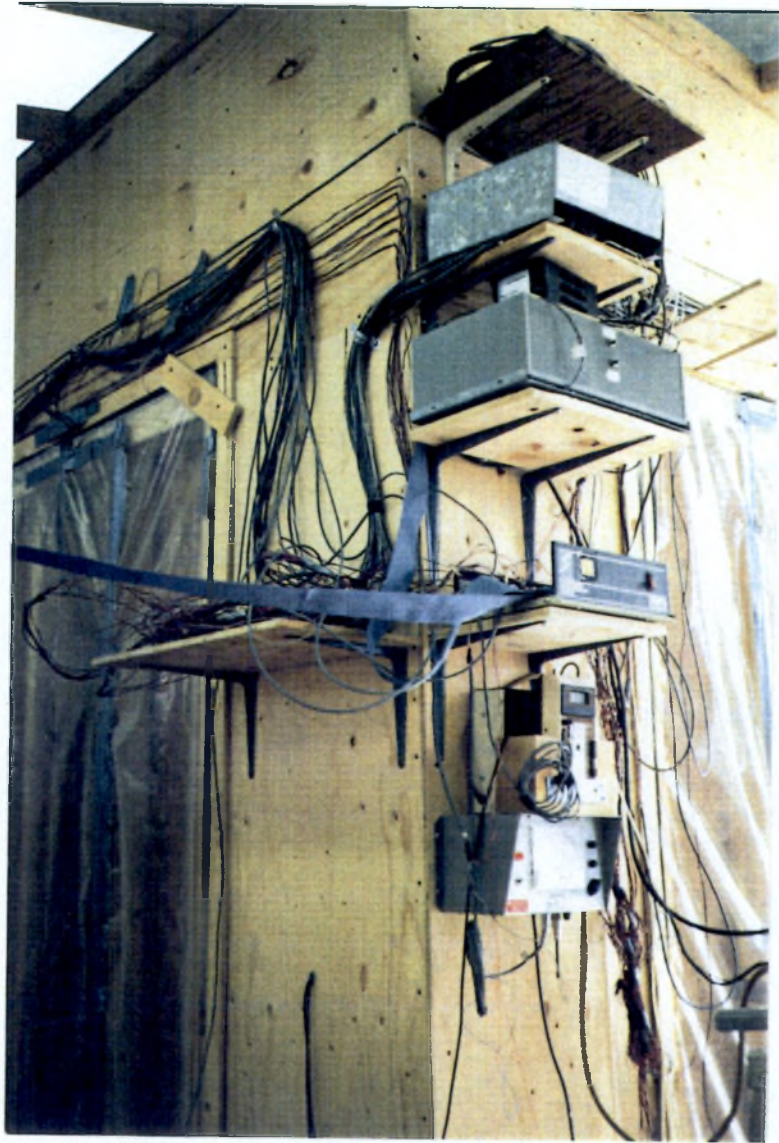
Photo 7
Data acquisition system mounted on chamber side.

Photo 8
Panel removed for dismantling.

Photo 9
Wood rot at bottom of test panel F (typical of all panels).

APPENDIX C
Temperature and Temperature Index Graphs

Temperature
WINTER
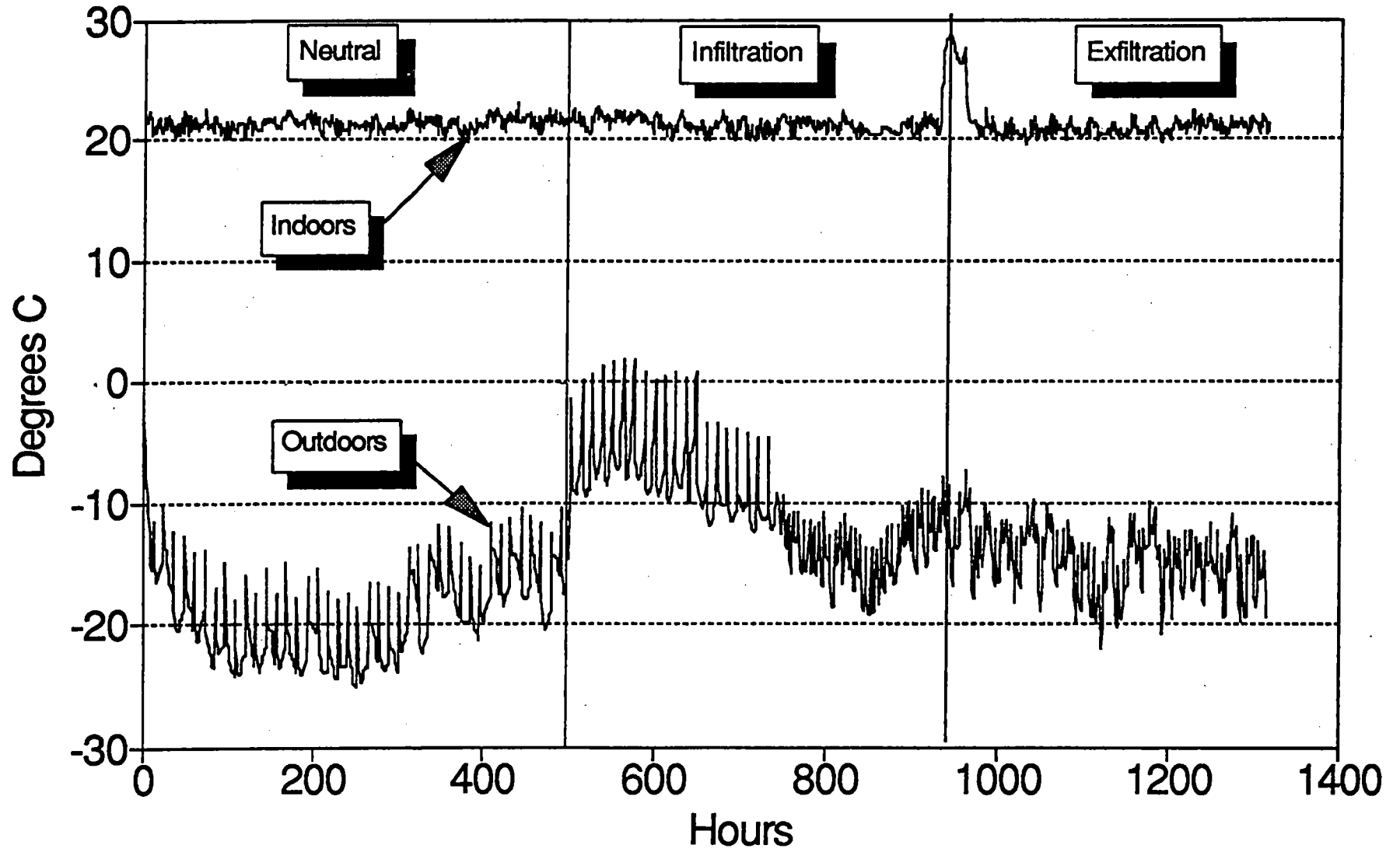
Cavity Temperatures
WINTER: Panel A, (Sealed/Wood Siding)
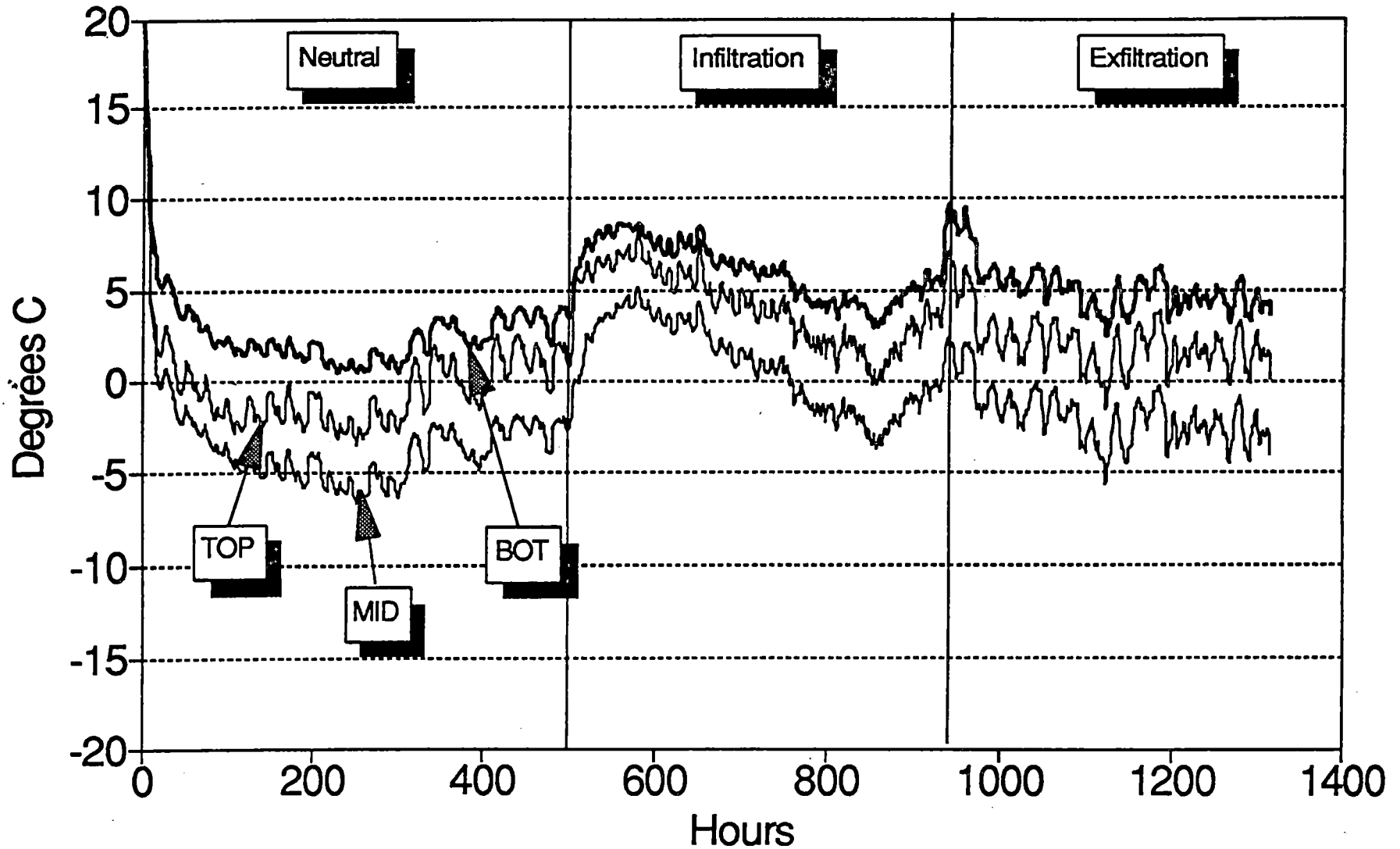
Cavity Temperatures
WINTER: Panel B, (Vented/Wood Siding)
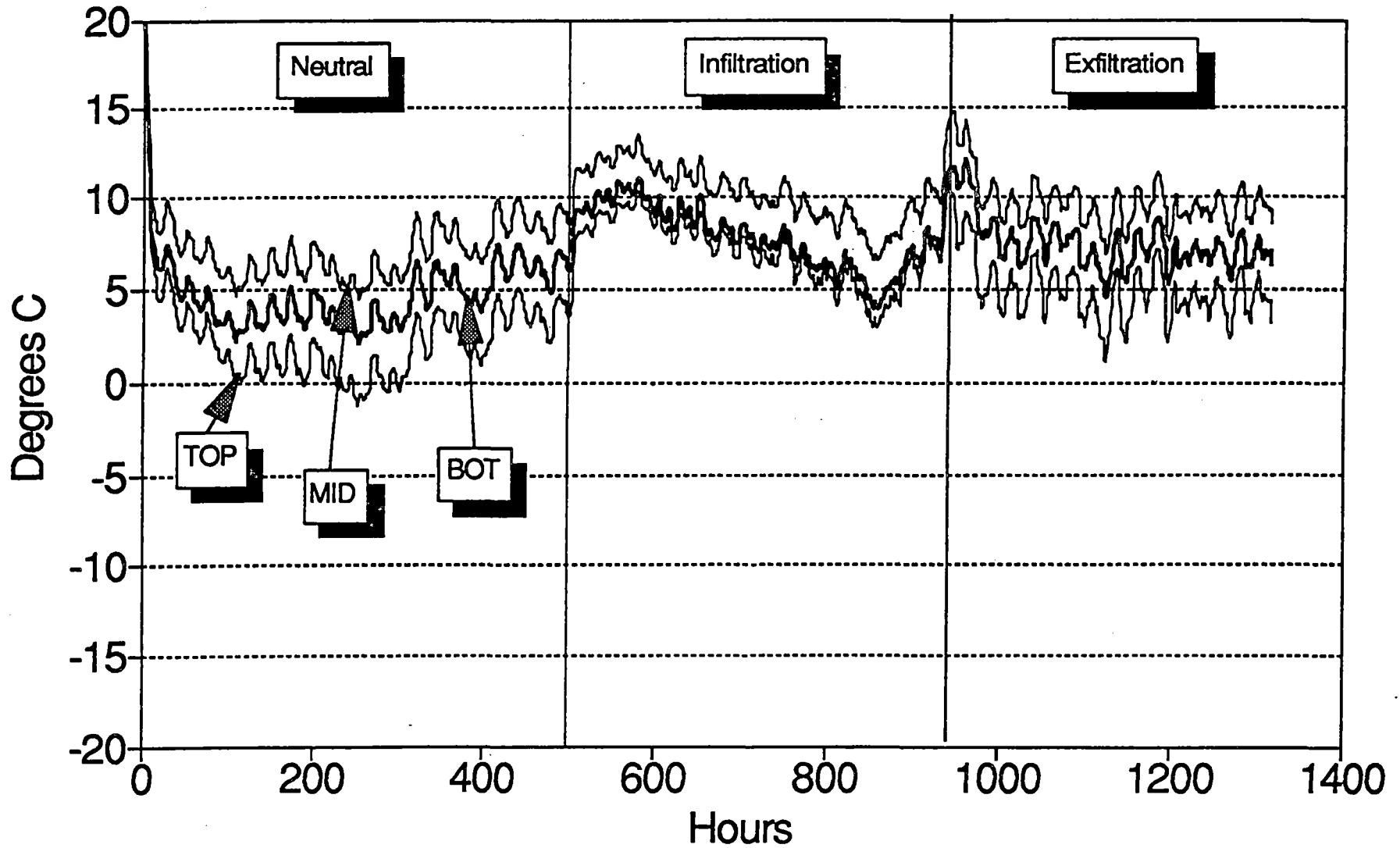
Cavity Temperatures
WINTER: Panel C, (Sealed/Vinyl Siding)
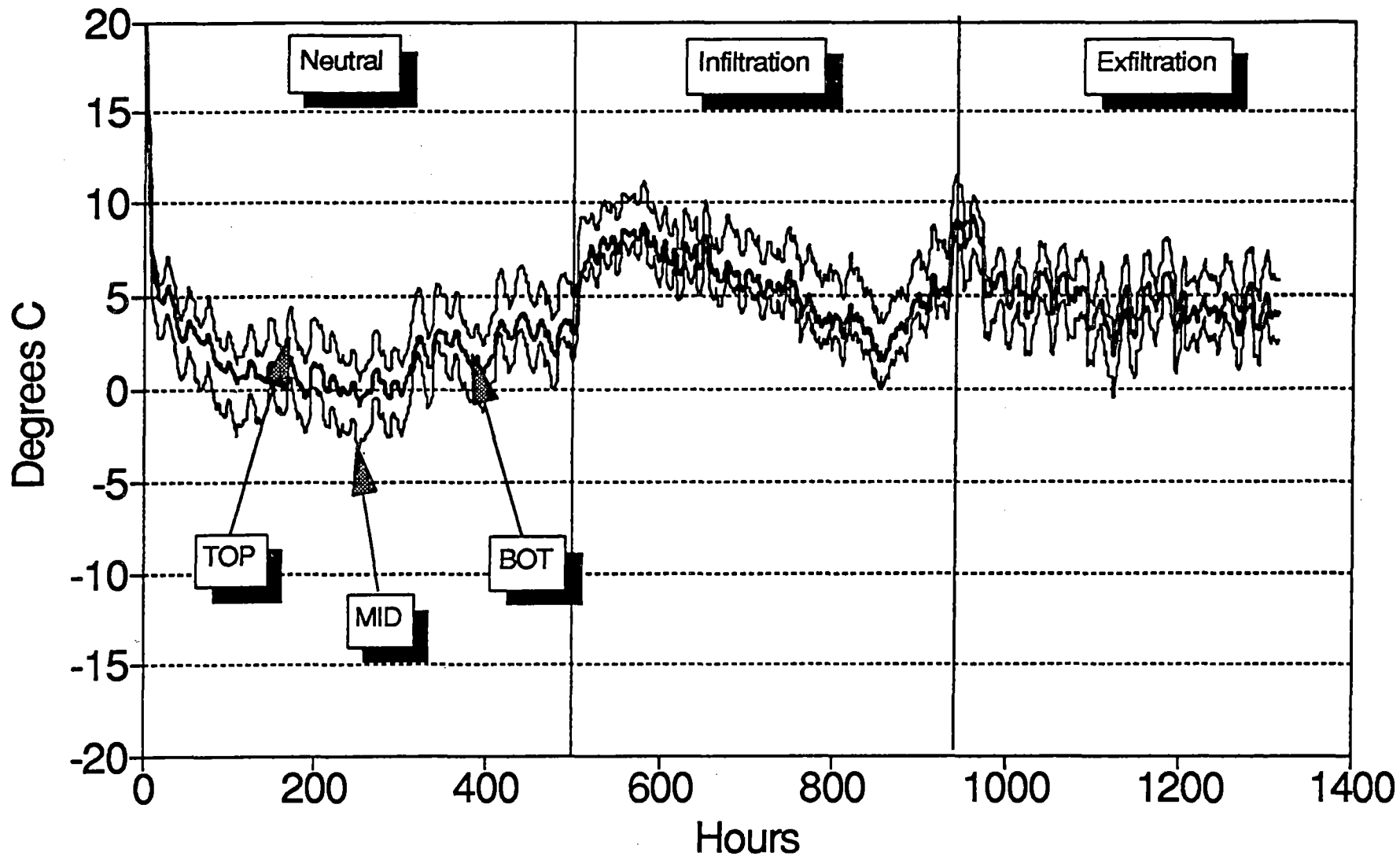
Cavity Temperatures
WINTER: Panel D, (Vented/Vinyl Siding)
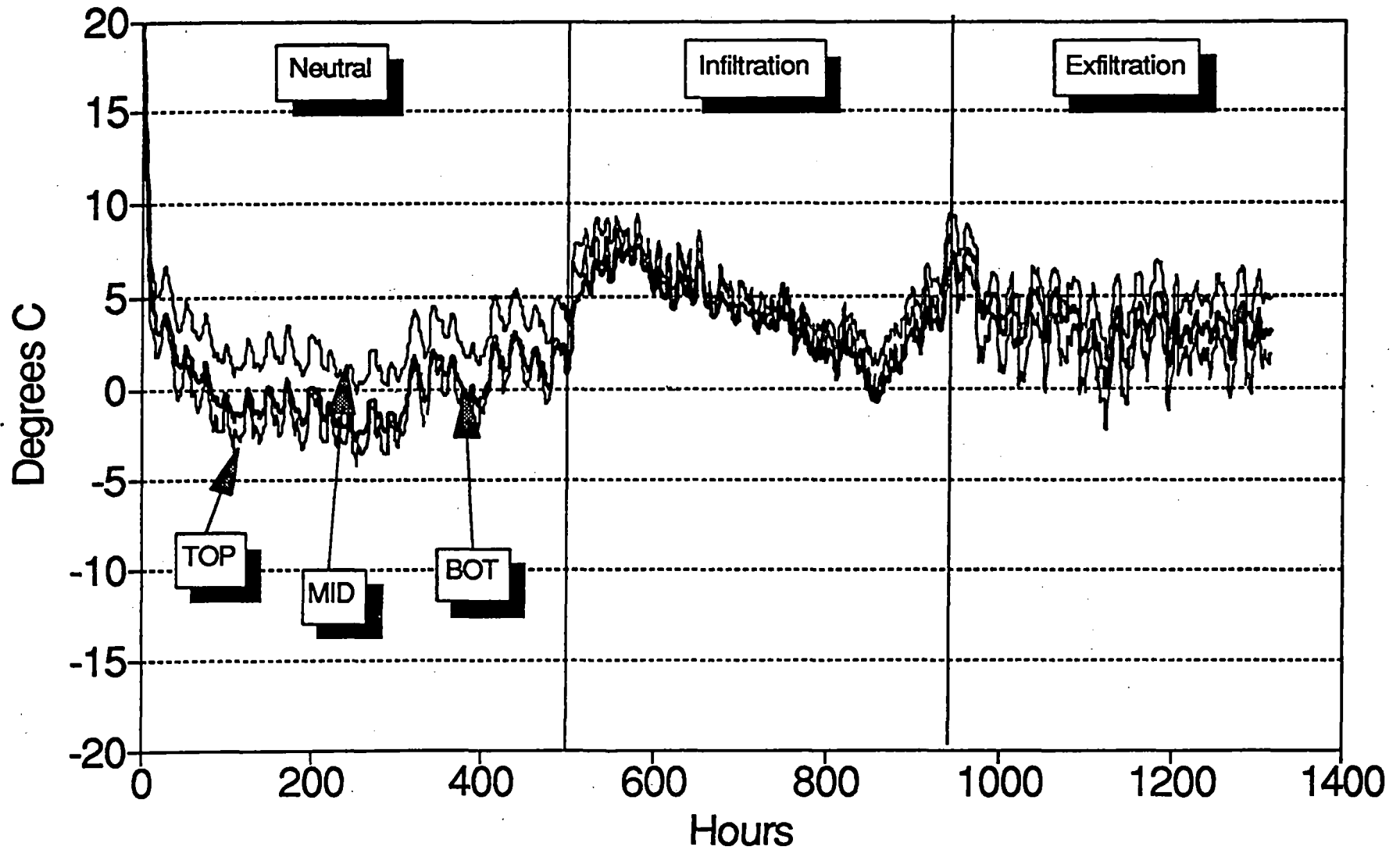
Cavity Temperatures
WINTER: Panel E, (Sealed/Vinyl/Strap)
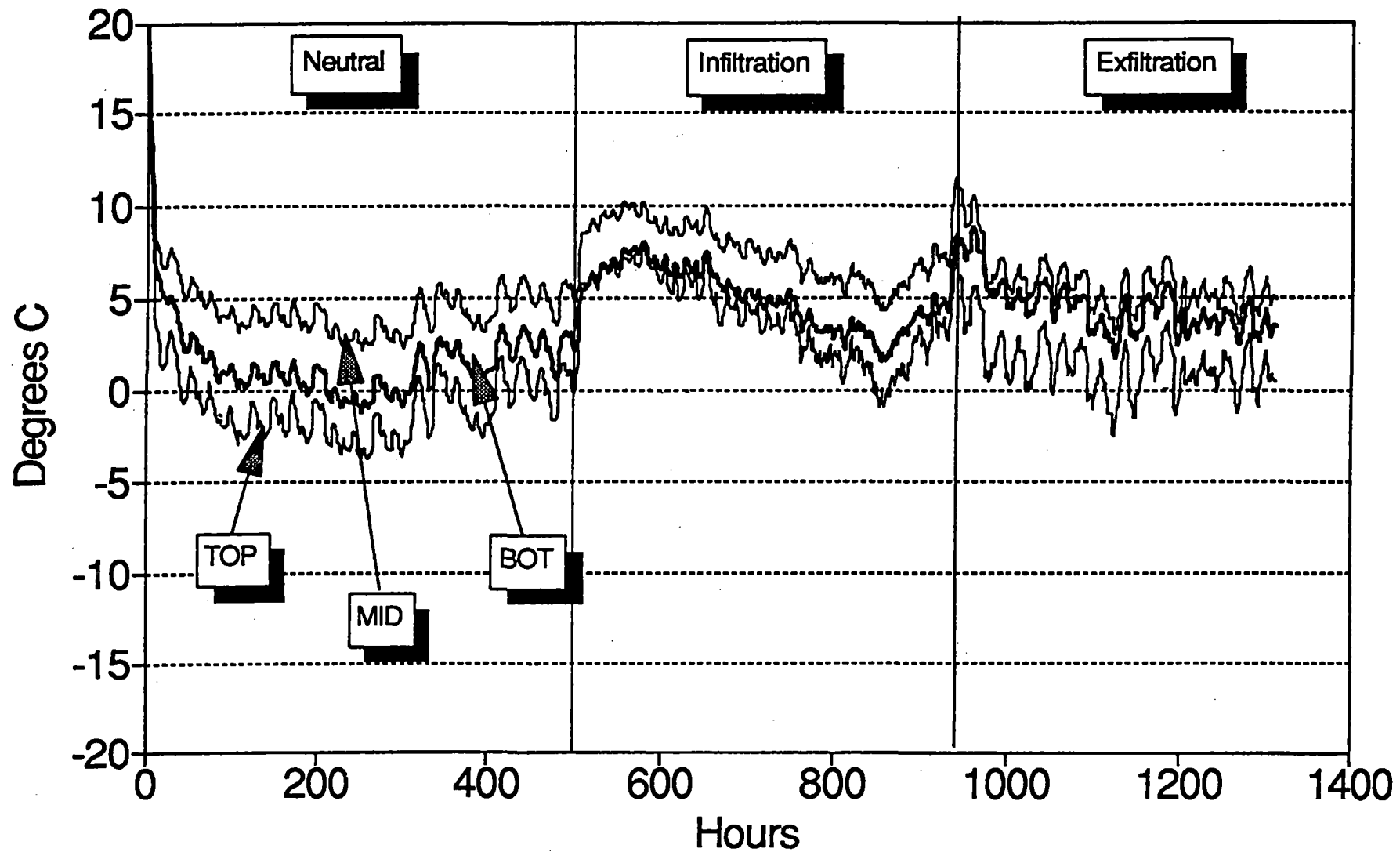
Cavity Temperatures
WINTER: Panel F, (Vented/Vinyl/Strap)

Temperature
SUMMER

Neutral | Infiltration | Exfiltration

Degrees C

Outdoors

Indoors

Hours
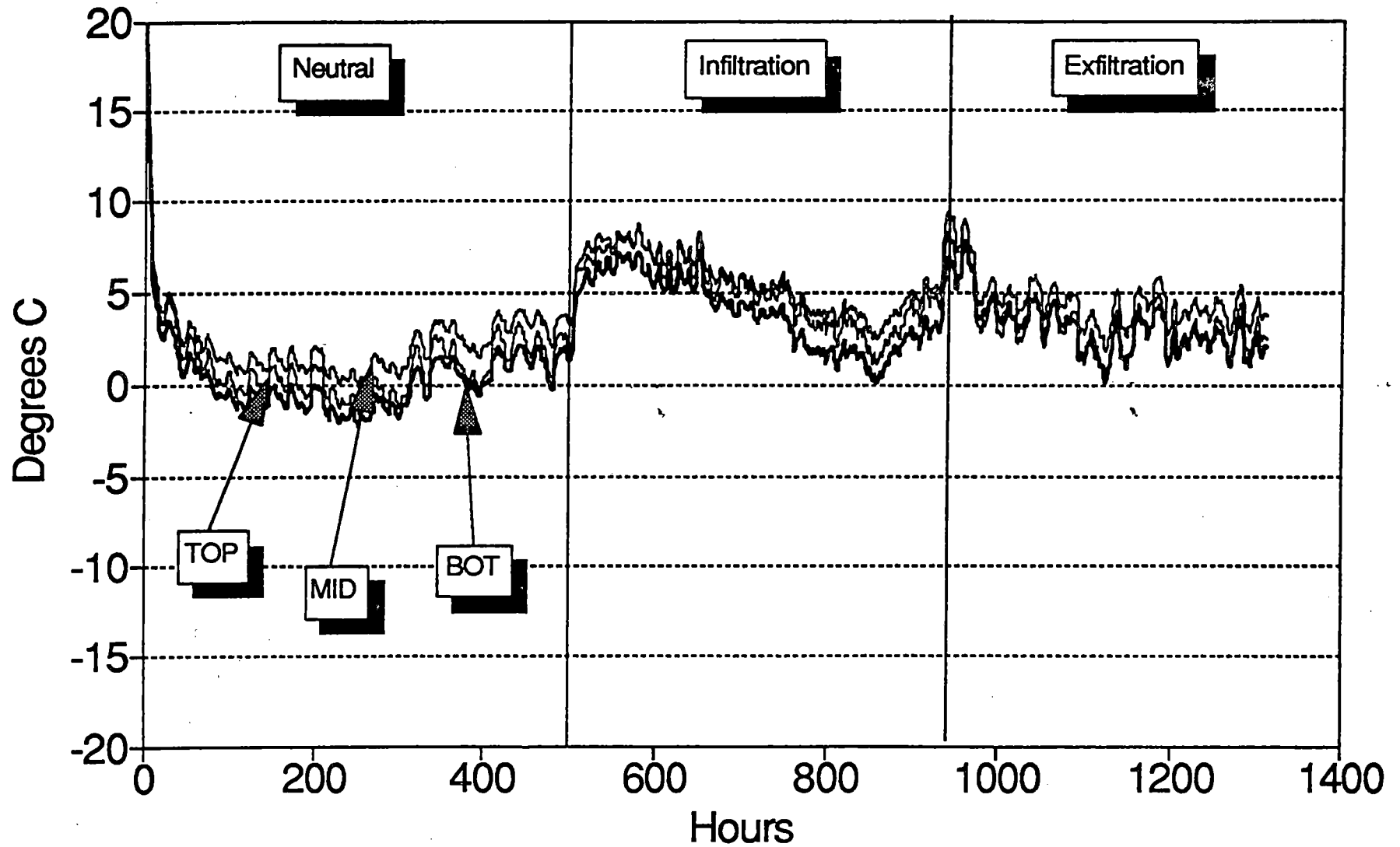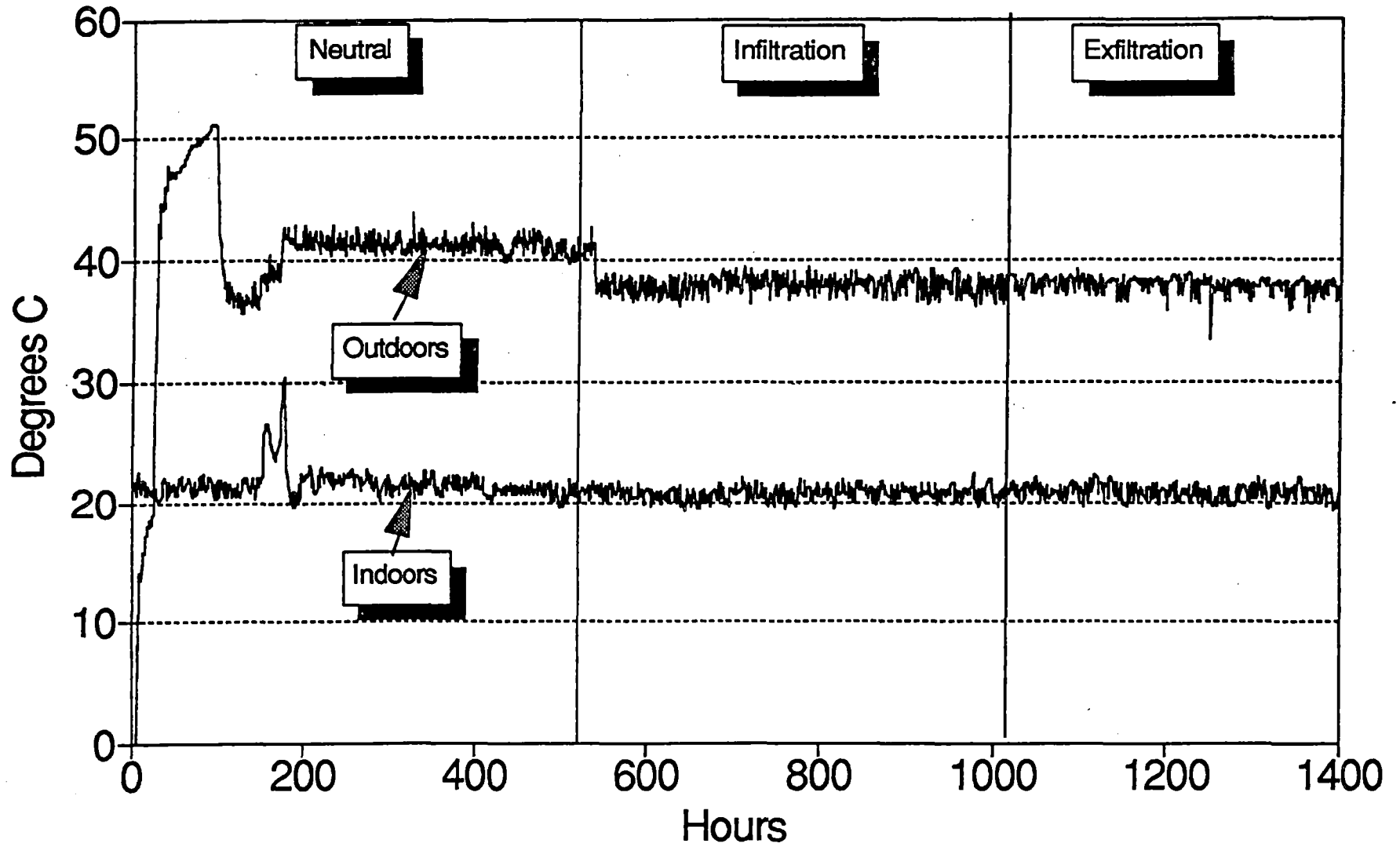
Cavity Temperatures
SUMMER: Panel A, (Sealed/Wood Siding)
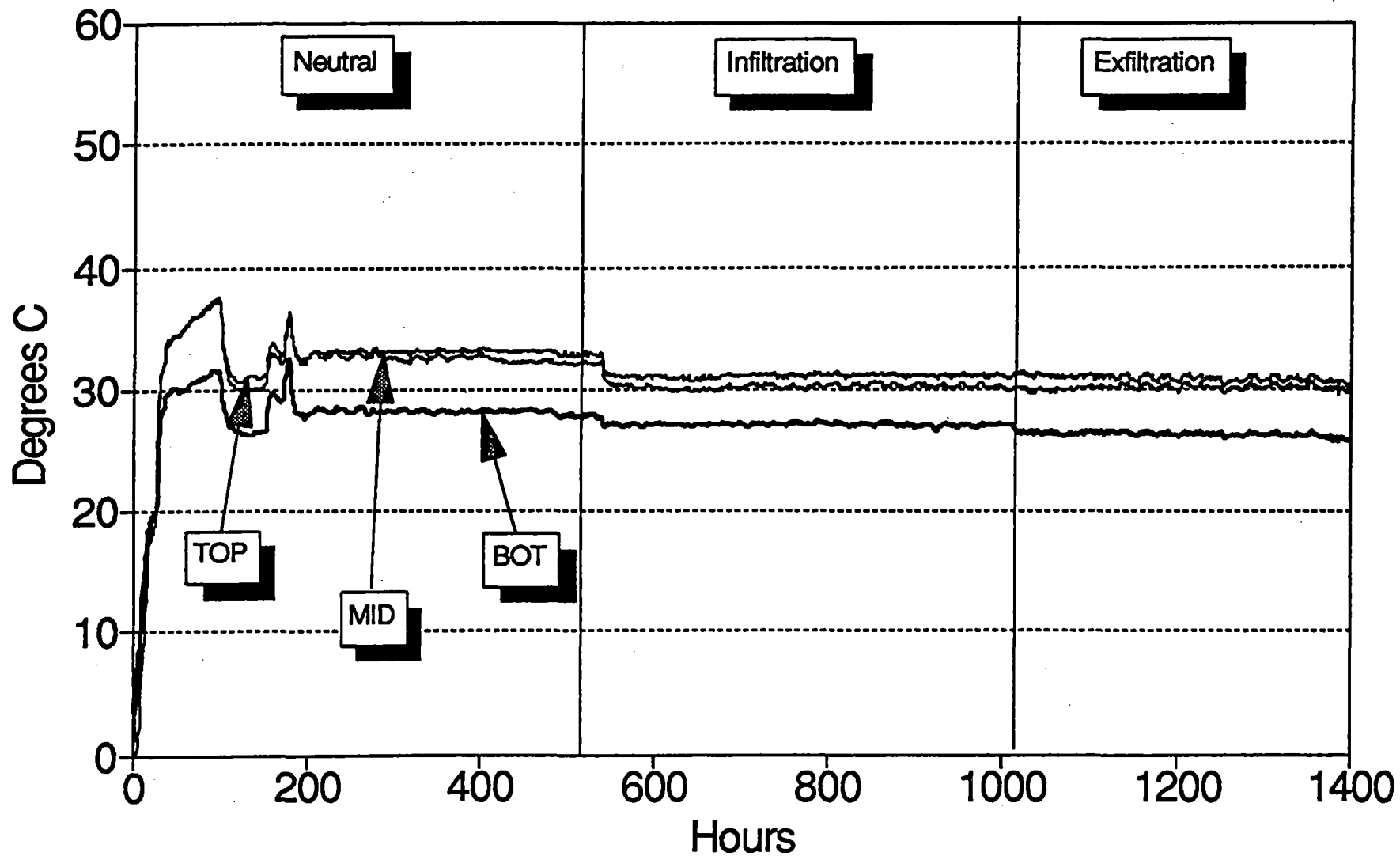
Cavity Temperatures
SUMMER: Panel B, (Vented/Wood Siding)
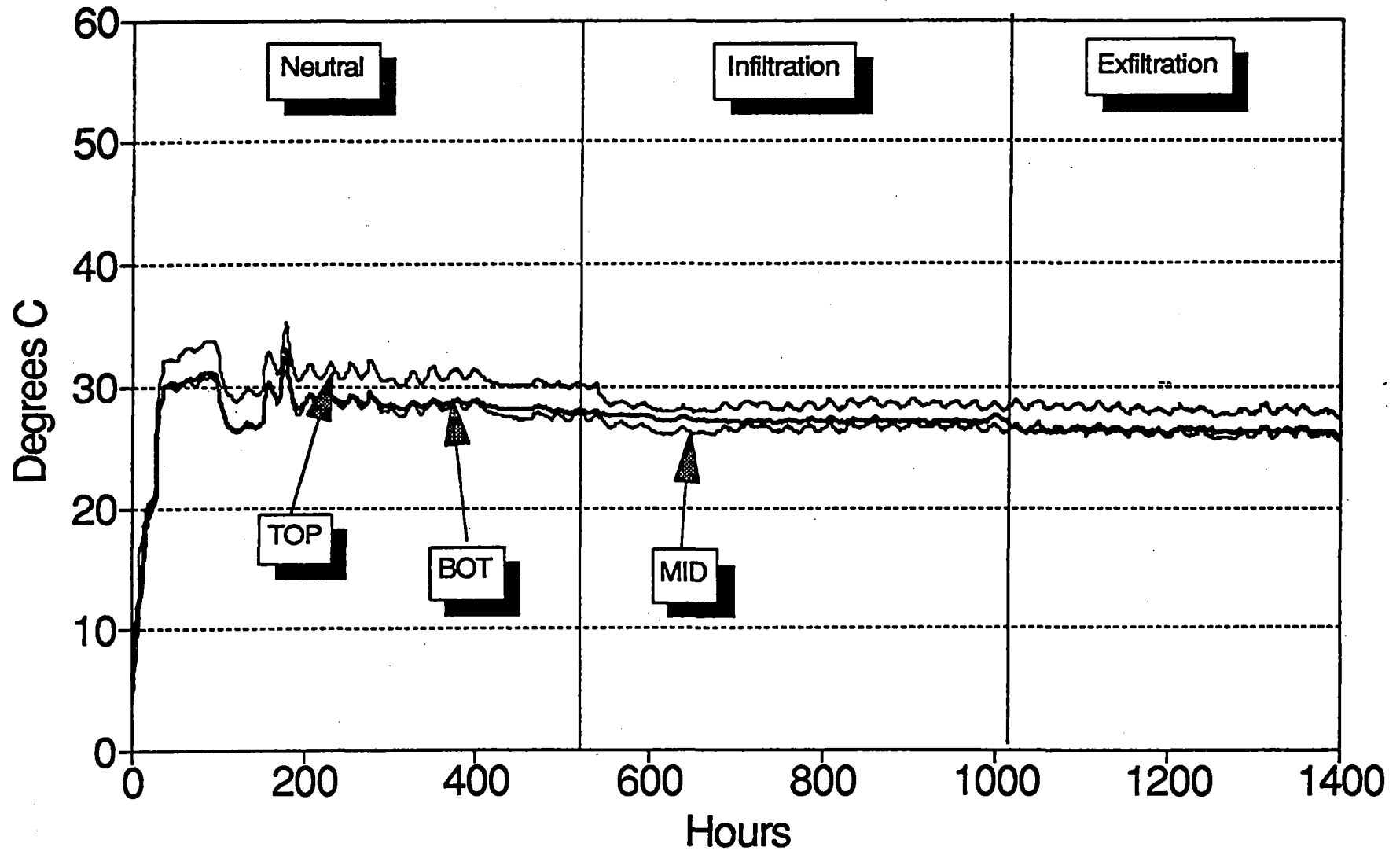
Cavity Temperatures
SUMMER: Panel C, (Sealed/Vinyl Siding)
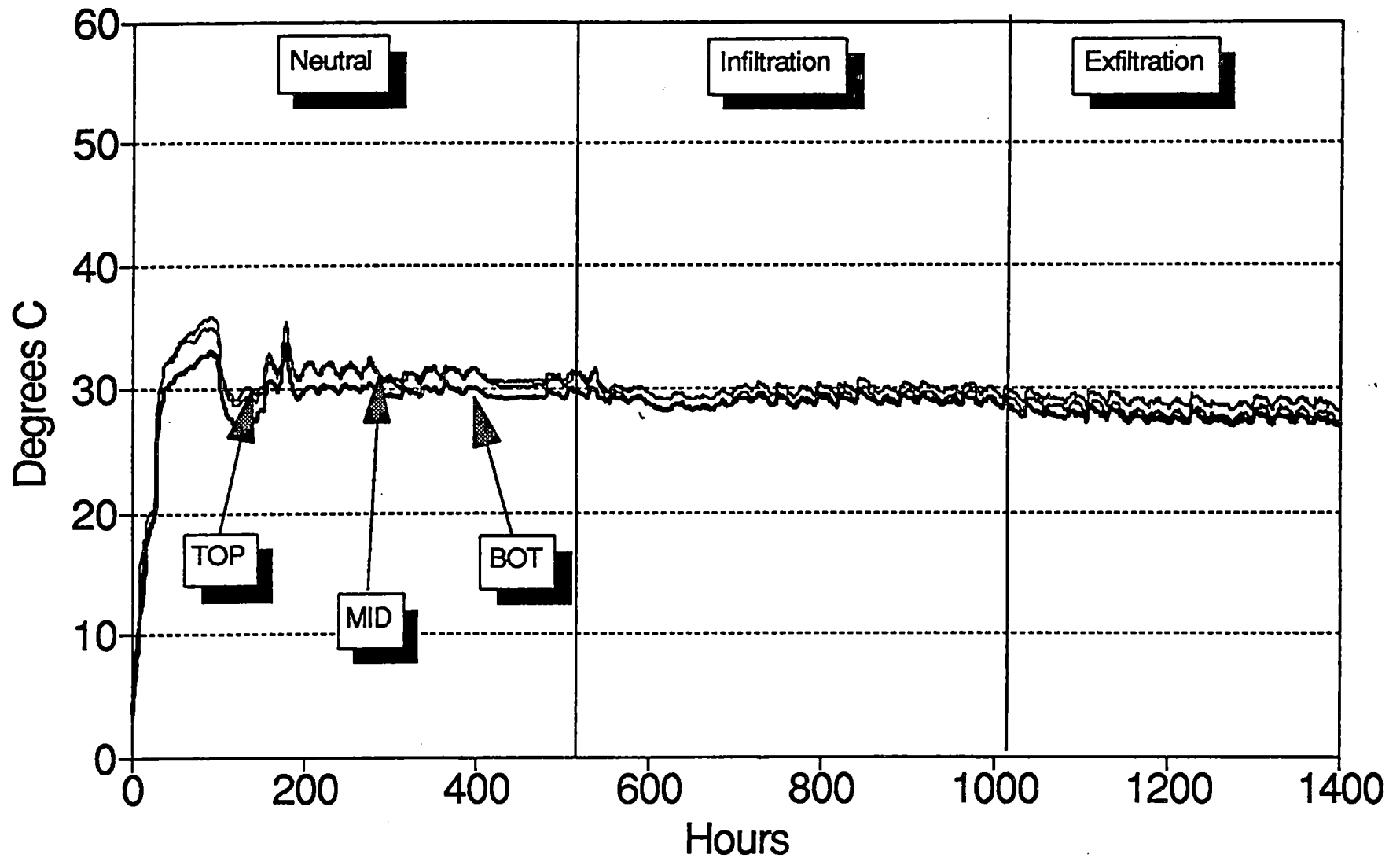
Cavity Temperatures
SUMMER: Panel D, (Vented/Vinyl Siding)
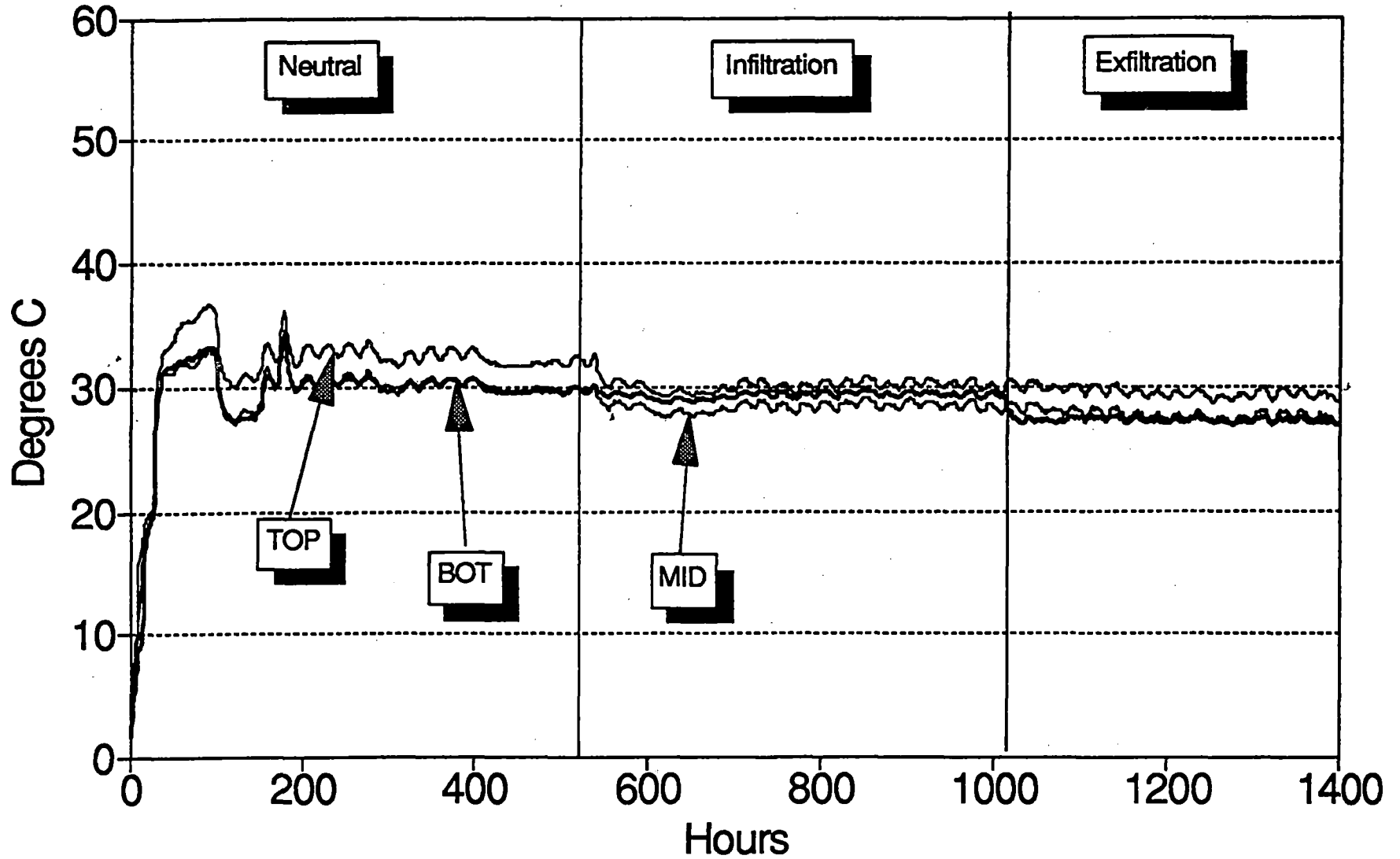
Cavity Temperatures
SUMMER: Panel E, (Sealed/Vinyl/Strap)
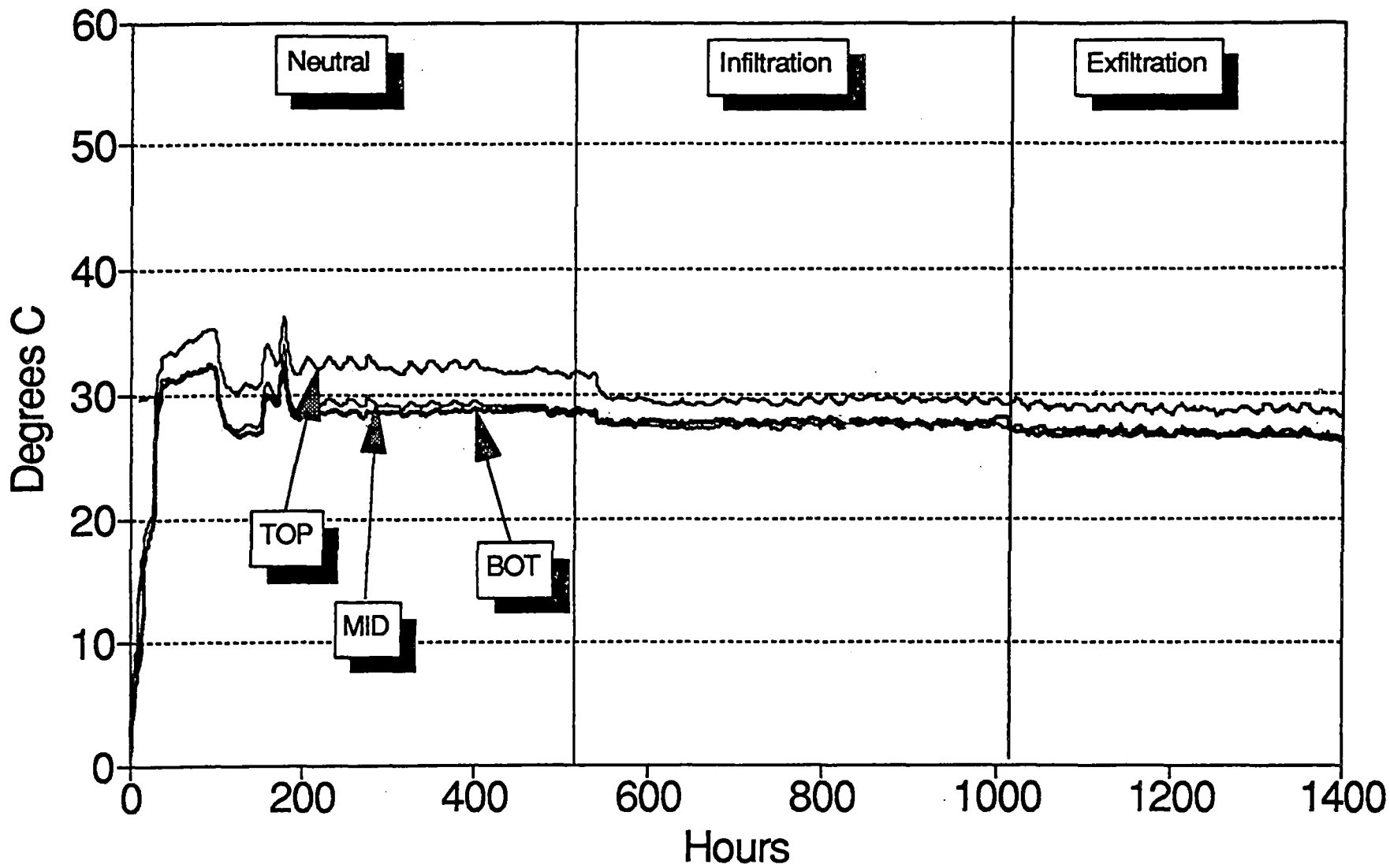
Cavity Temperatures
SUMMER: Panel F, (Vented/Vinyl/Strap)
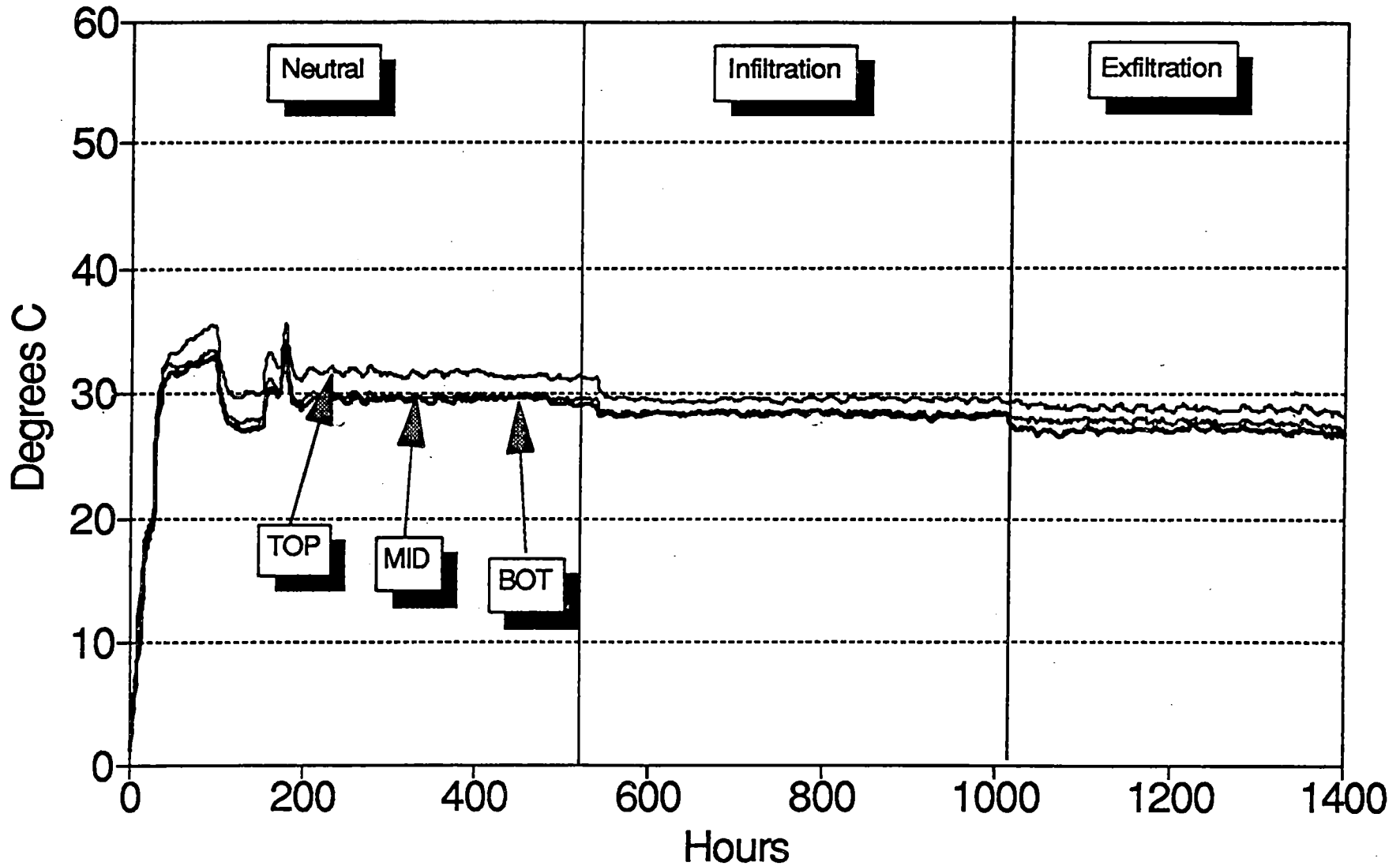
Temperature Index
WINTER: Panel A, (Sealed/Wood Siding)
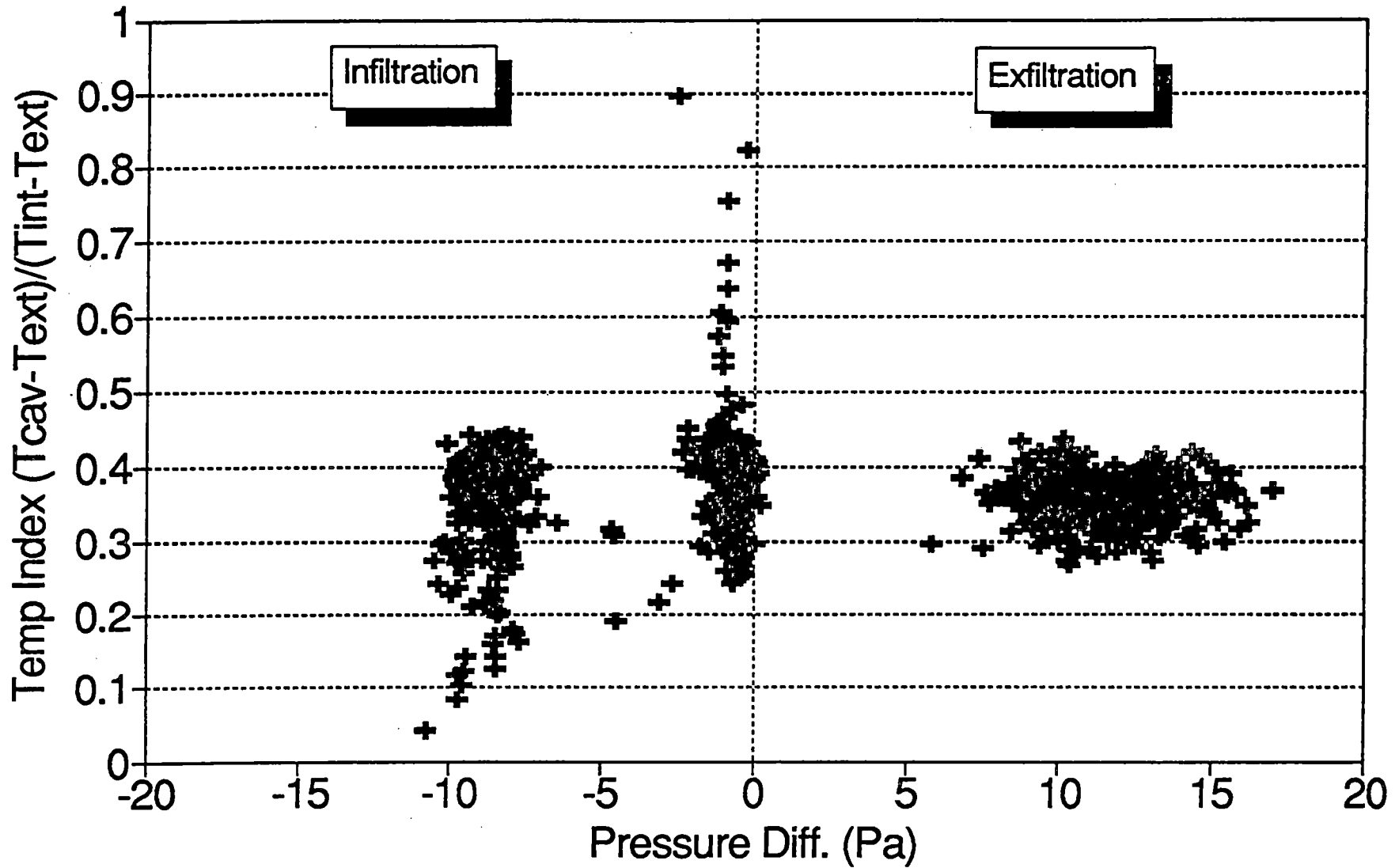
Temperature Index
WINTER: Panel B, (Vented/Wood Siding)
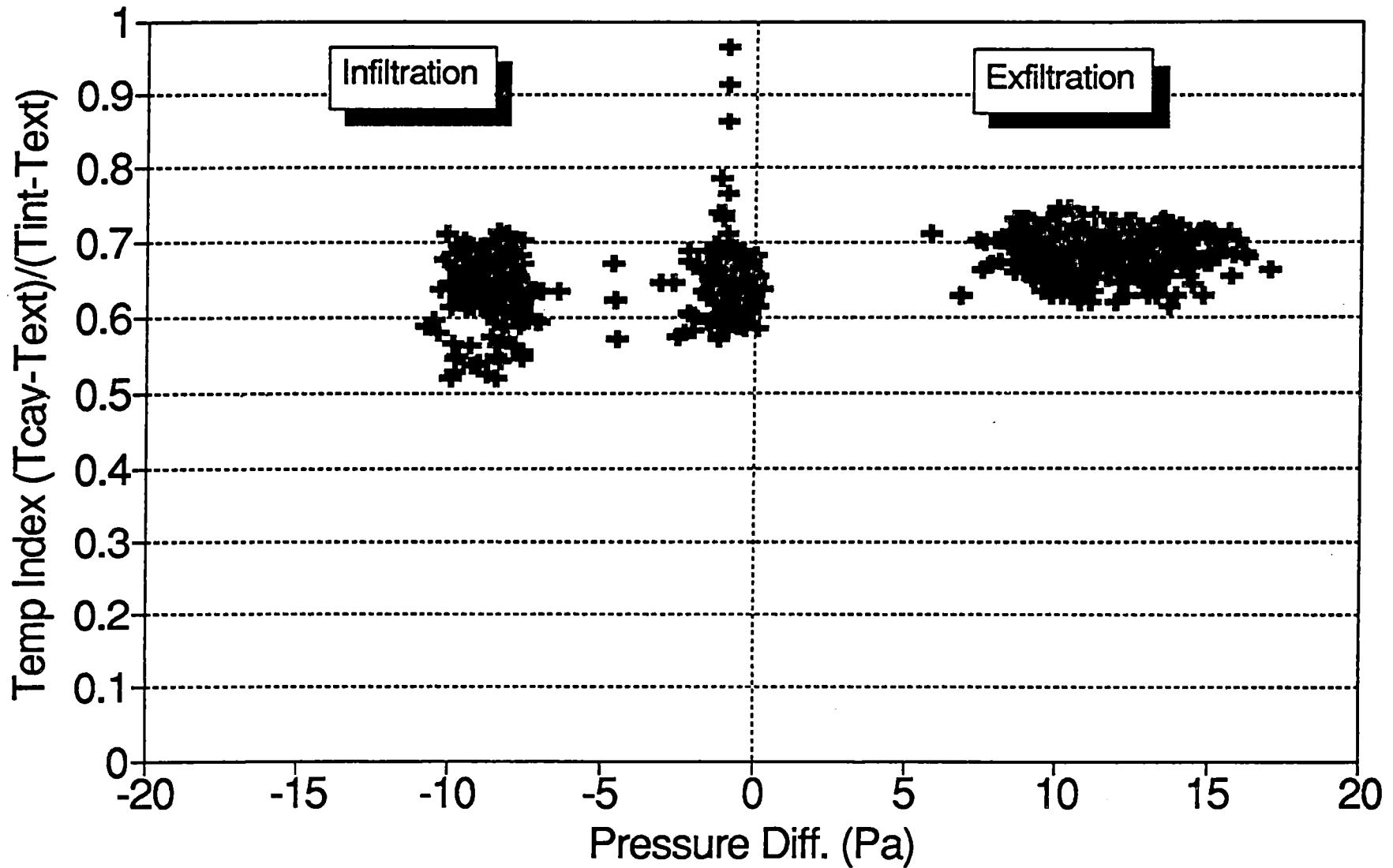
Temperature Index
WINTER: Panel C, (Sealed/Vinyl Siding)
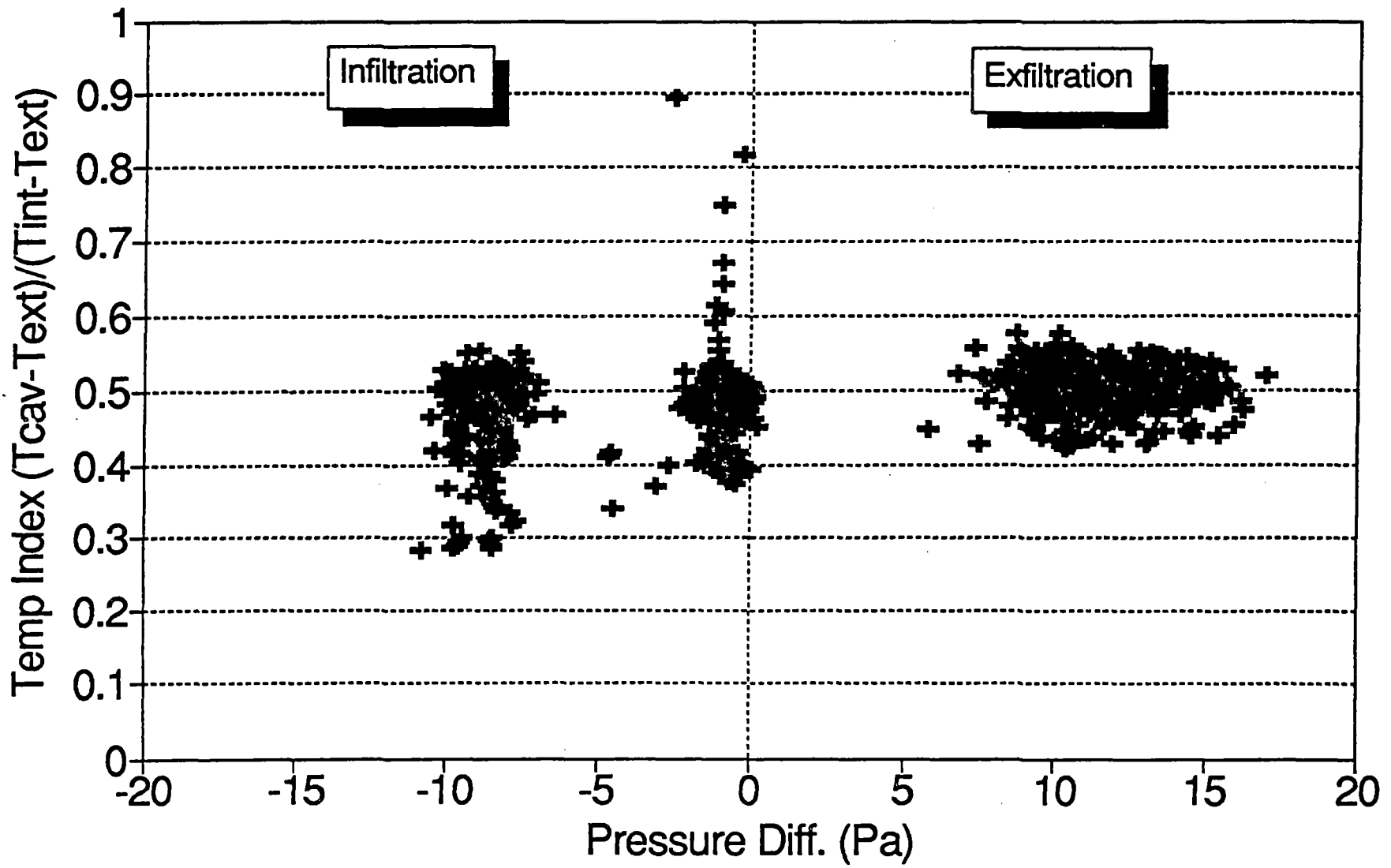
Temperature Index
WINTER: Panel D, (Vented/Vinyl Siding)
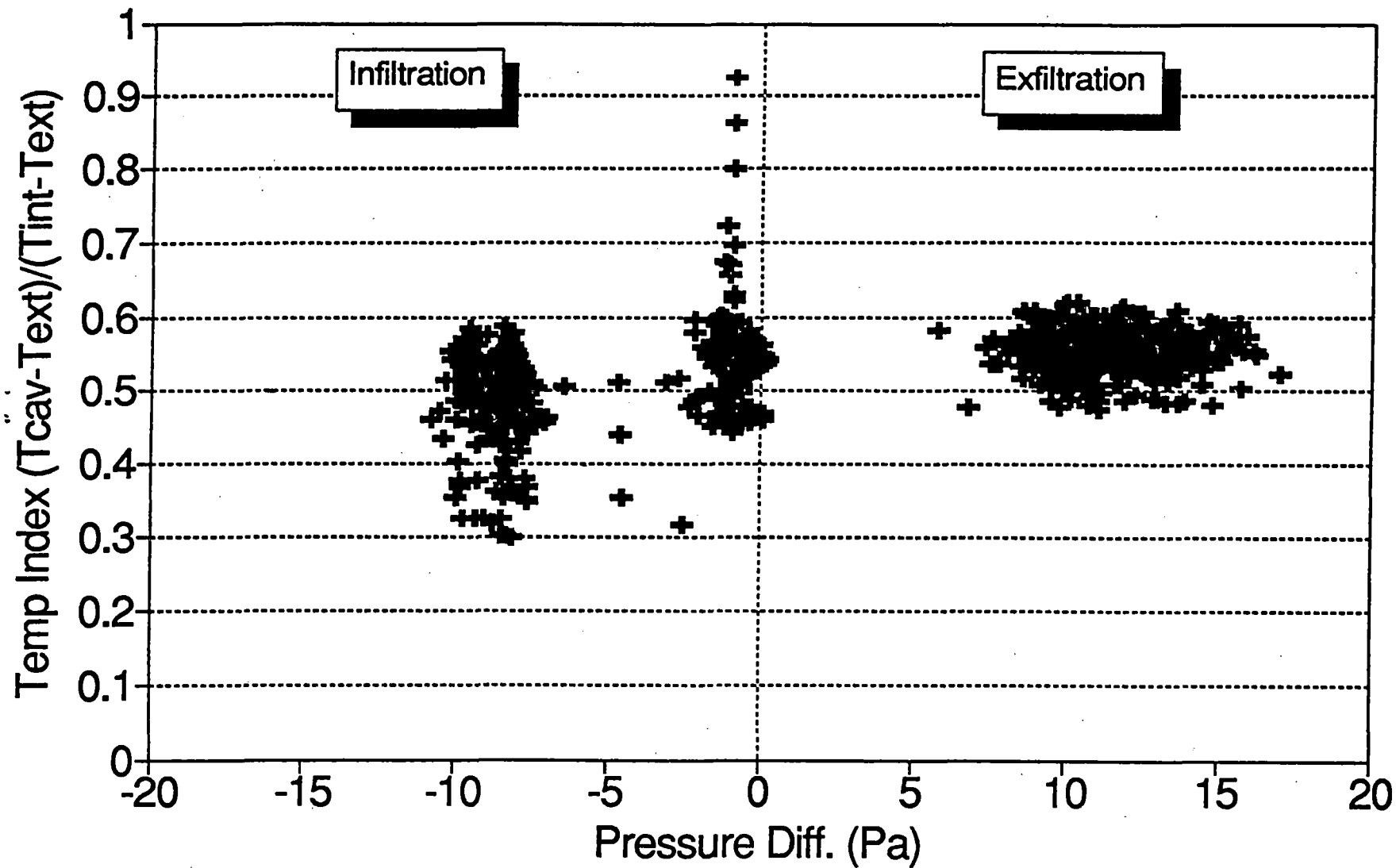
Temperature Index
WINTER: Panel E, (Sealed/Vinyl/Strap)
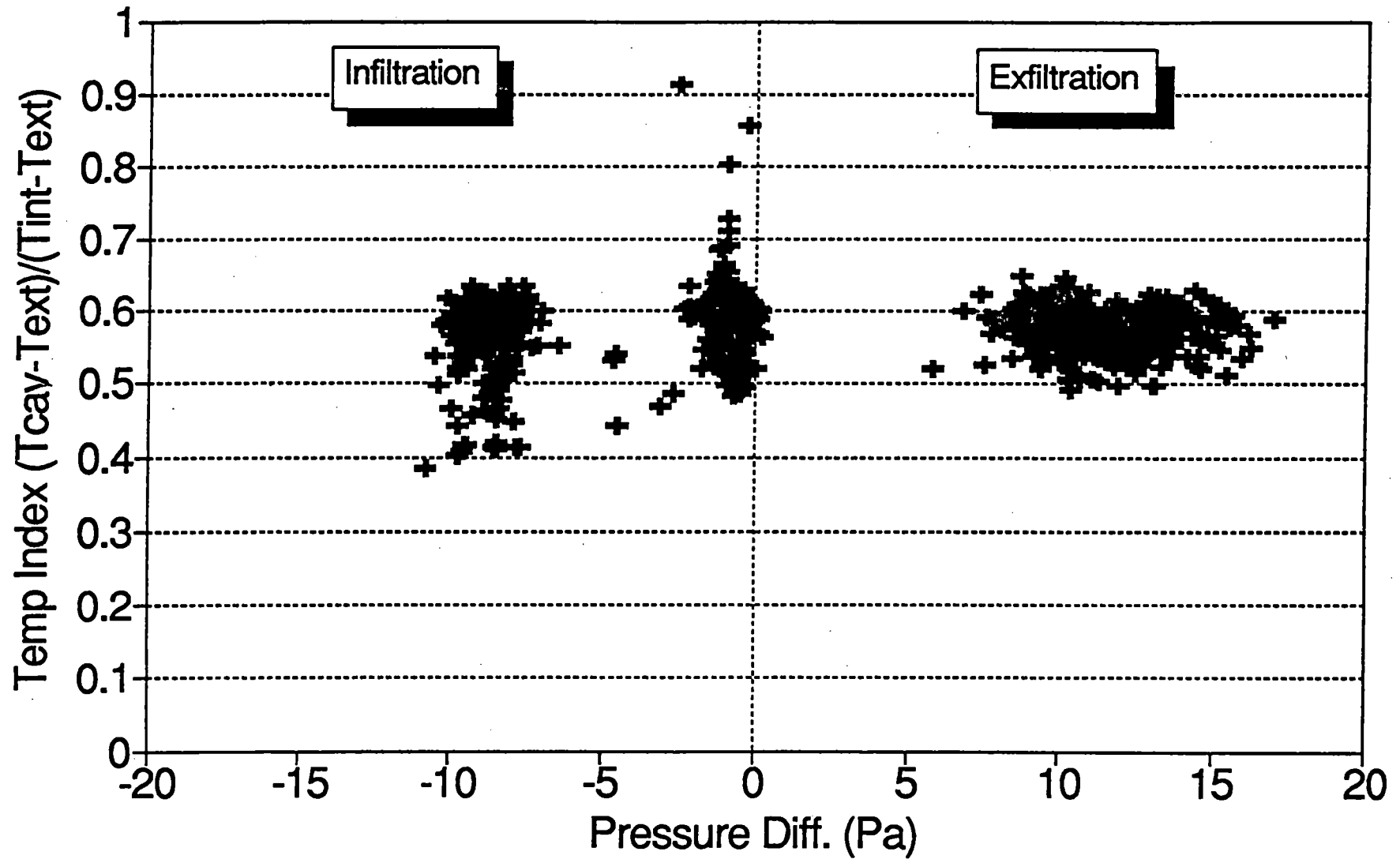
Temperature Index
WINTER: Panel F, (Vented/Vinyl/Strap)
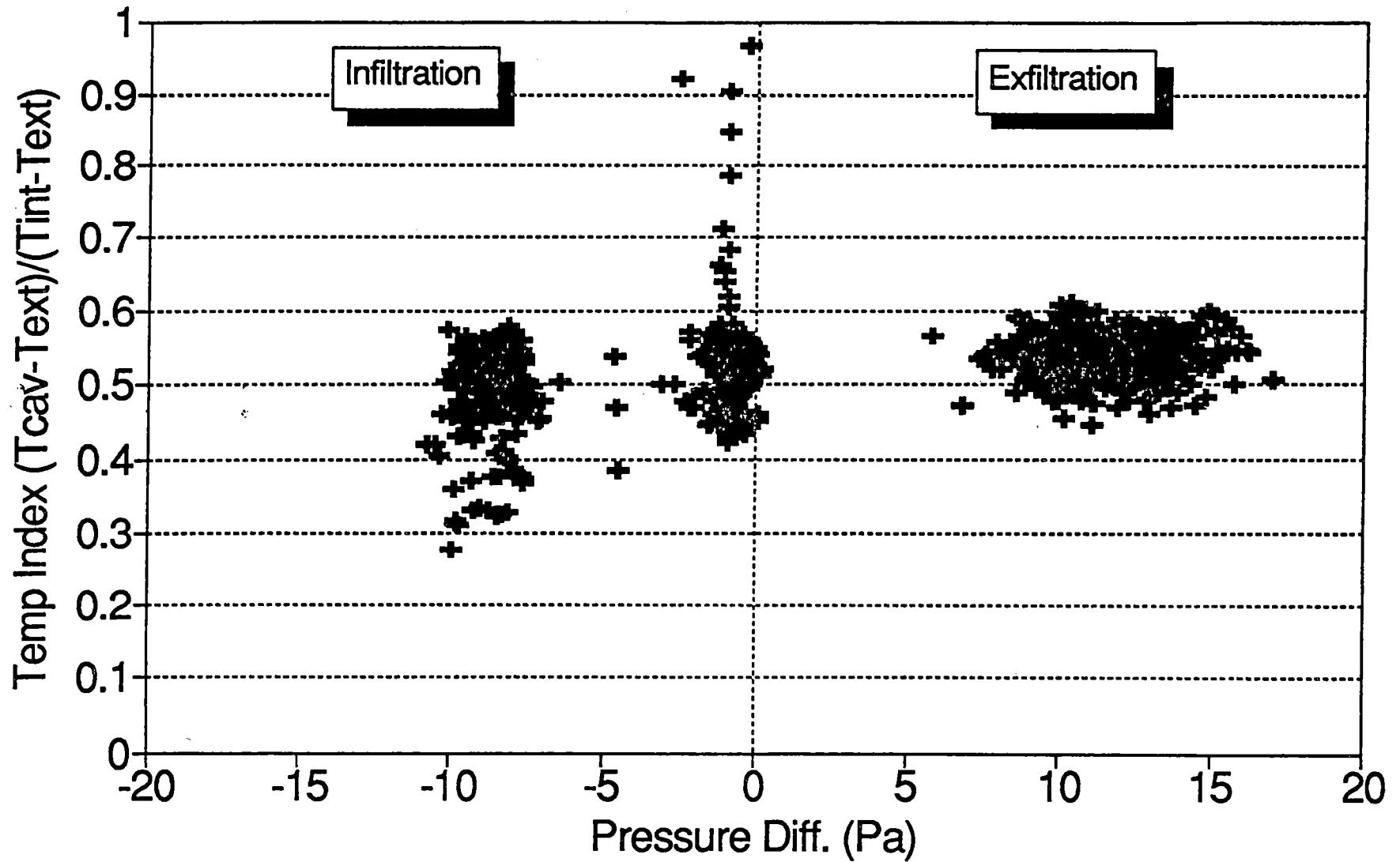
Temperature Index
SUMMER: Panel A, (Sealed/Wood Siding)
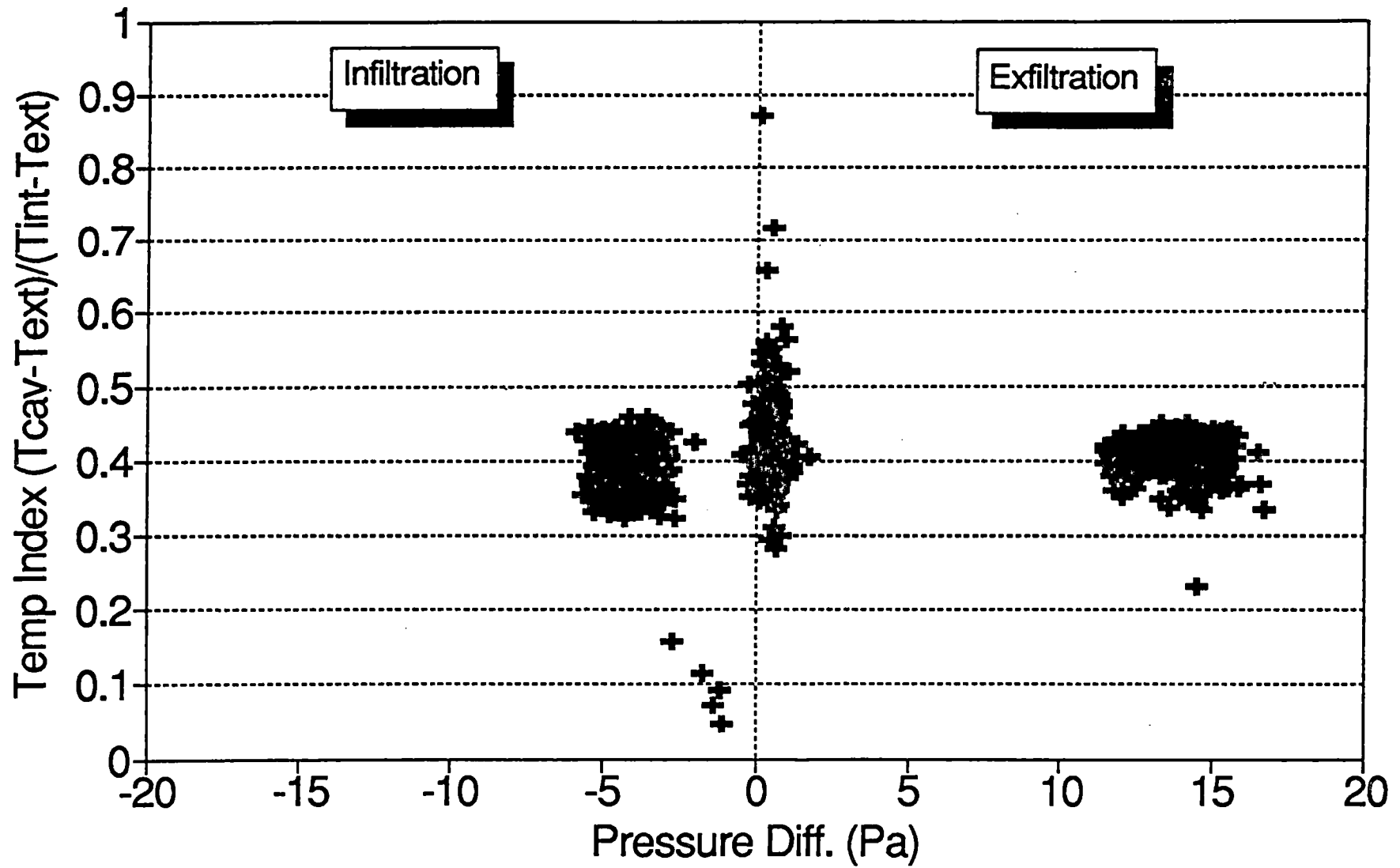
Temperature Index
SUMMER: Panel B, (Vented/Wood Siding)
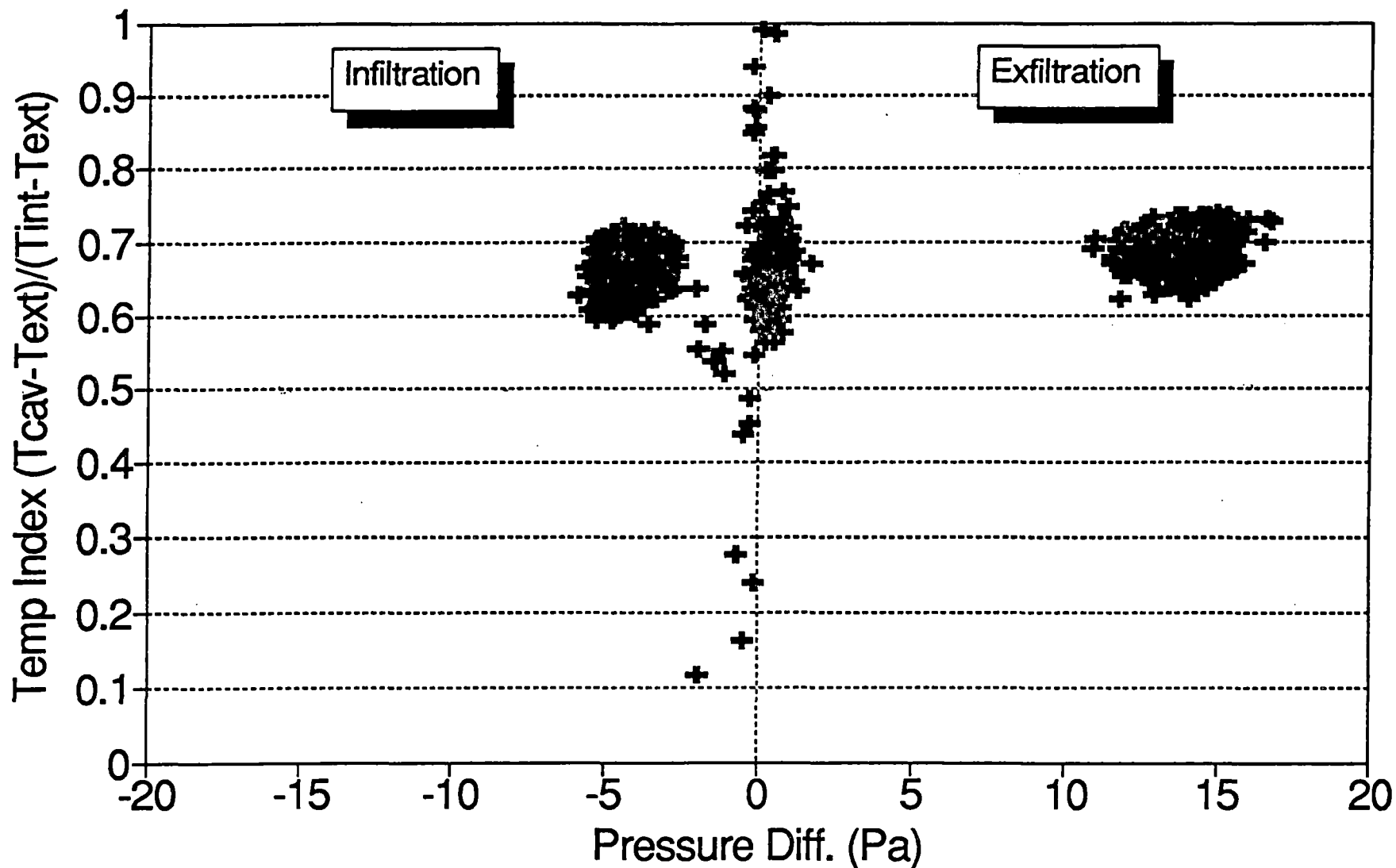
Temperature Index
SUMMER: Panel C, (Sealed/Vinyl Siding)
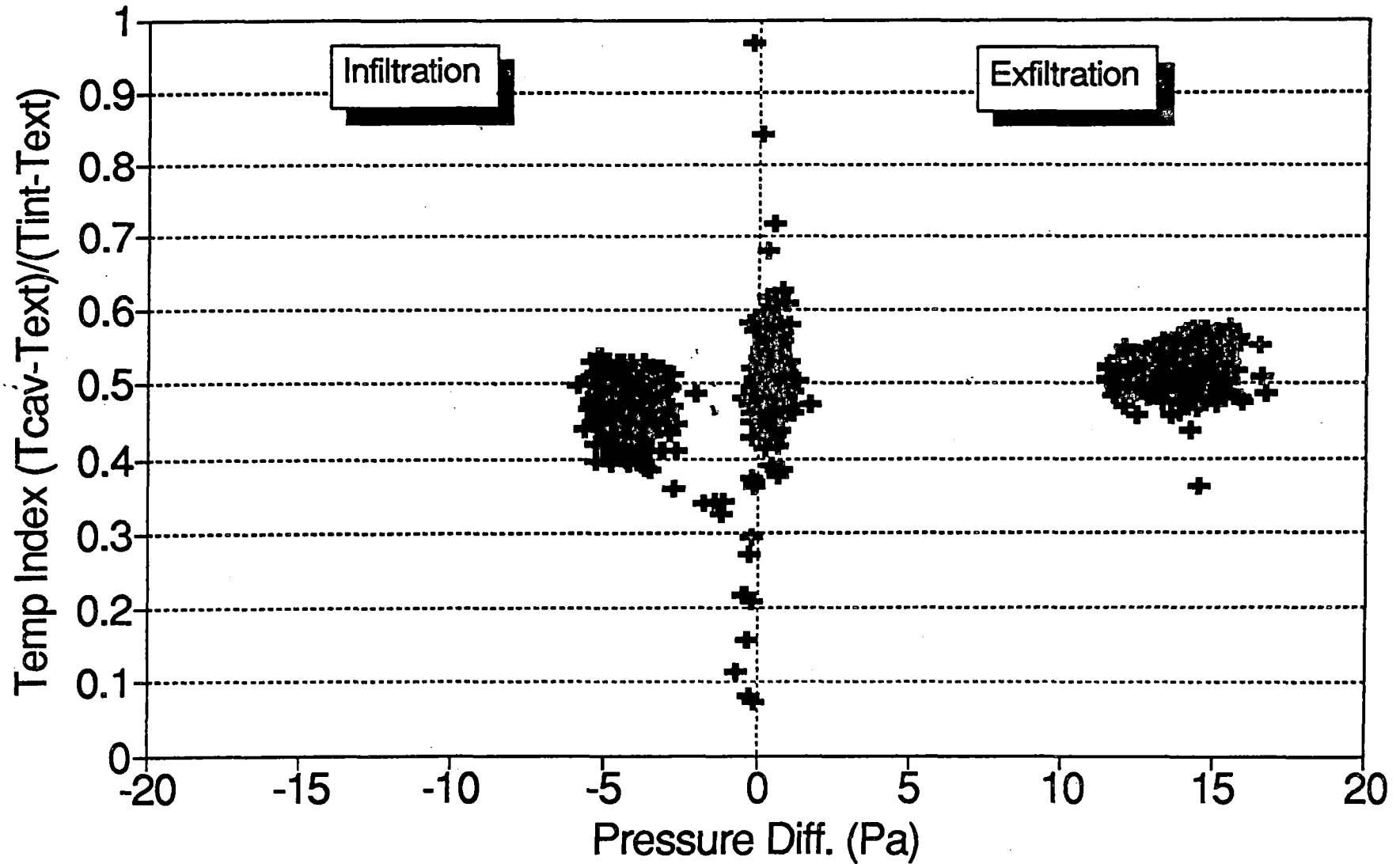
Temperature Index
SUMMER: Panel D, (Vented/Vinyl Siding)
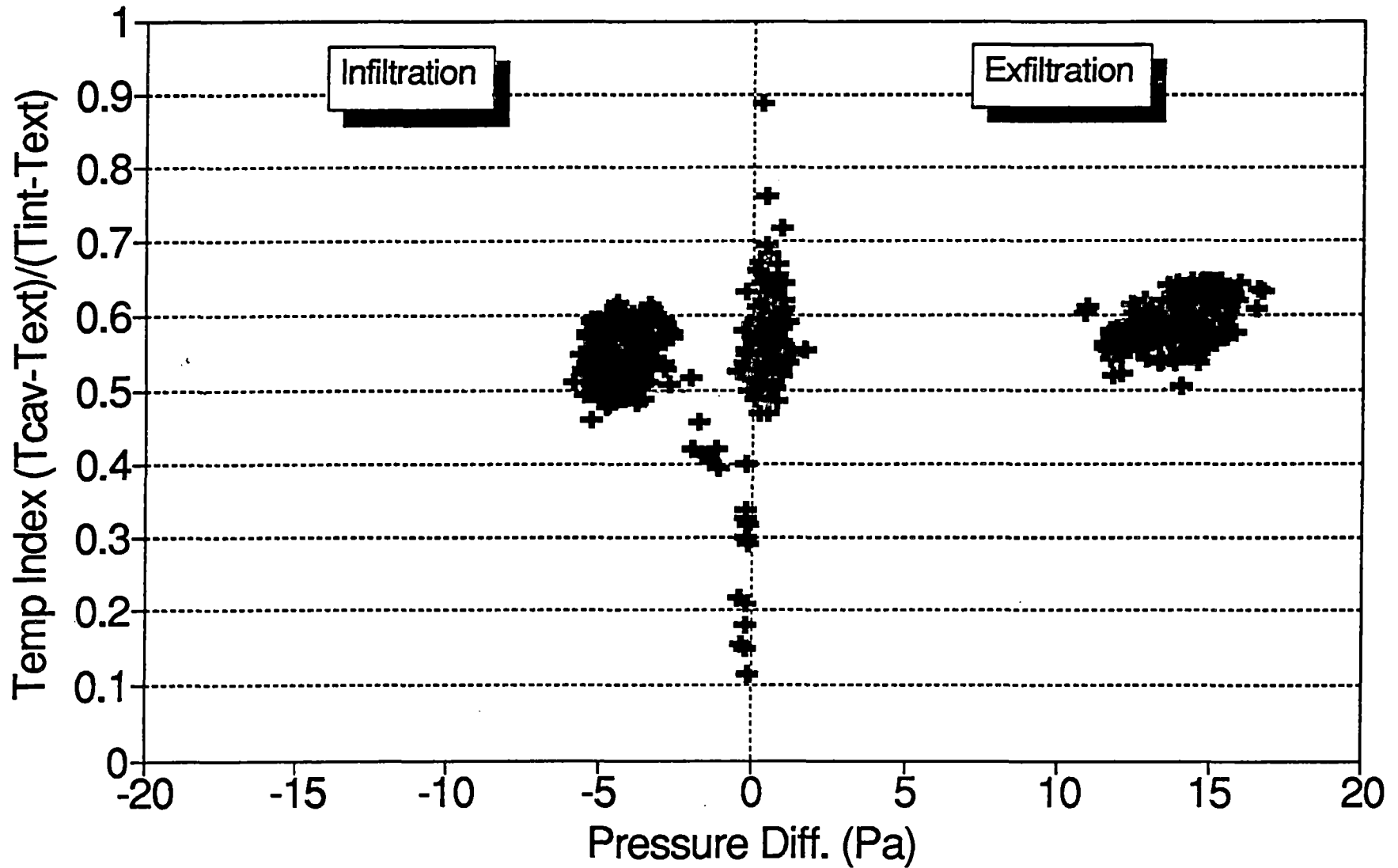
Temperature Index
SUMMER: Panel E, (Sealed/Vinyl/Strap)
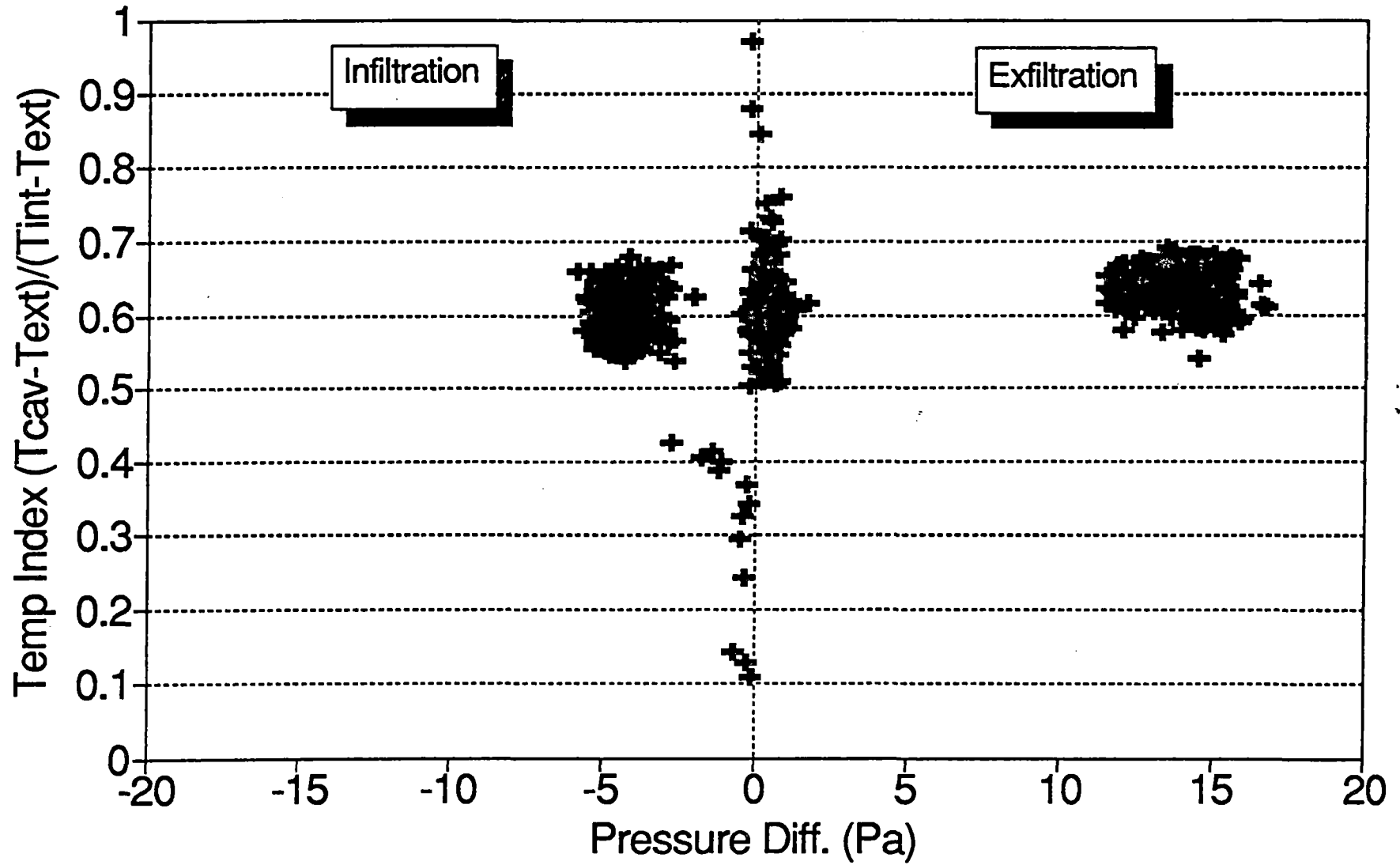
Temperature Index
SUMMER: Panel F, (Vented/Vinyl/Strap)
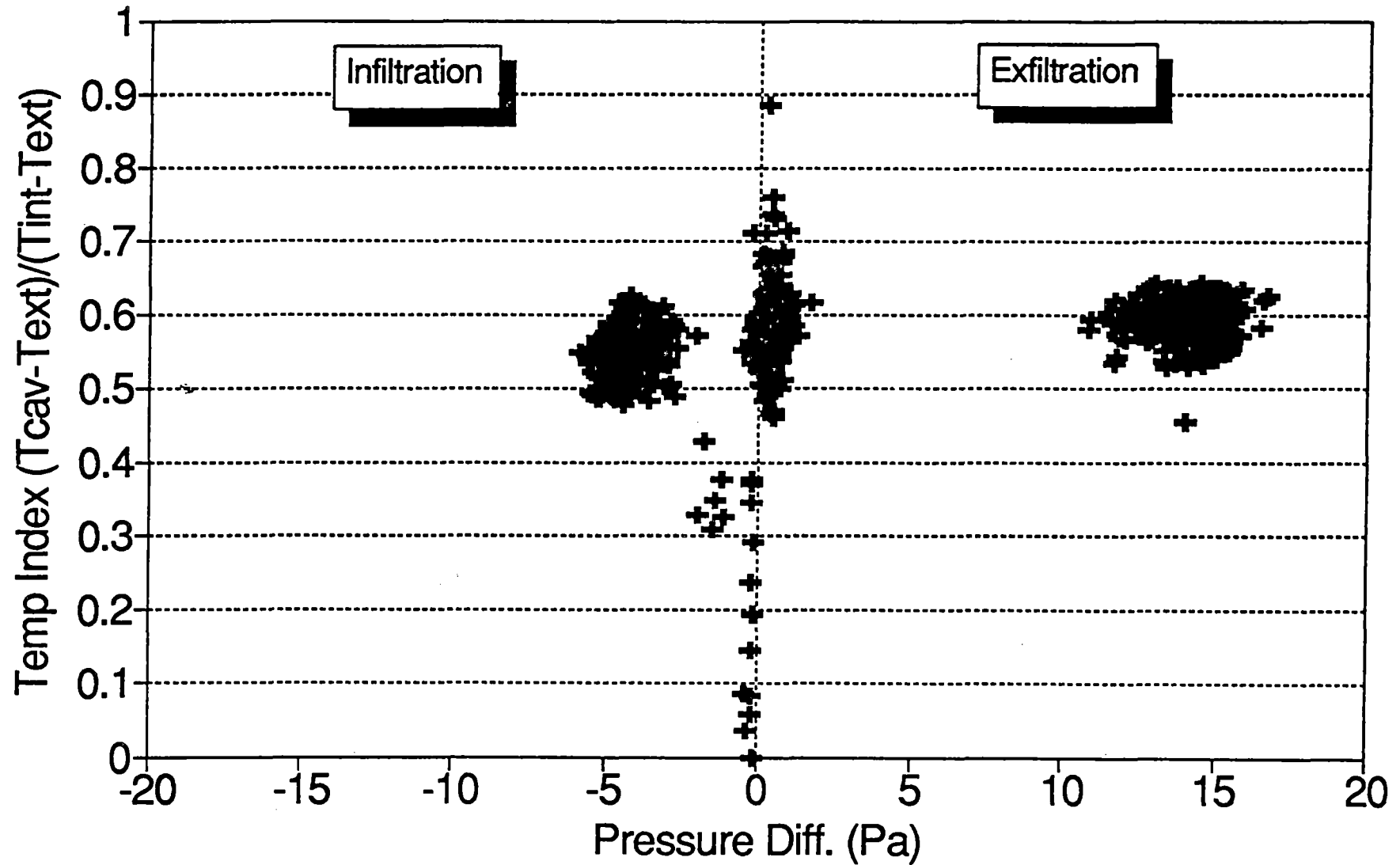
APPENDIX D
Differential Pressure Graphs

Pressure Differential
WINTER

Neutral

Infiltration

Exfiltration

Avg. Infiltration: -8.4 Pa

Avg. Exfiltration: 11.5 Pa

Avg. Neutral: -0.7 Pa

Pressure Differential (Pa)

Hours
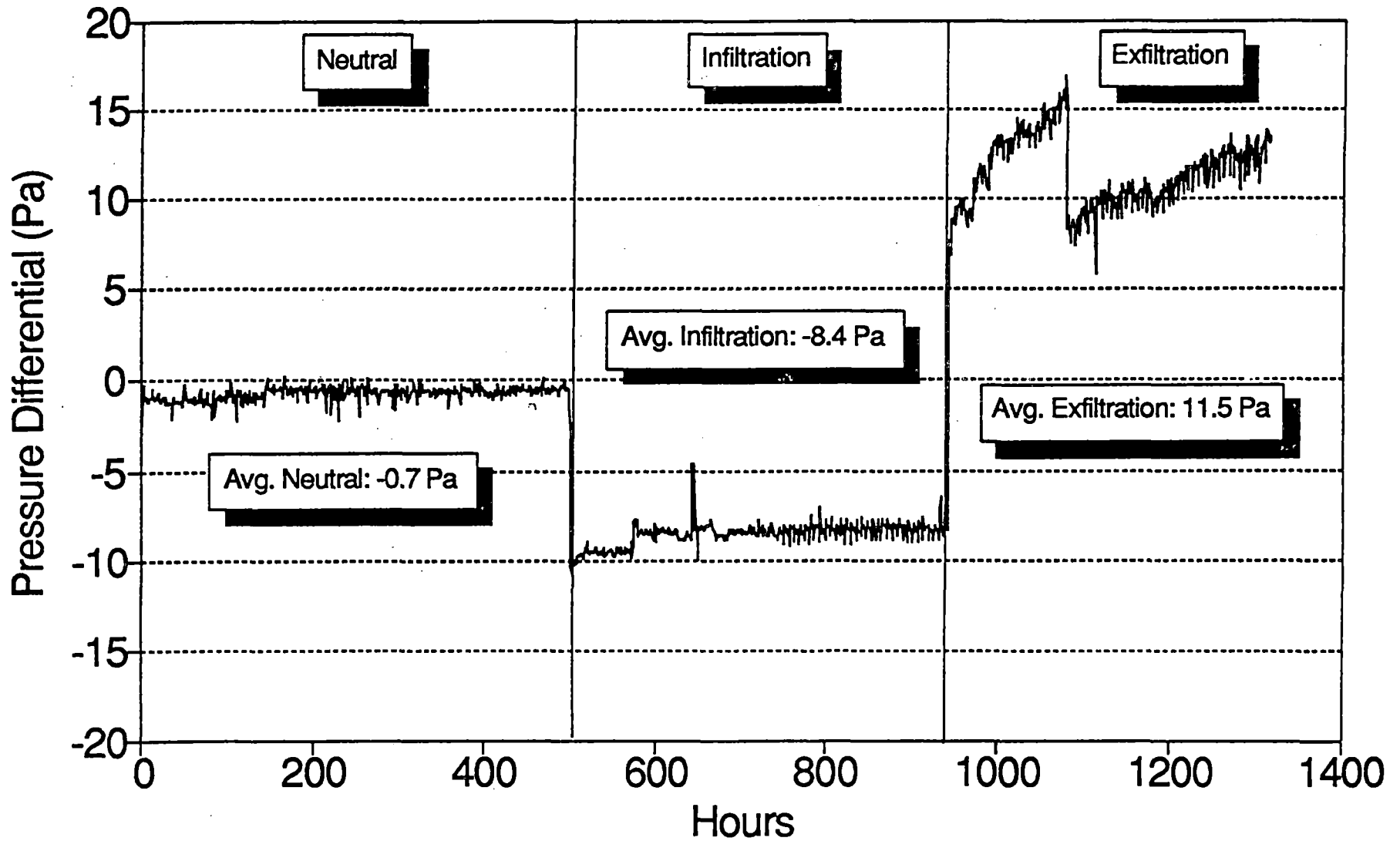
Average Cavity Comparison
WINTER, Panel A and B
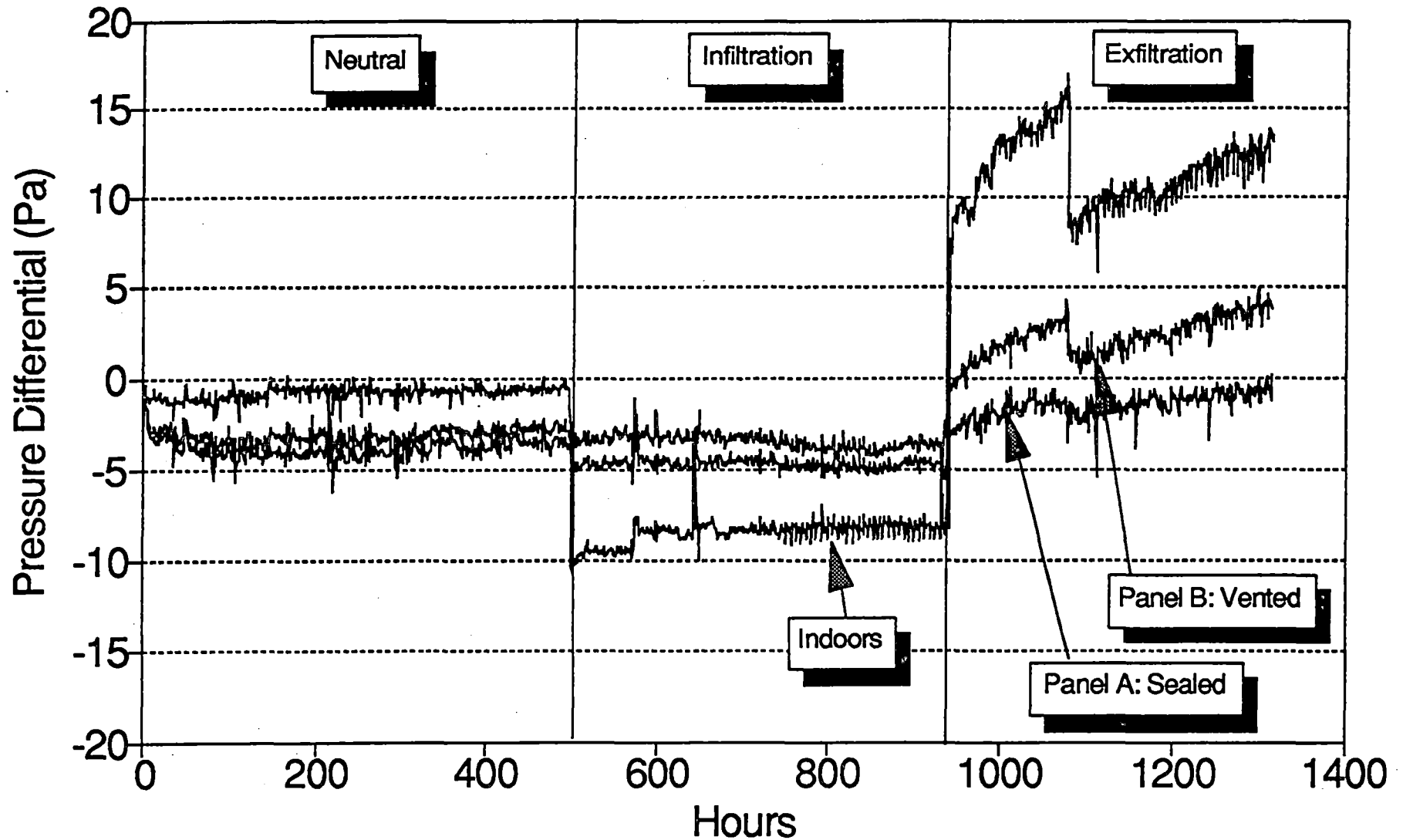
Average Cavity Comparison
WINTER: Panel C and D
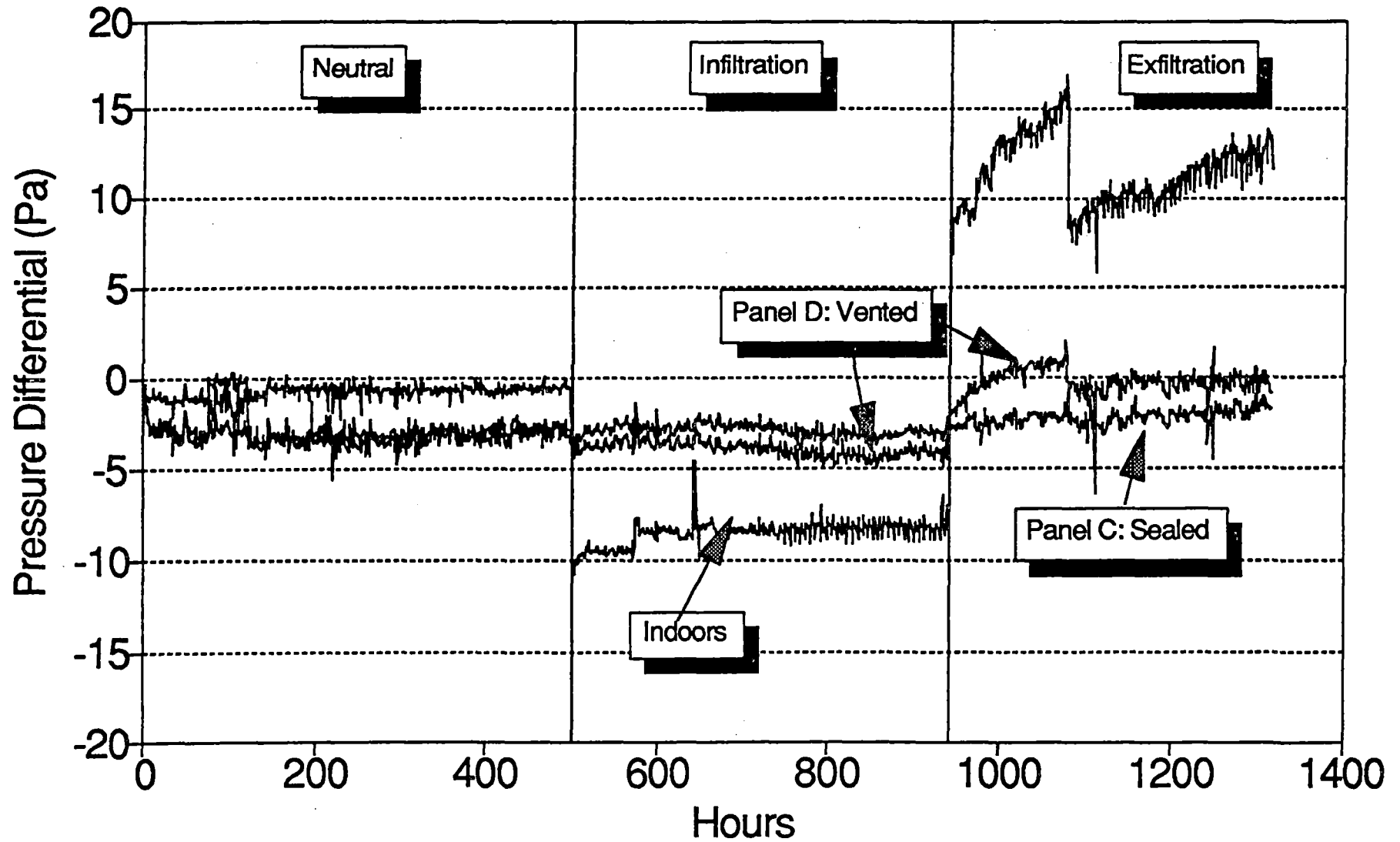
Average Cavity Comparison
WINTER: Panel E and F
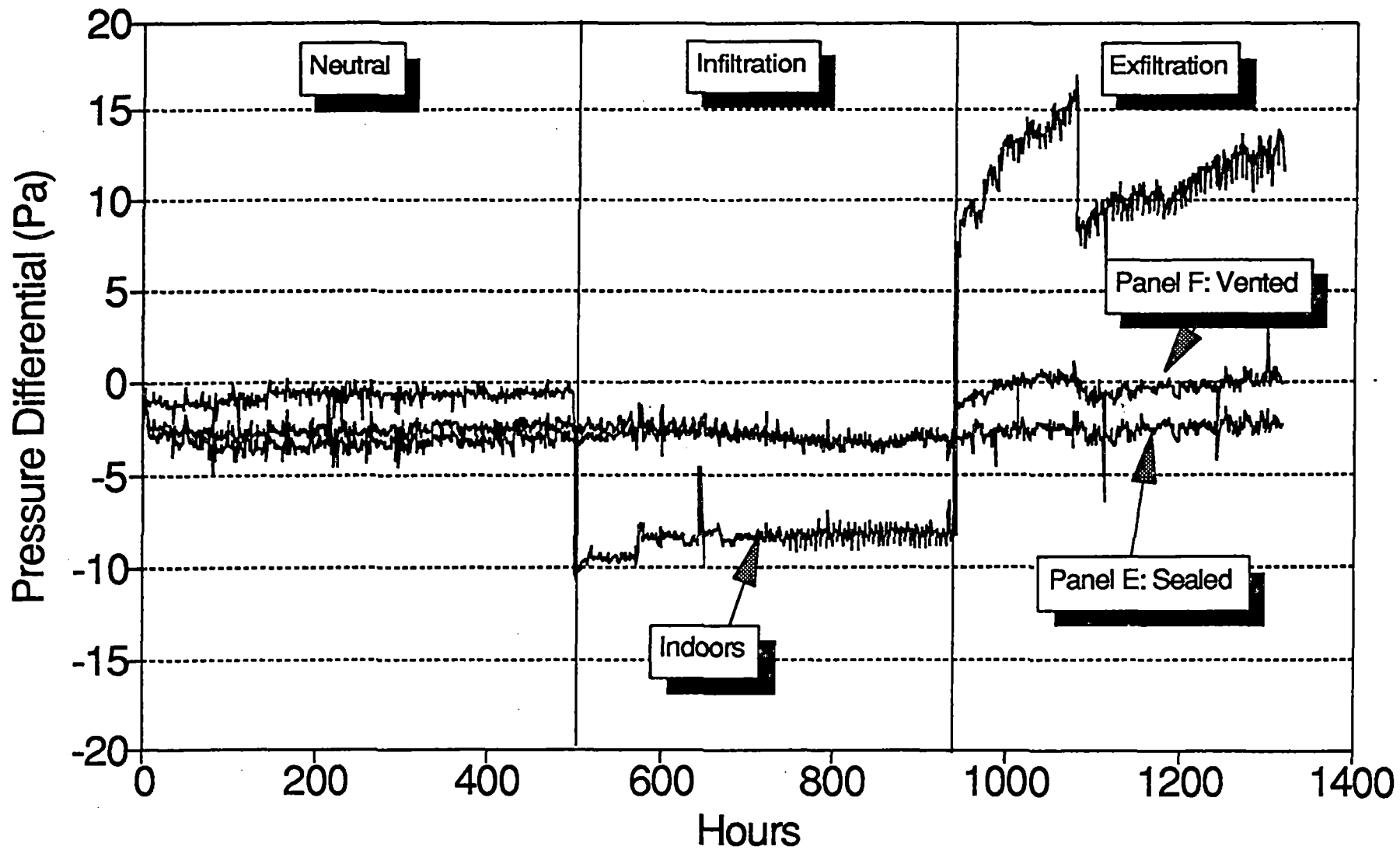
Pressure Differential
SUMMER
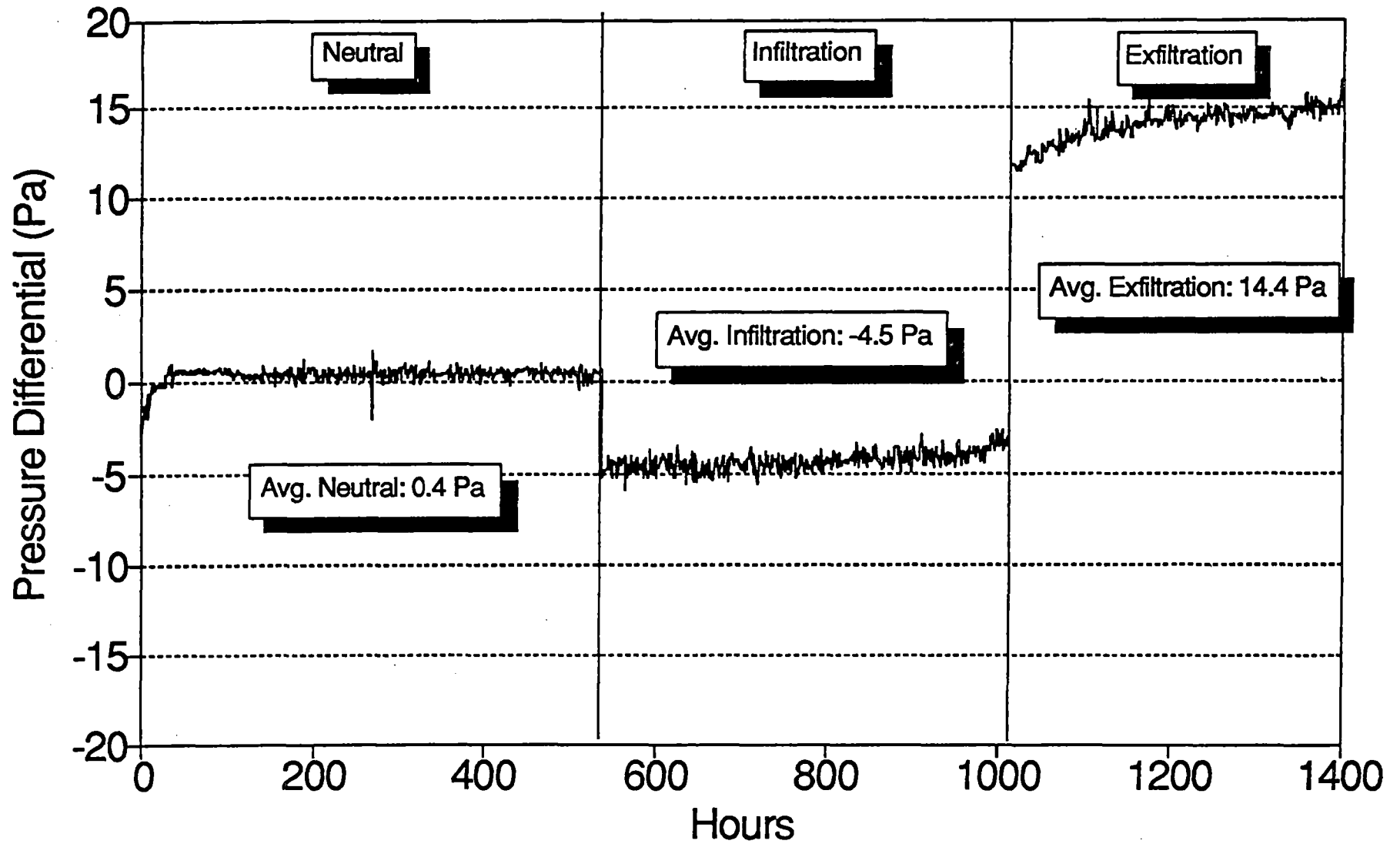
Average Cavity Comparison
SUMMER: Panel A and B
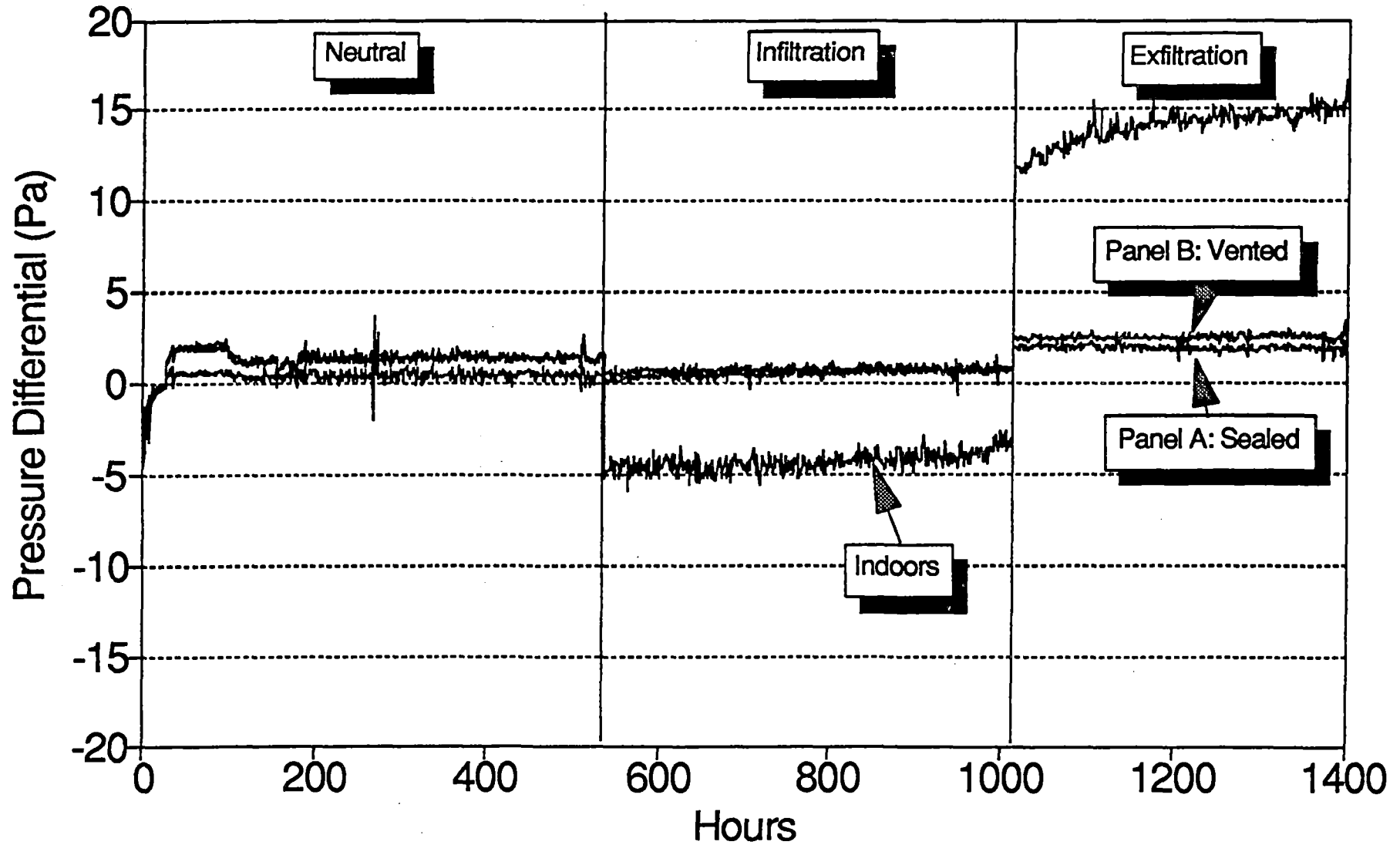
Average Cavity Comparison
SUMMER: Panel C and D
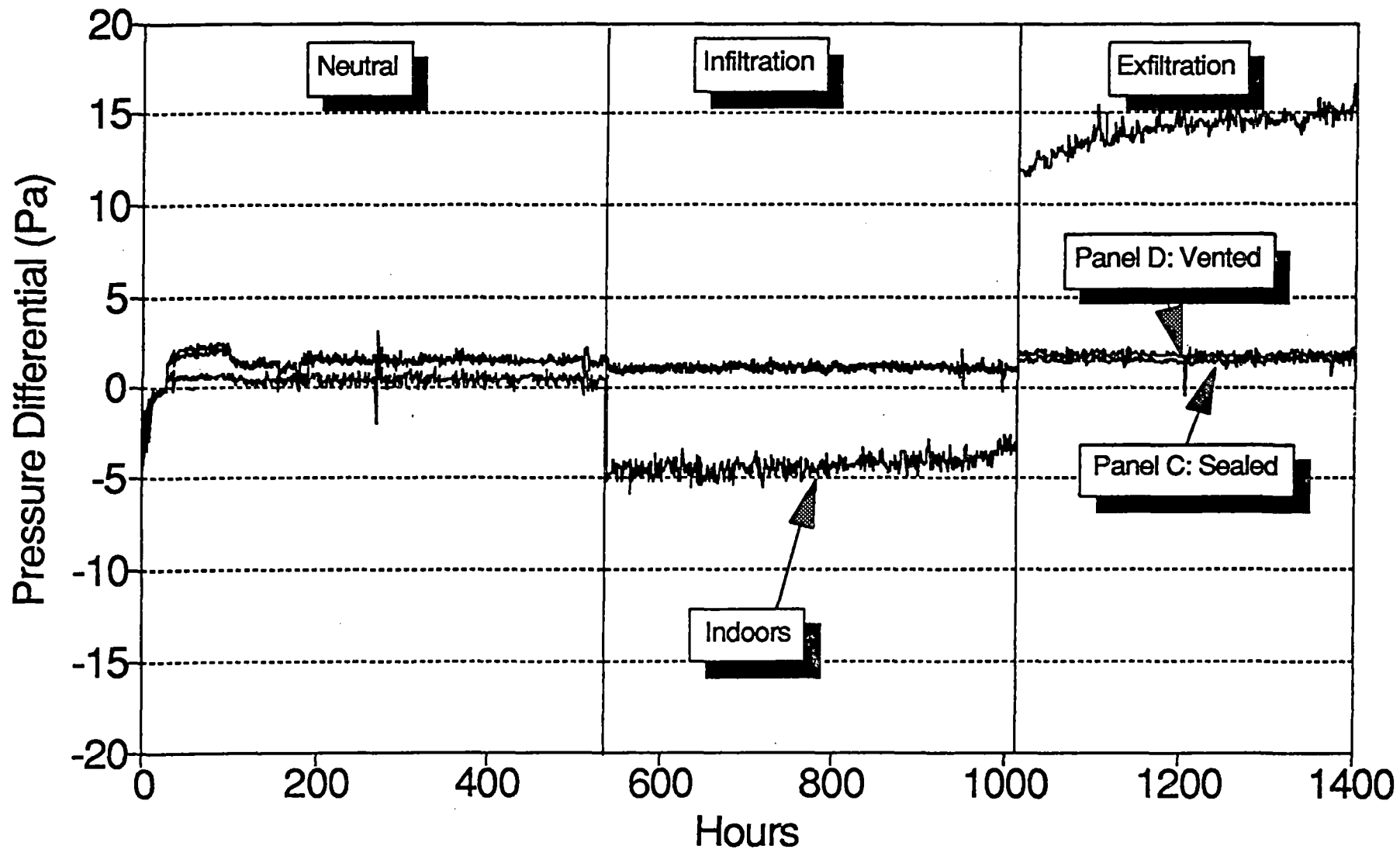
Average Cavity Comparisons
SUMMER: Panel E and F

Neutral

Infiltration

Exfiltration

Panel F: Vented

Panel E: Sealed

Indoors

Pressure Differential (Pa)

Hours
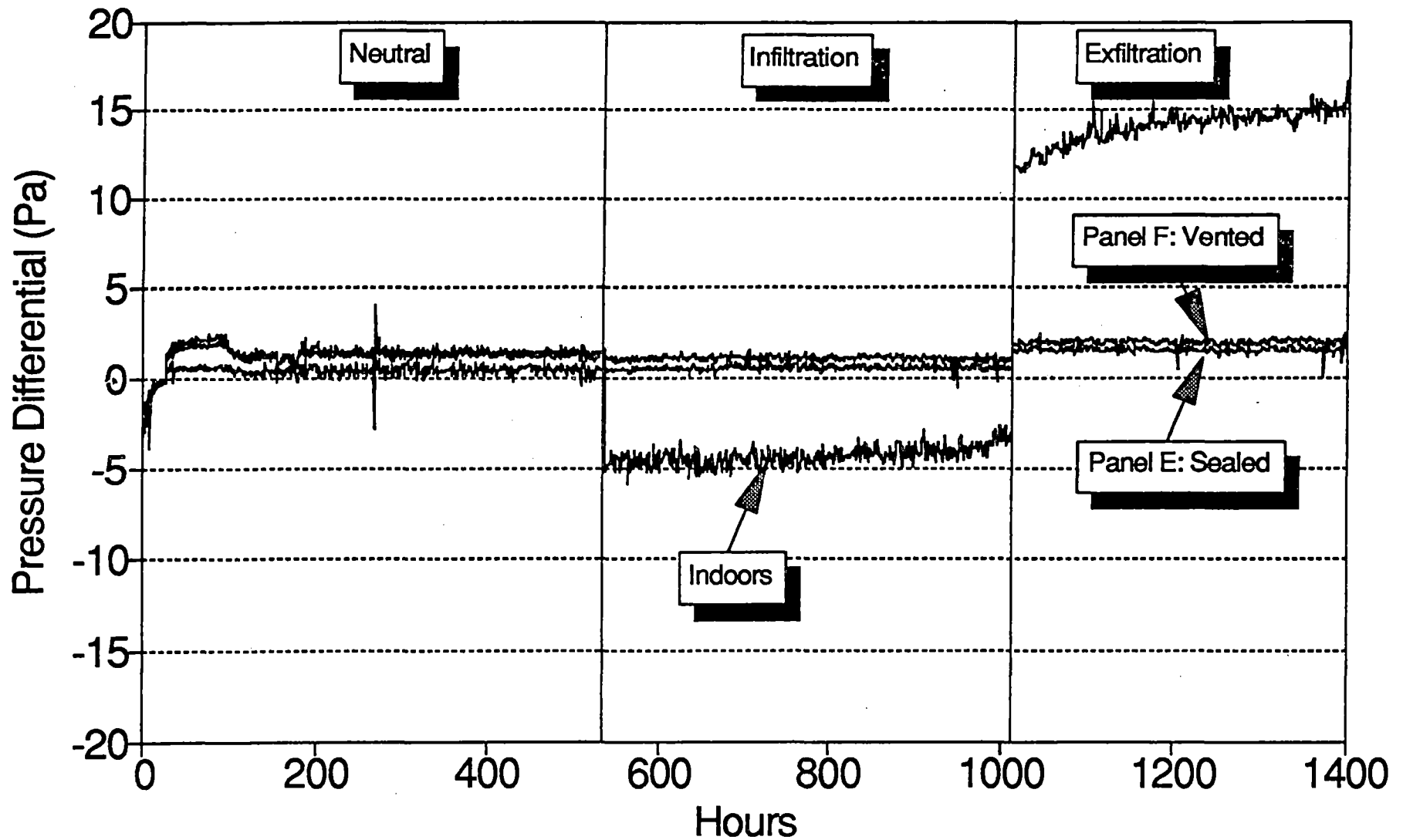
APPENDIX E
Relative Humidity and Humidity Index Graphs

Relative Humidity
WINTER
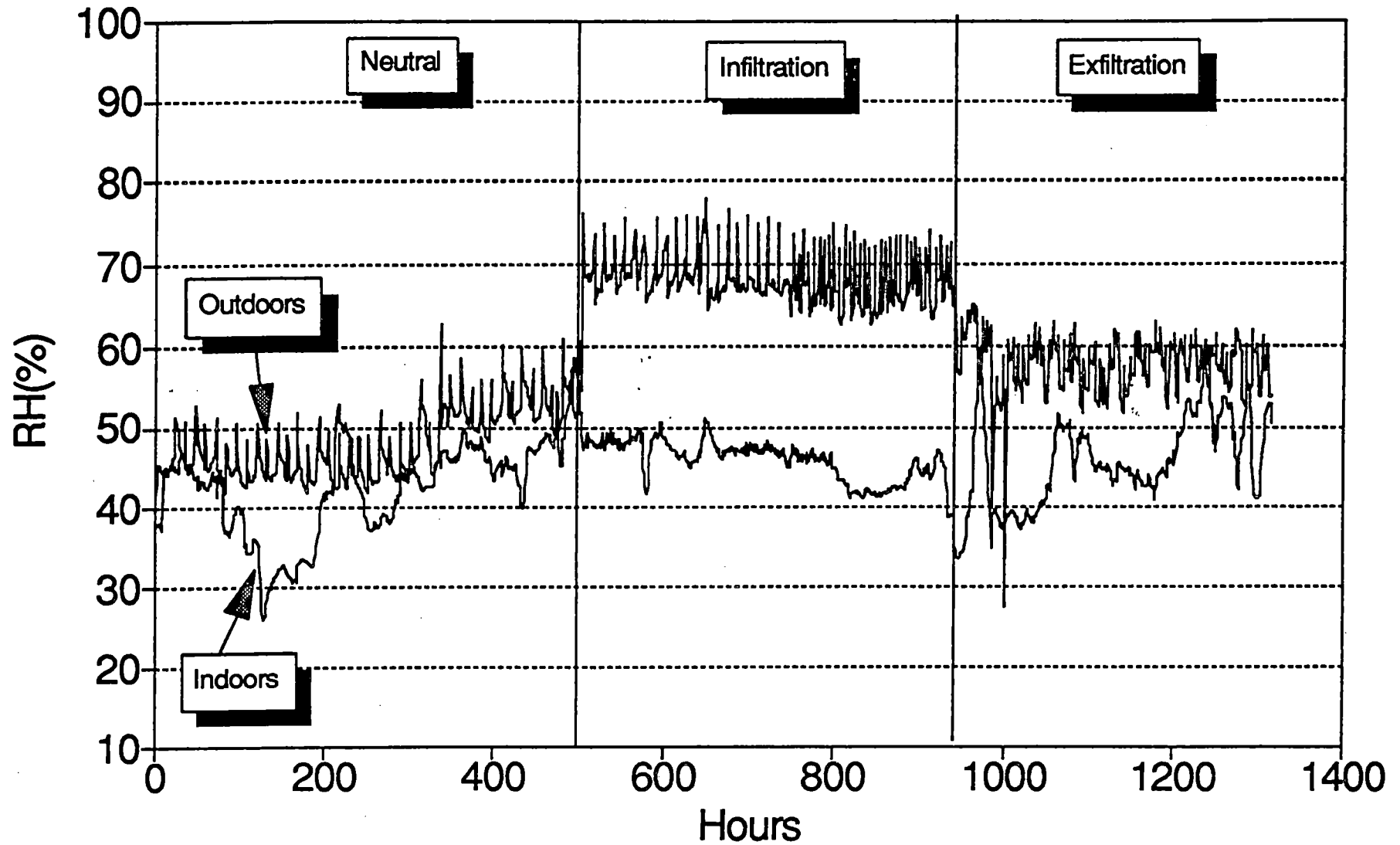
Relative Humidity-Stud Cavities
WINTER: Panel A and B
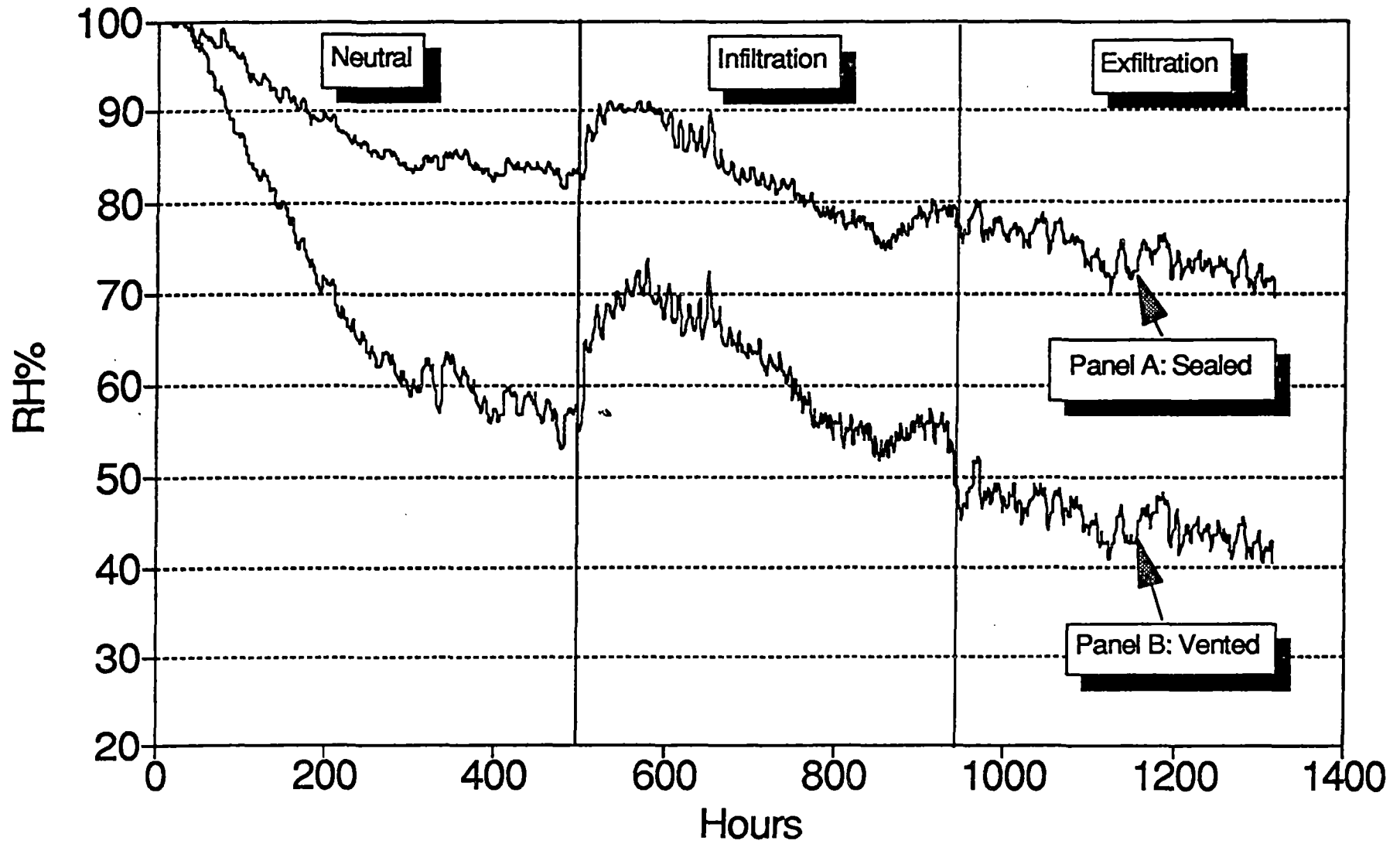
Relative Humidity-Stud Cavities
WINTER: Panel C and D
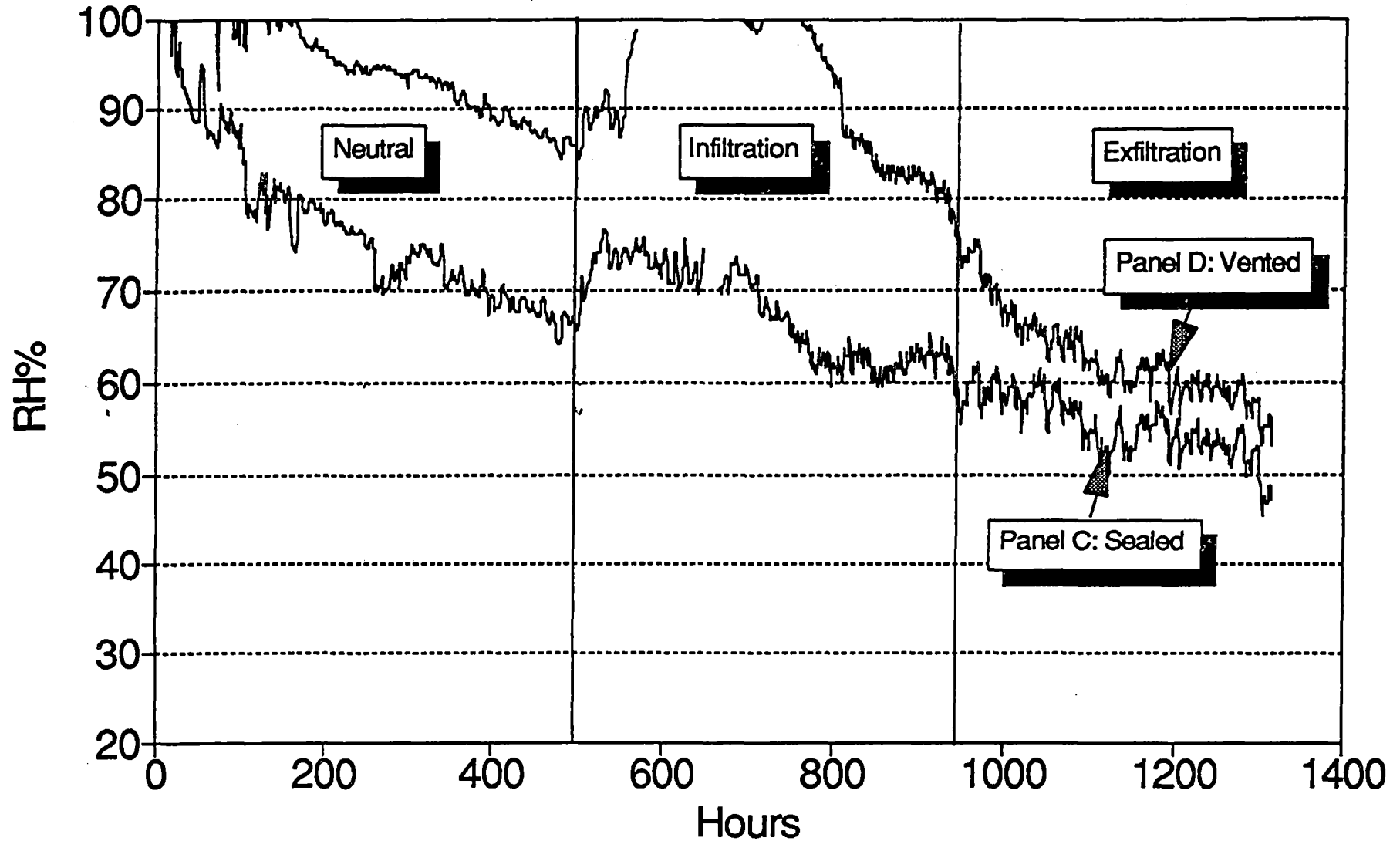
Relative Humidity-Stud Cavities
WINTER: Panel E and F
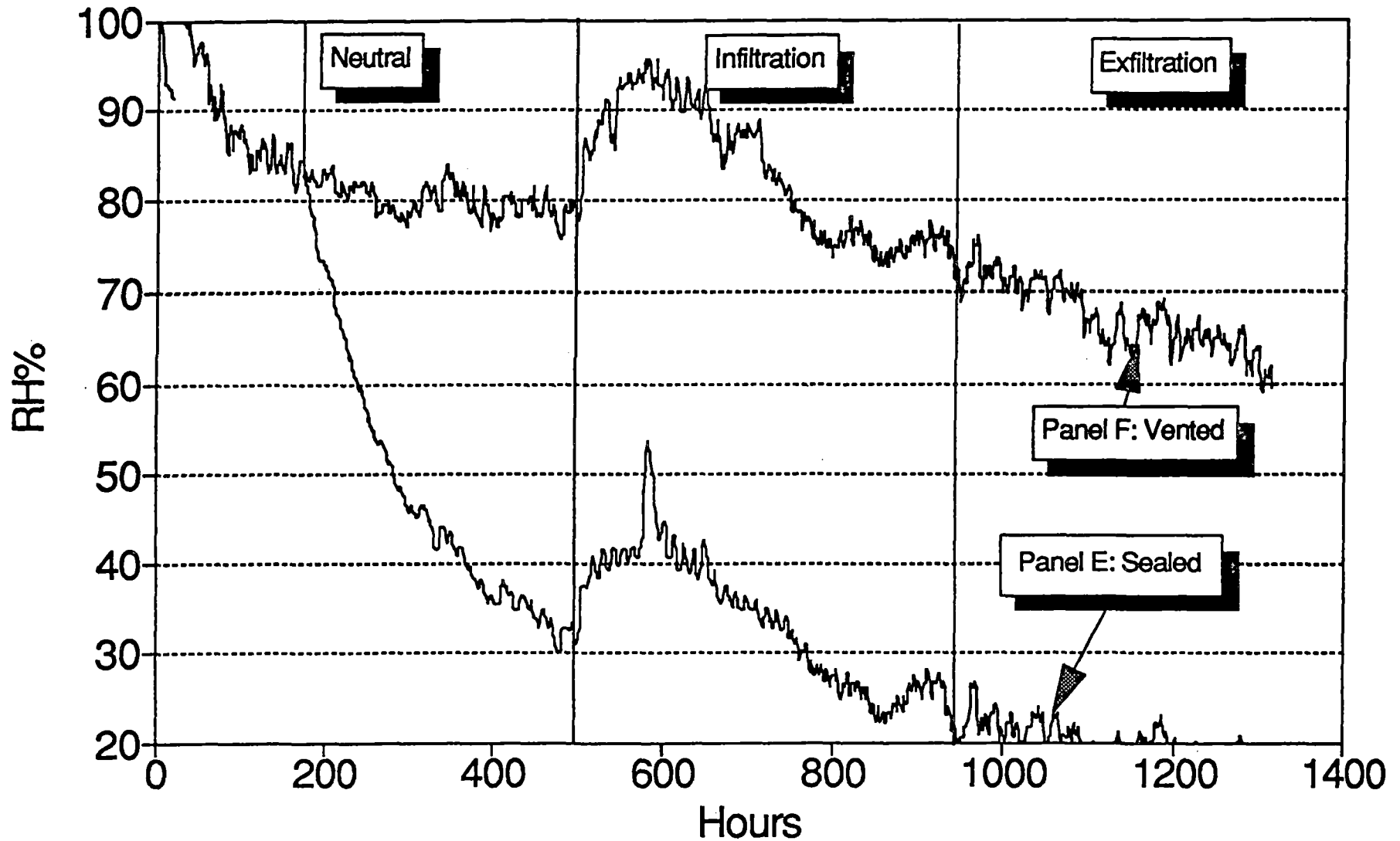
Relative Humidity
SUMMER
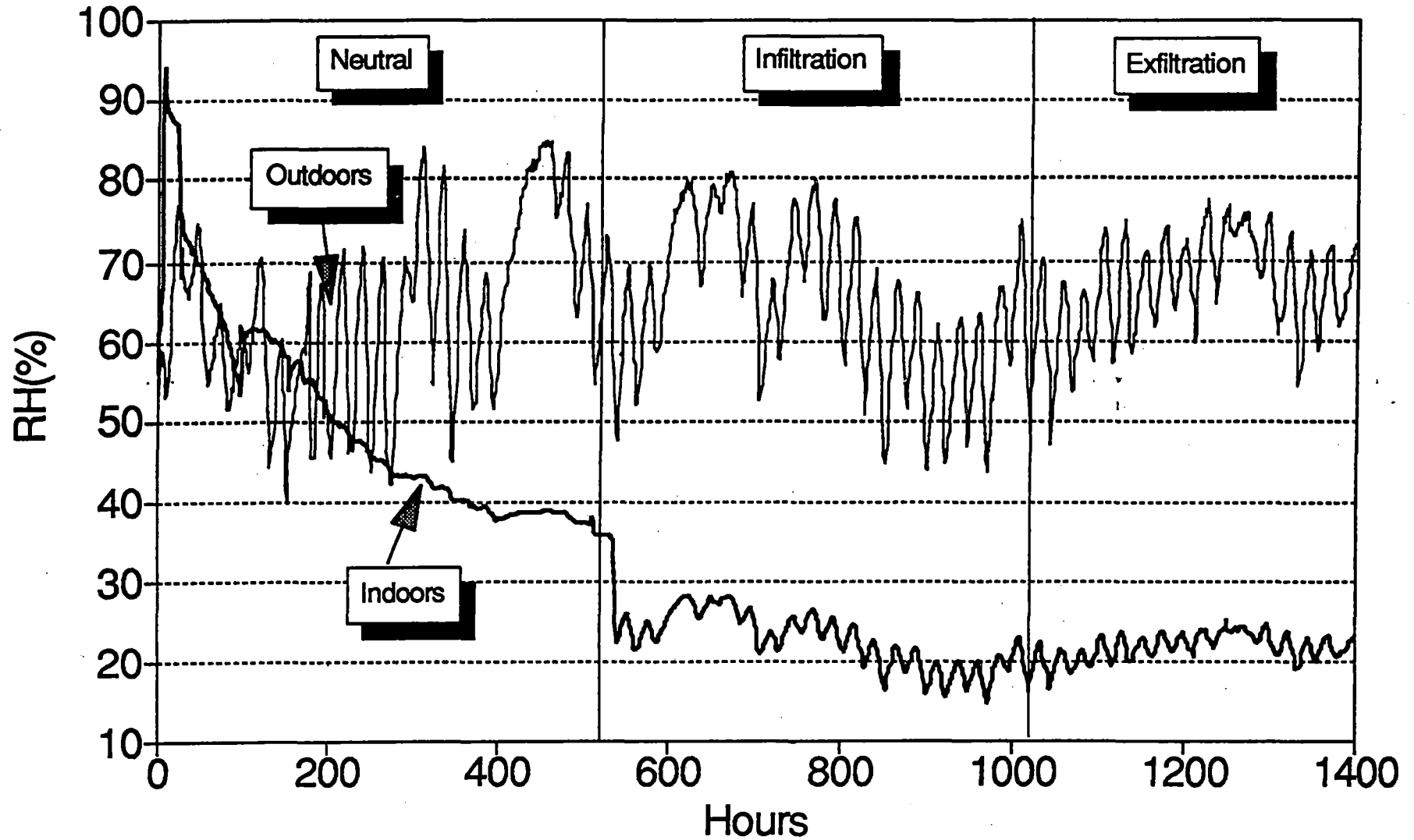
Relative Humidity-Stud Cavities
SUMMER: Panel A and B
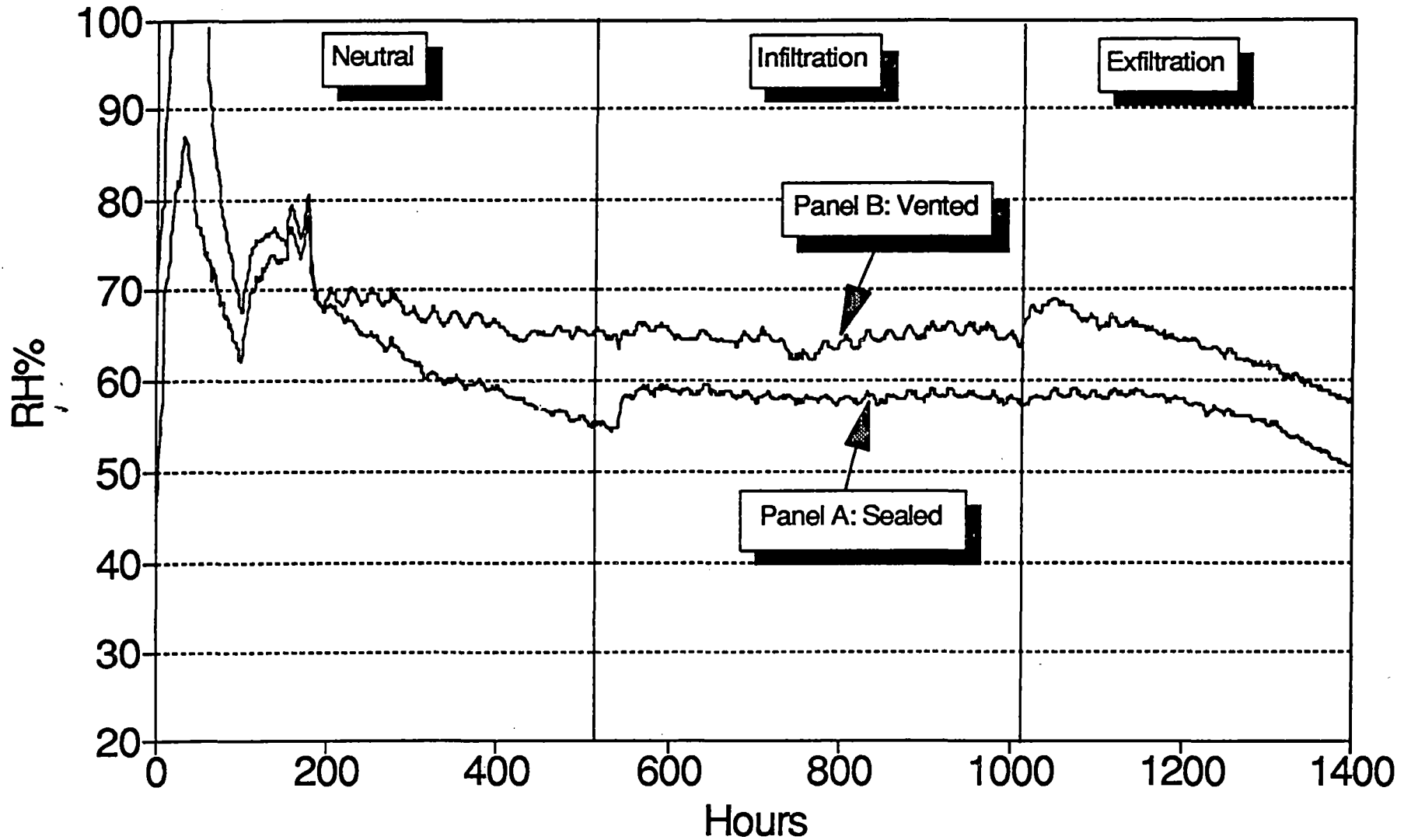
Relative Humidity-Stud Cavities
SUMMER: Panel C and D
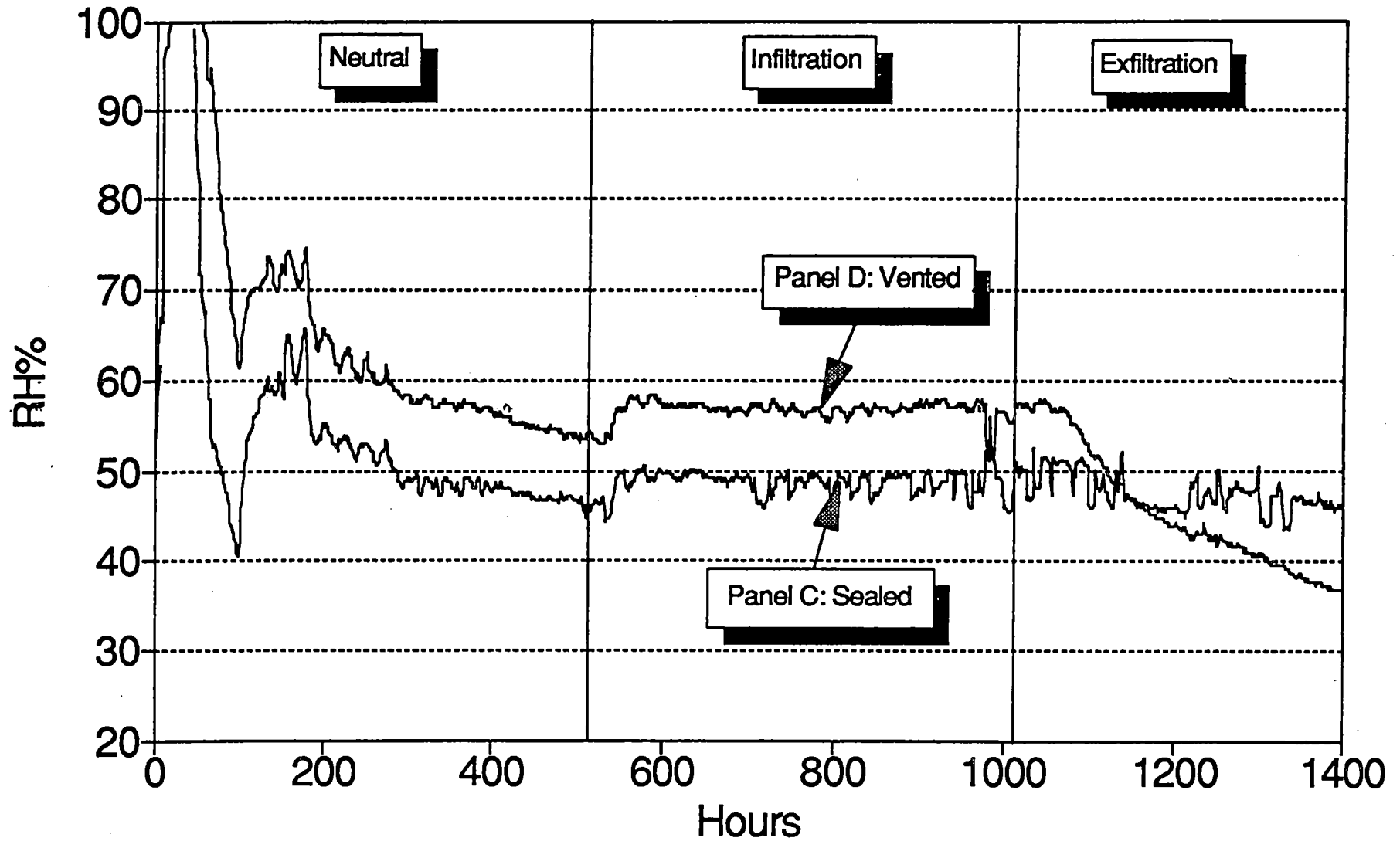
Relative Humidity-Stud Cavities
SUMMER: Panel E and F
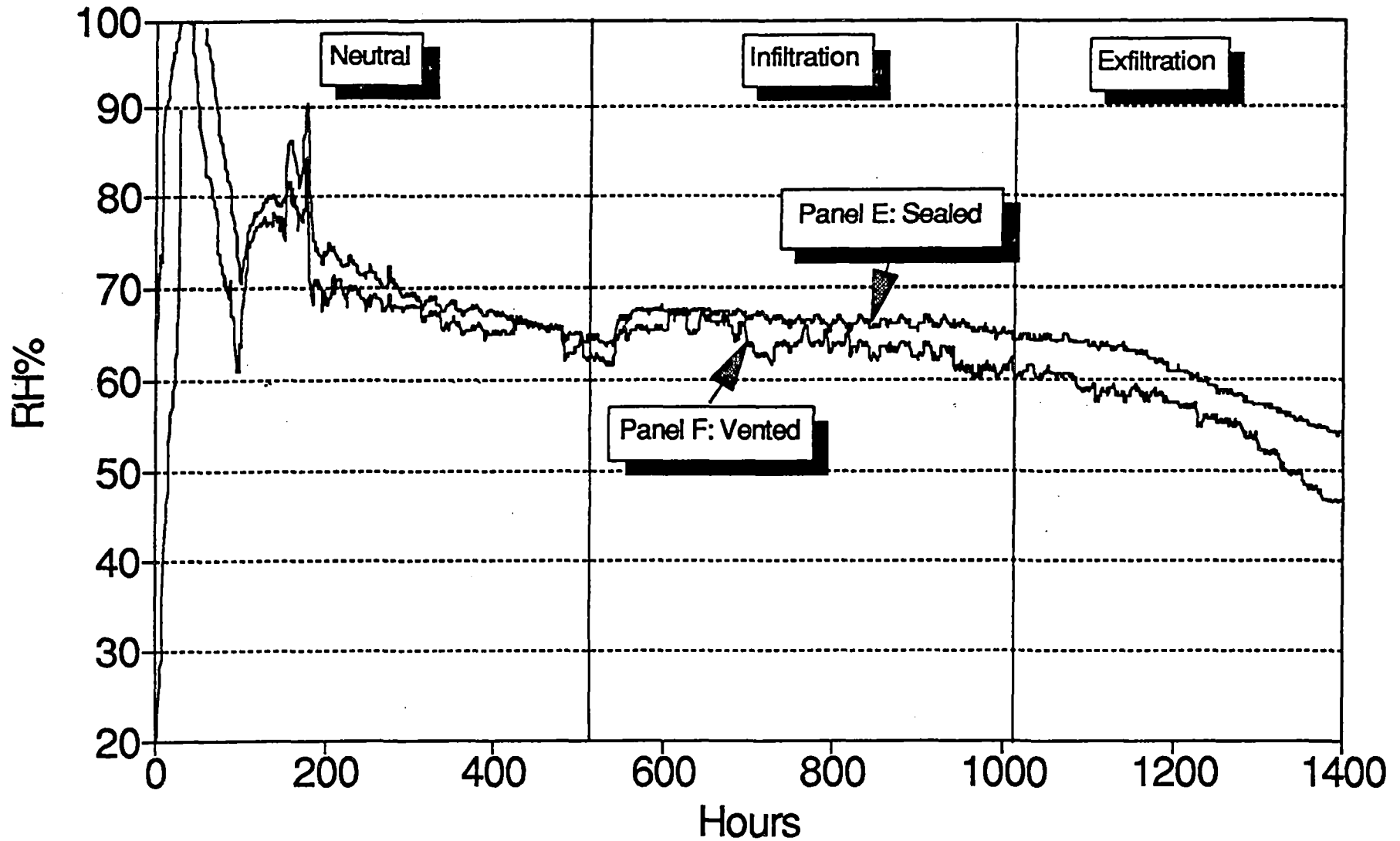
Humidity Index
WINTER: Panel A, (Sealed/Wood Siding)
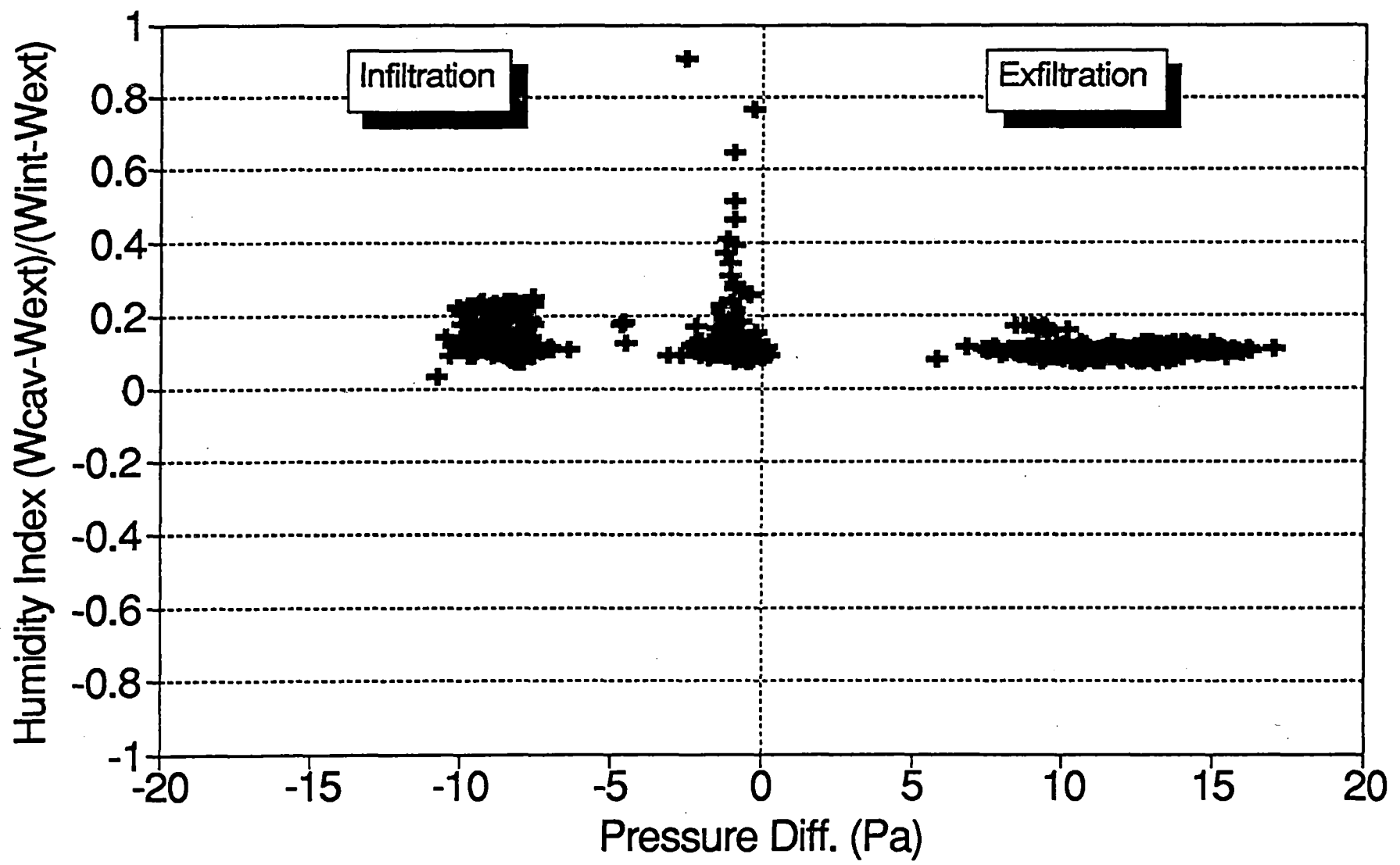
Humidity Index
WINTER: Panel B, (Vented/Wood Siding)

Humidity Index
SUMMER: Panel A, (Sealed/Wood Siding)
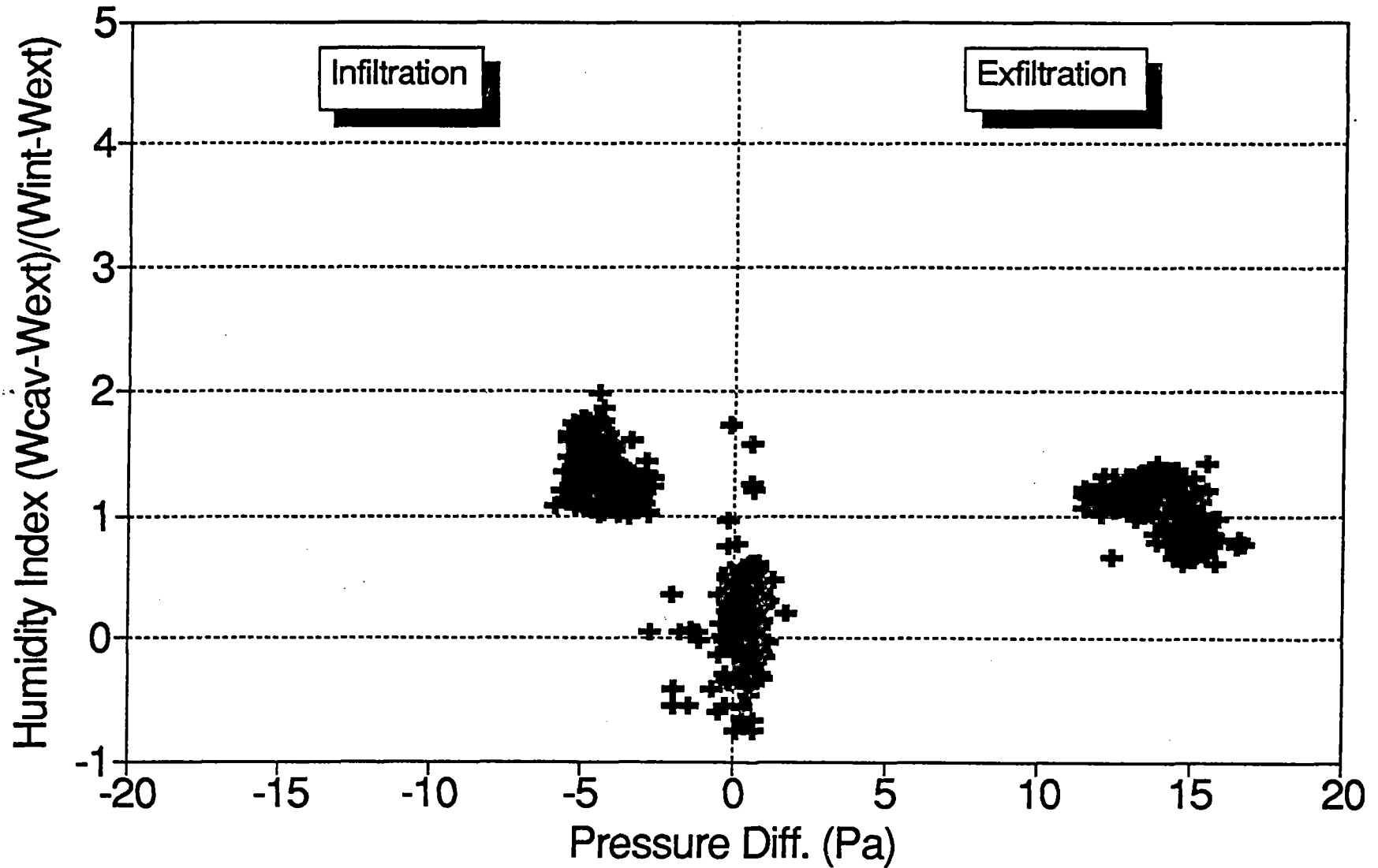
Humidity Index
SUMMER: Panel B, (Vented/Wood Siding)
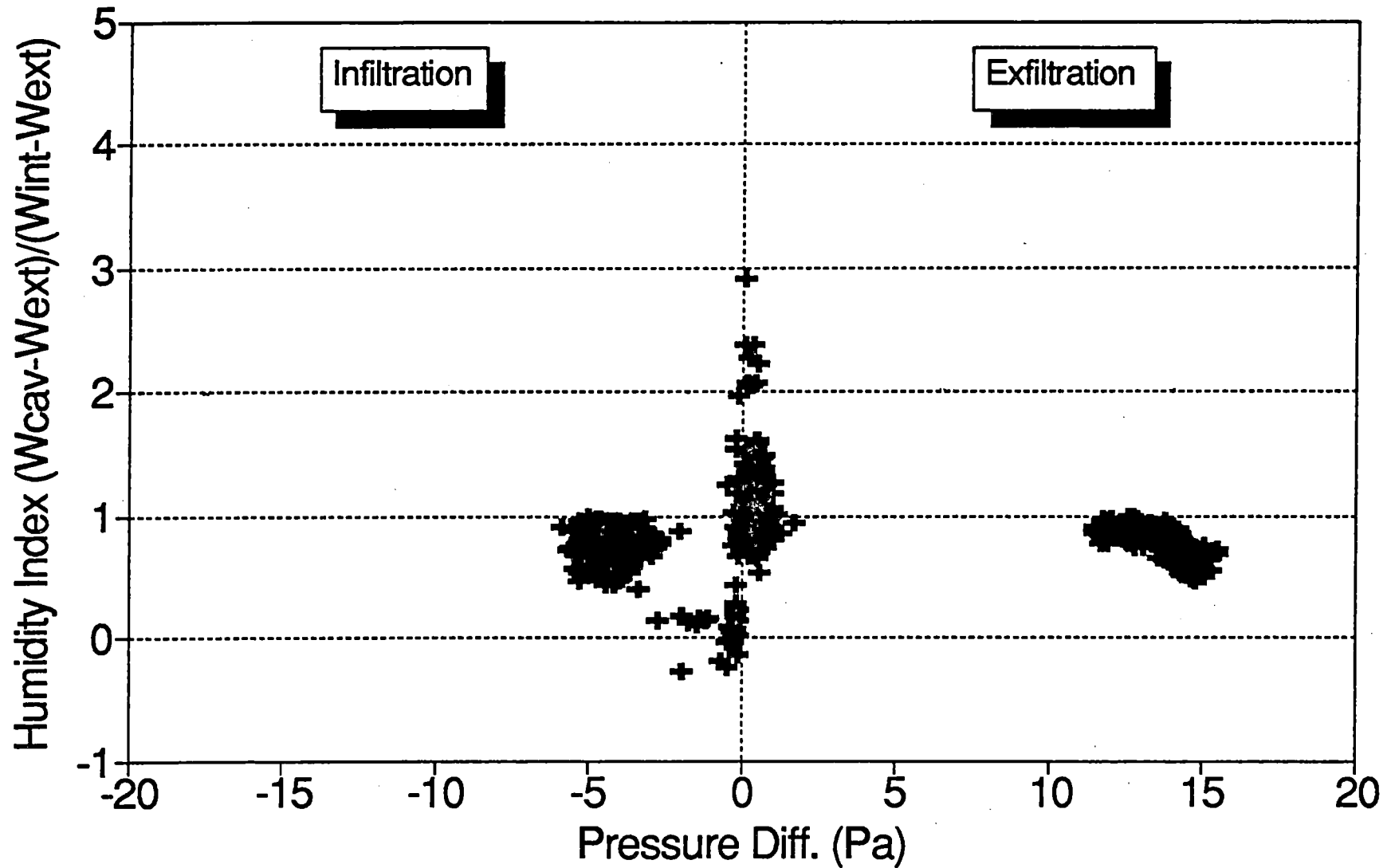
Stud Moisture Content
Winter: Panel A, (Sealed/Wood Siding)
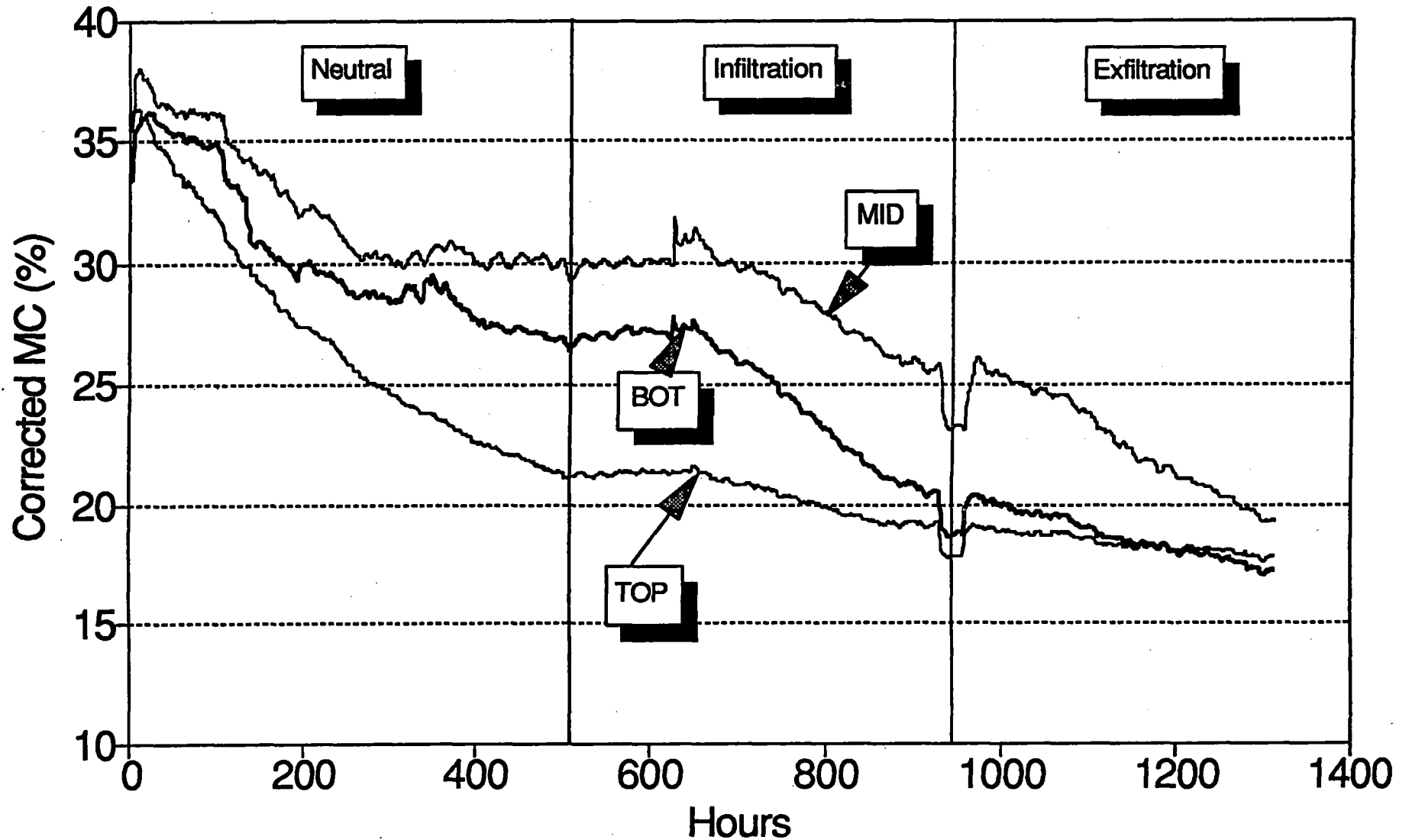
Stud Moisture Content
WINTER: Panel B, (Vented/Wood Siding)
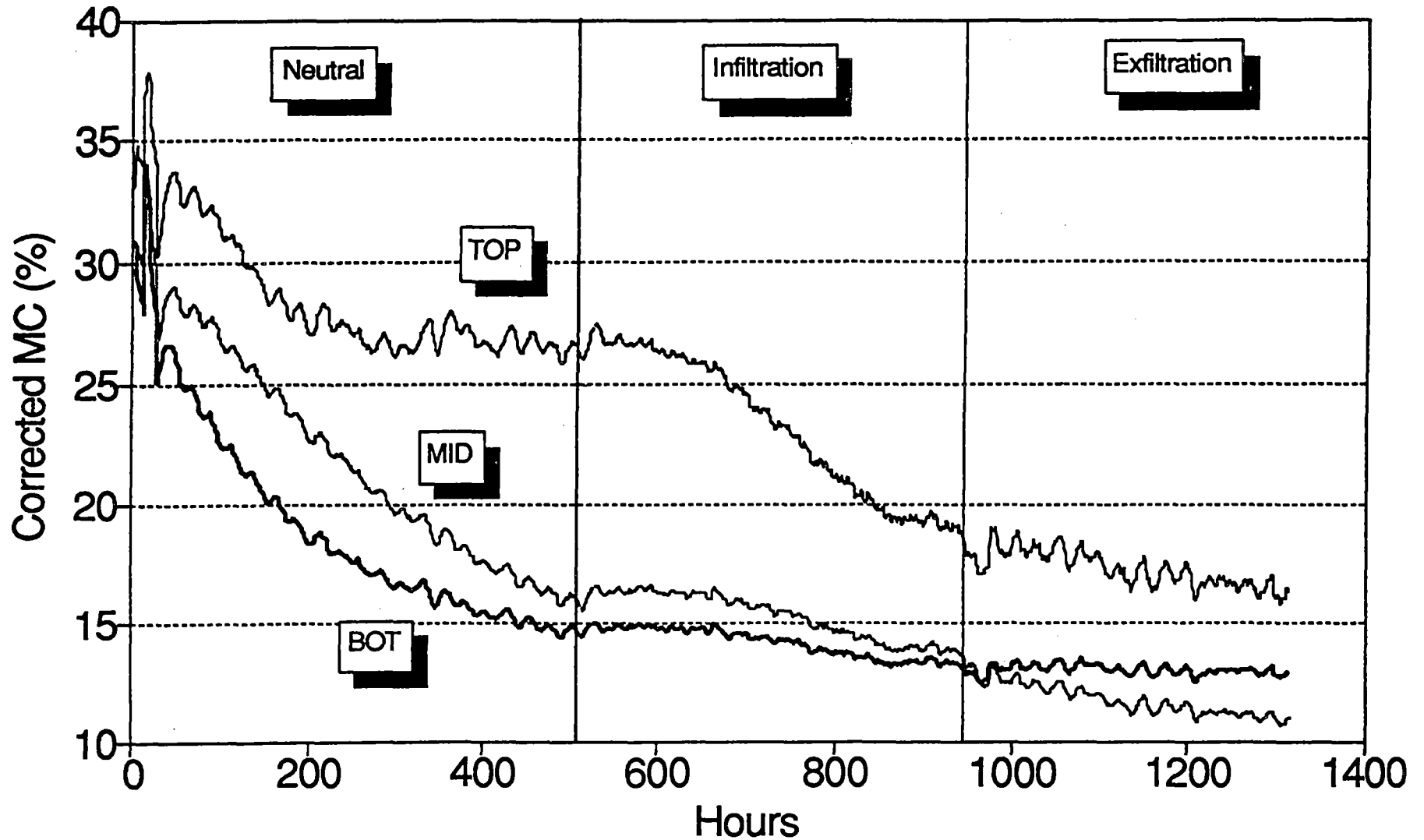
Stud Moisture Content
WINTER: Panel C, (Sealed/Vinyl Siding)
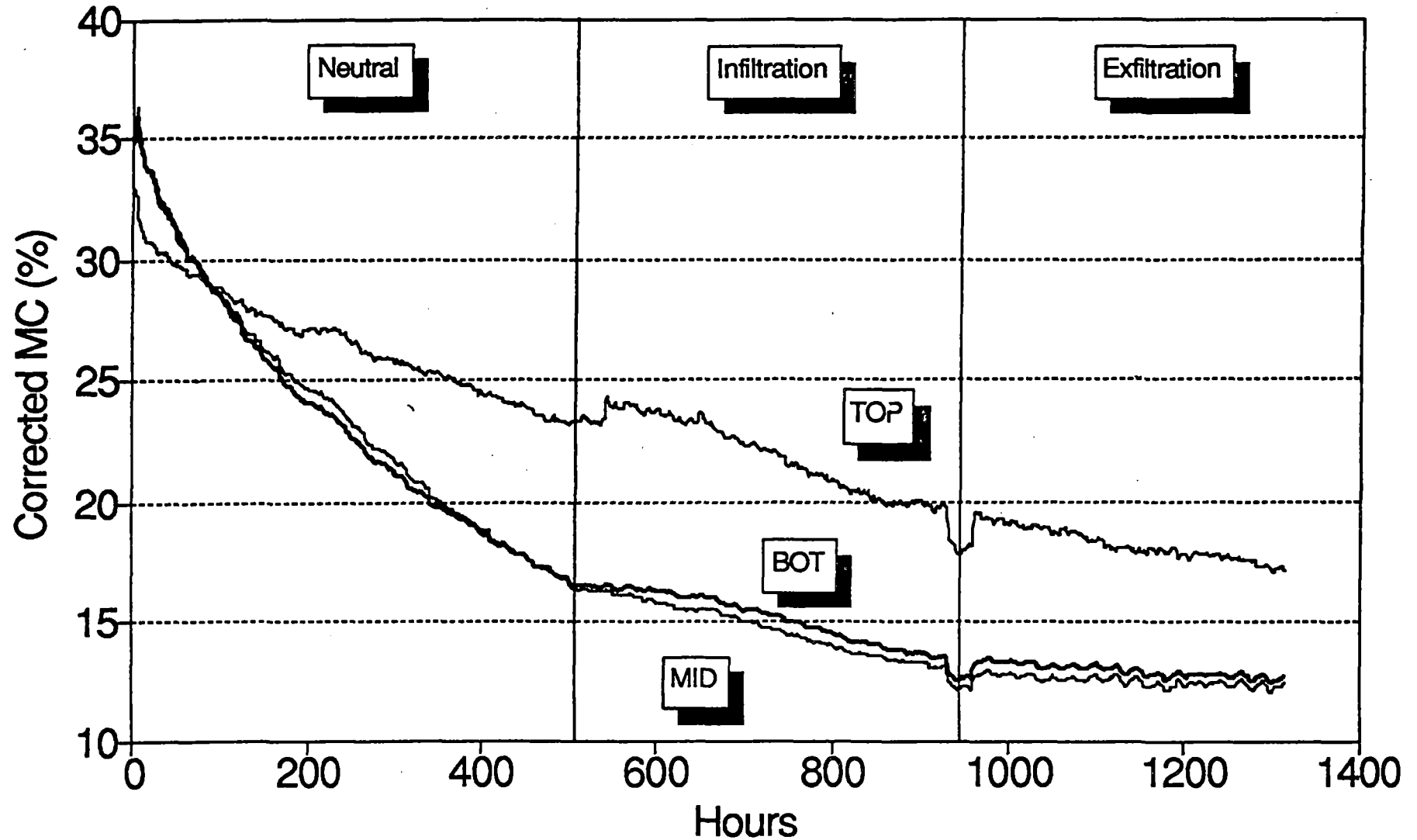
Stud Moisture Content
WINTER: Panel D, (Vented/Vinyl Siding)
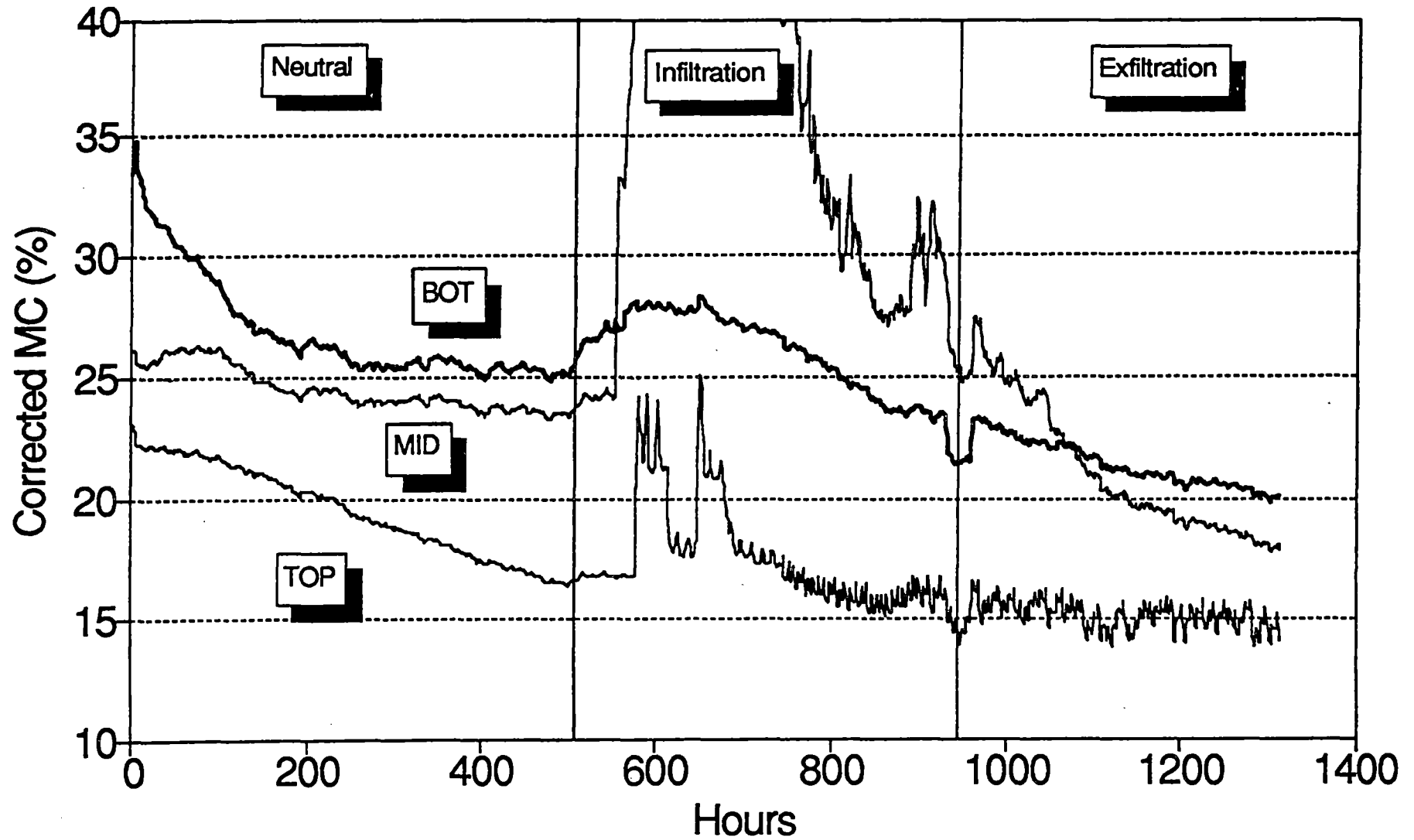
Stud Moisture Content
WINTER: Panel E, (Sealed/Vinyl/Strap)
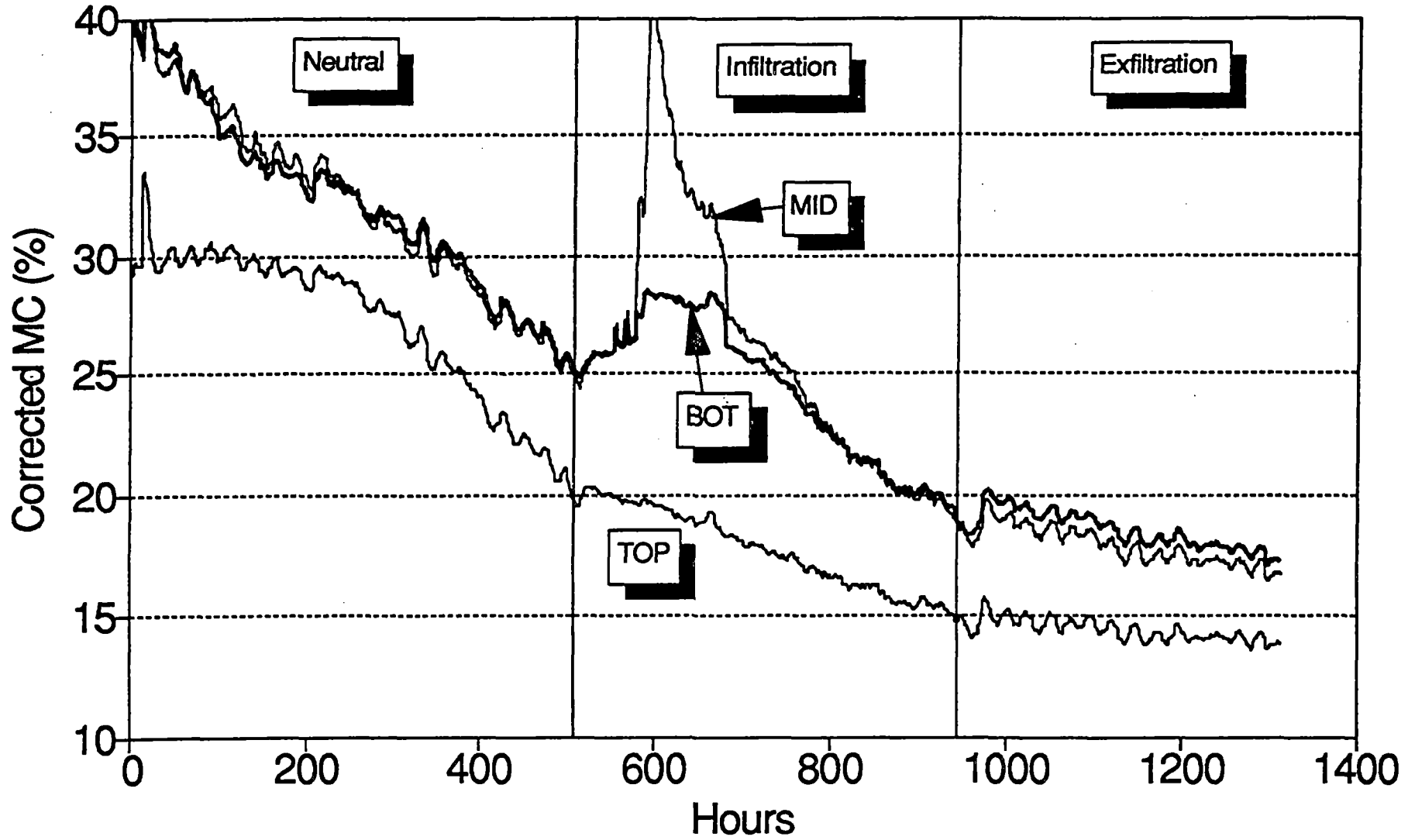
Stud Moisture Content
WINTER: Panel F, (Vented/Vinyl/Strap)
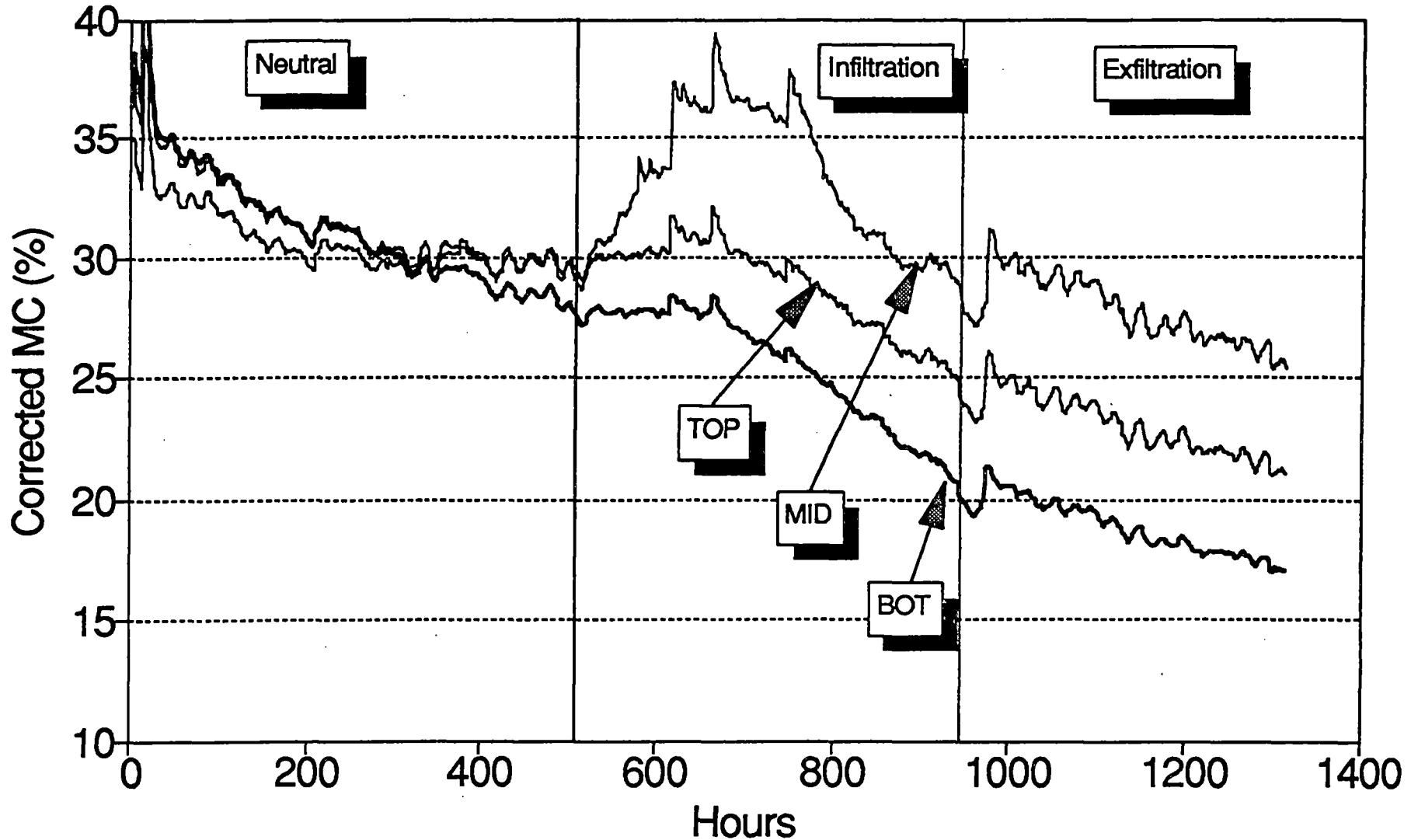
APPENDIX F
Moisture Content Graphs

Stud Moisture Content
SUMMER: Panel A, (Sealed/Wood Siding)

Neutral

Infiltration

Exfiltration

MID

TOP

BOT
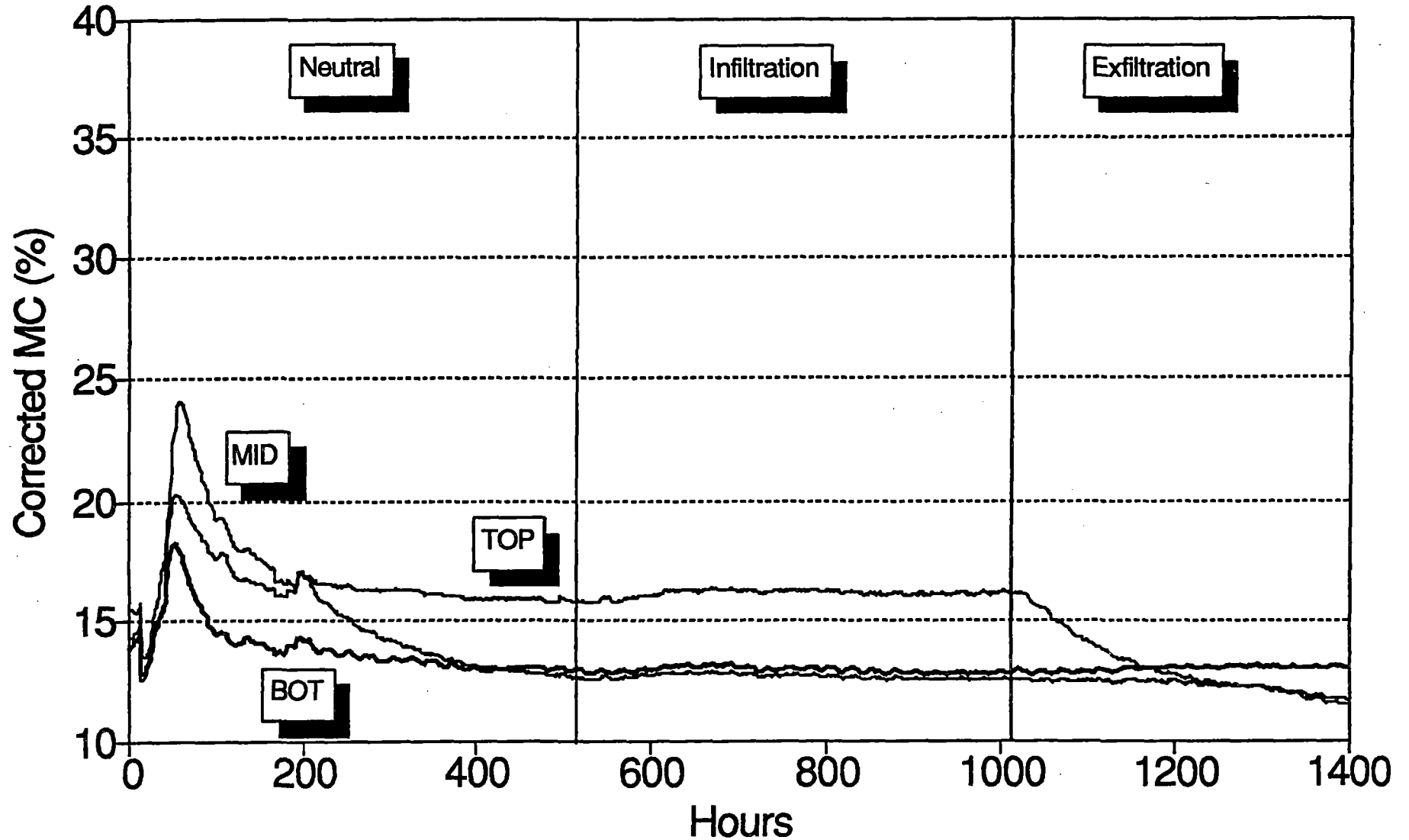
Stud Moisture Content
SUMMER: Panel B, (Vented/Vinyl Siding)
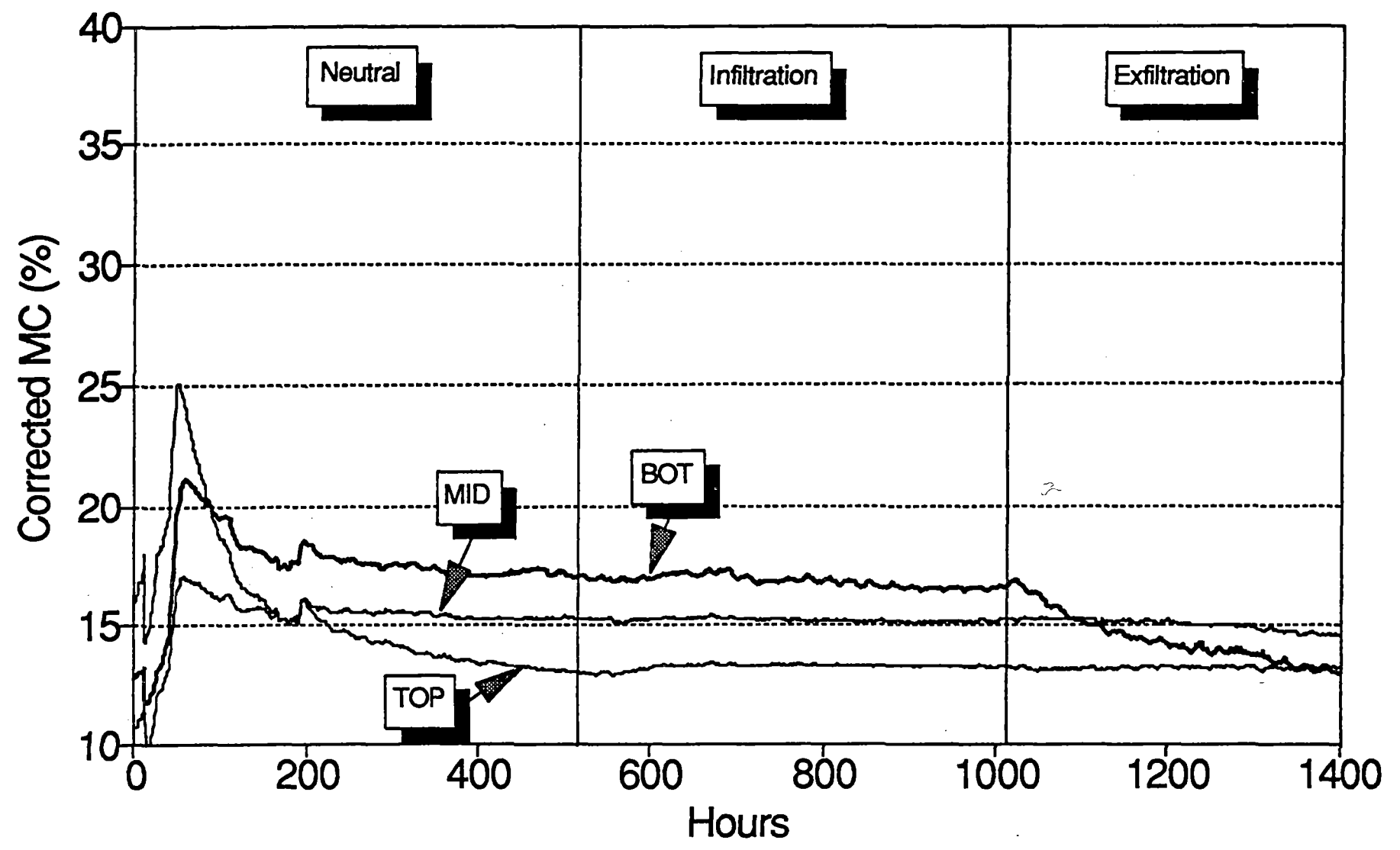
Stud Moisture Content
SUMMER: Panel C, (Sealed/Vinyl Siding)
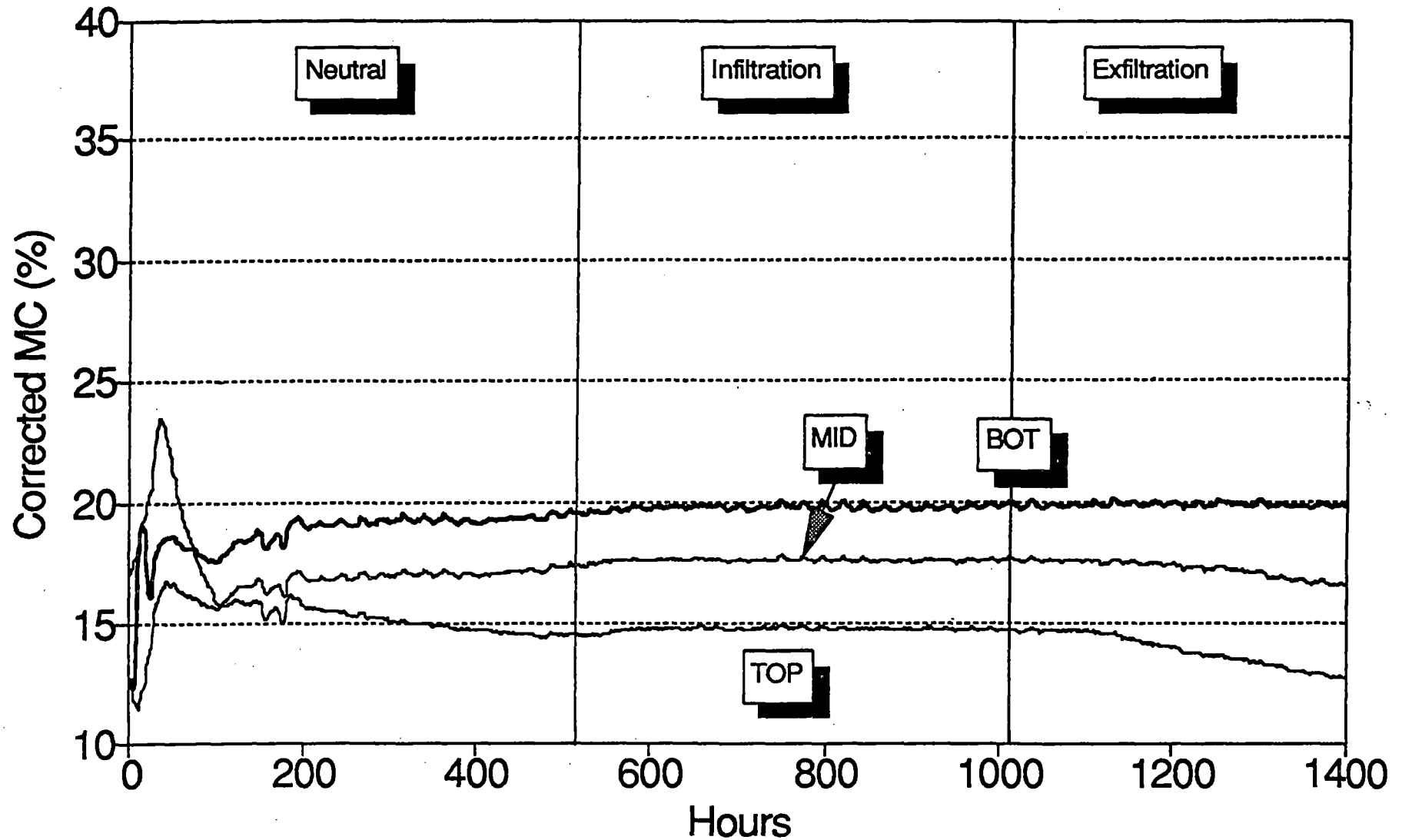
Stud Moisture Content
SUMMER: Panel D, (Vented/Vinyl Siding)
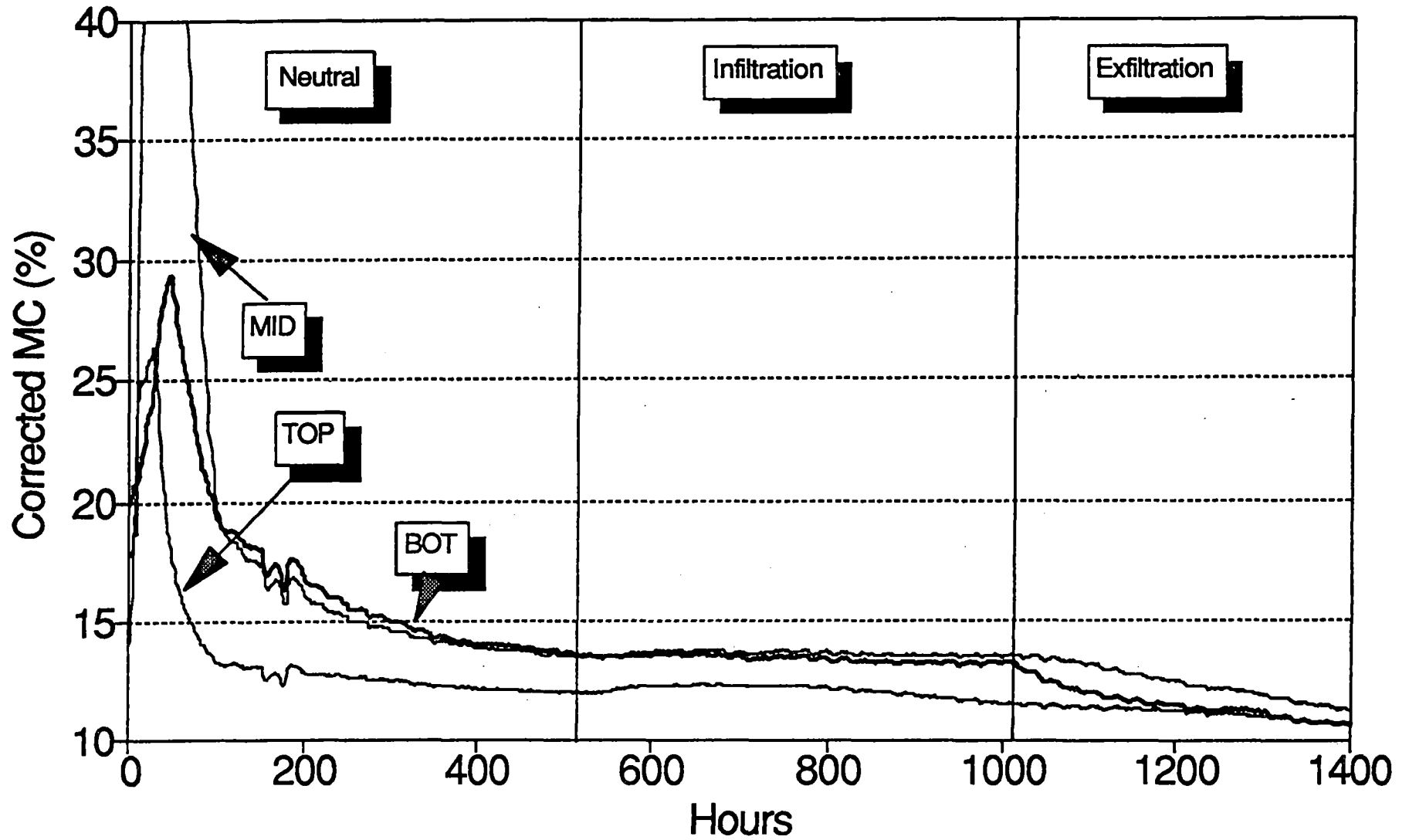
Stud Moisture Content
SUMMER: Panel E, (Sealed/Vinyl/Strap)
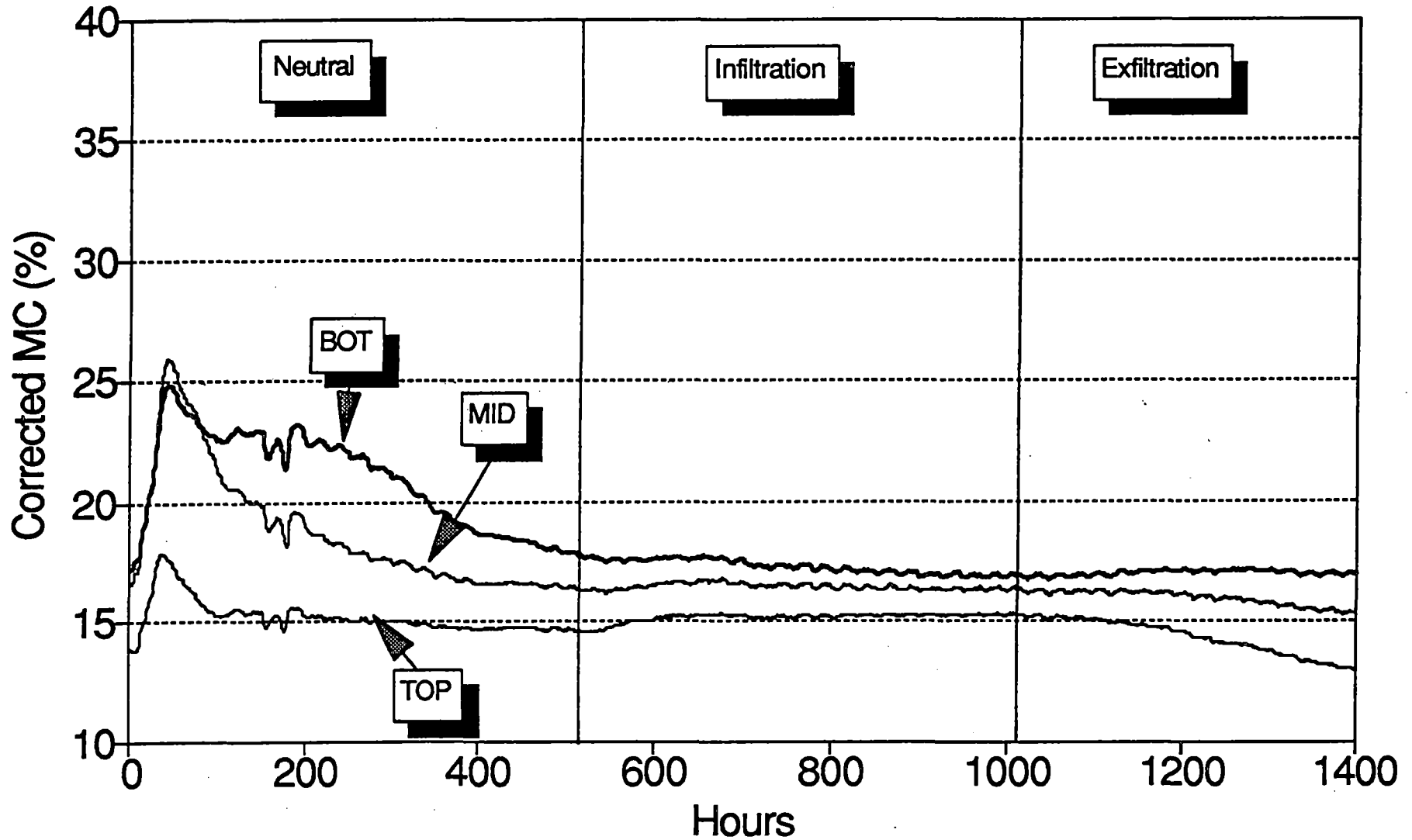
Stud Moisture Content
SUMMER: Panel F, (Vented/Vinyl/Strap)
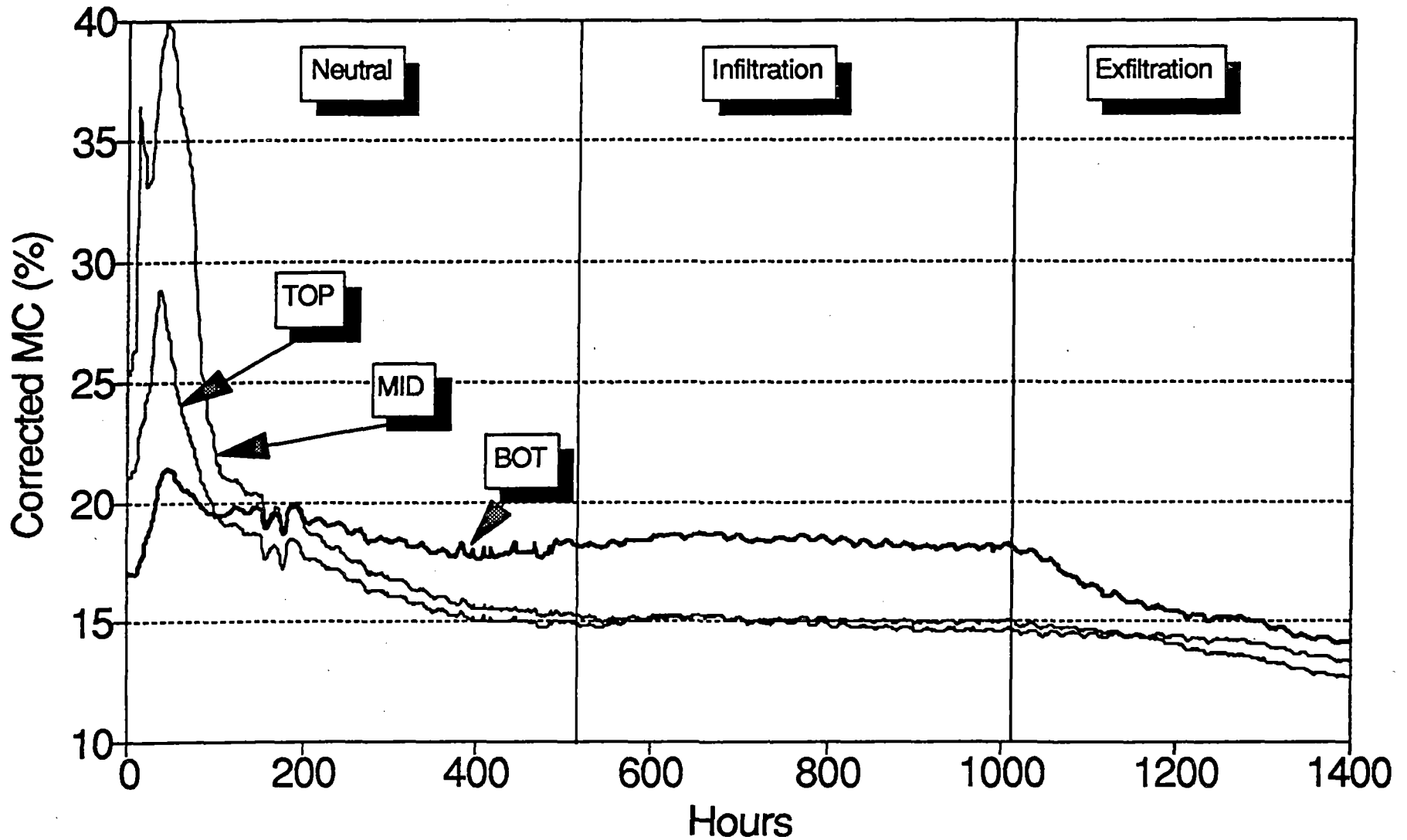
Sheathing Moisture Content (uncorr.)
Winter: Panel A, (Sealed/Wood Siding)
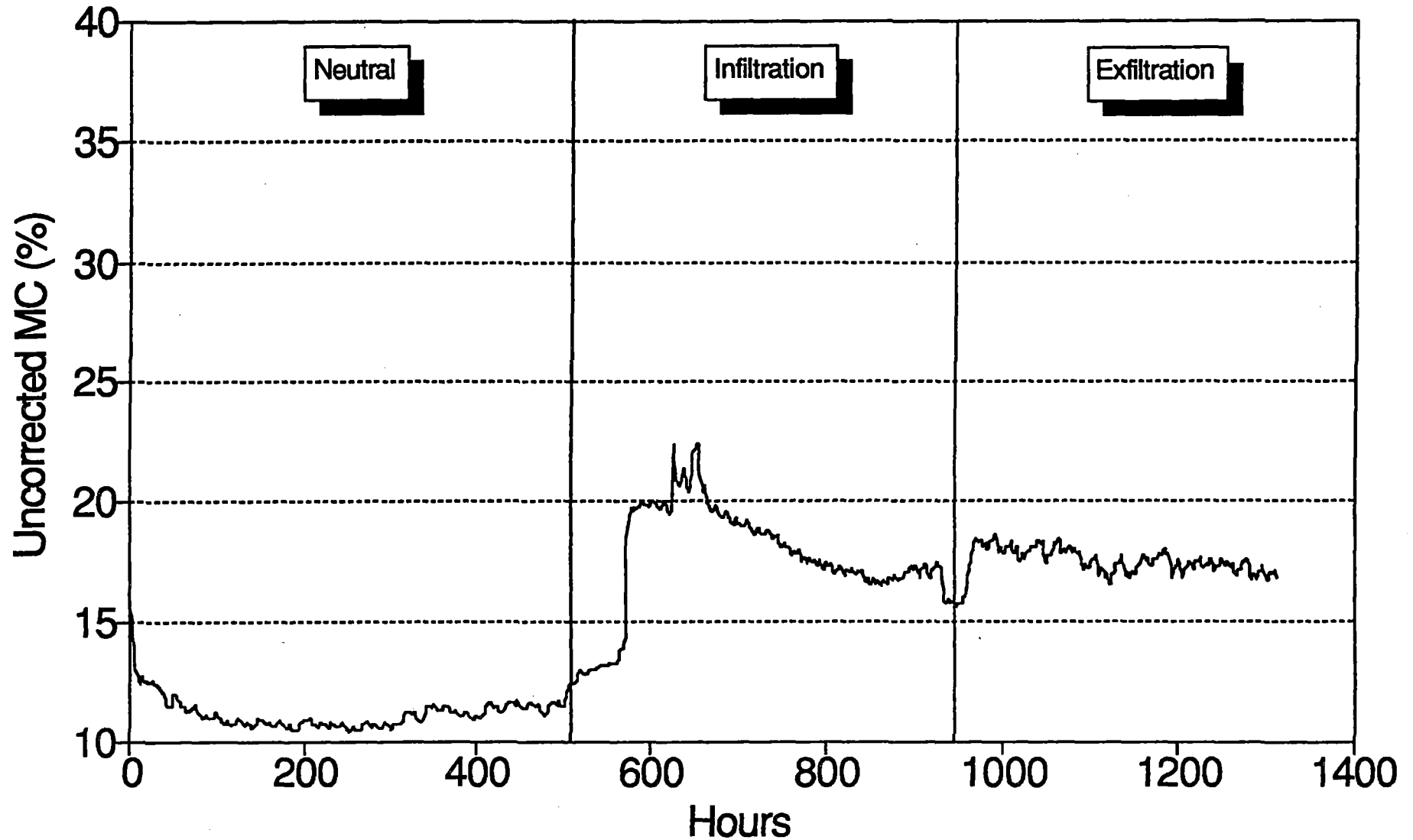
Sheathing Moisture Content (uncorr.)
SUMMER: Panel A, (Sealed/Wood Siding)
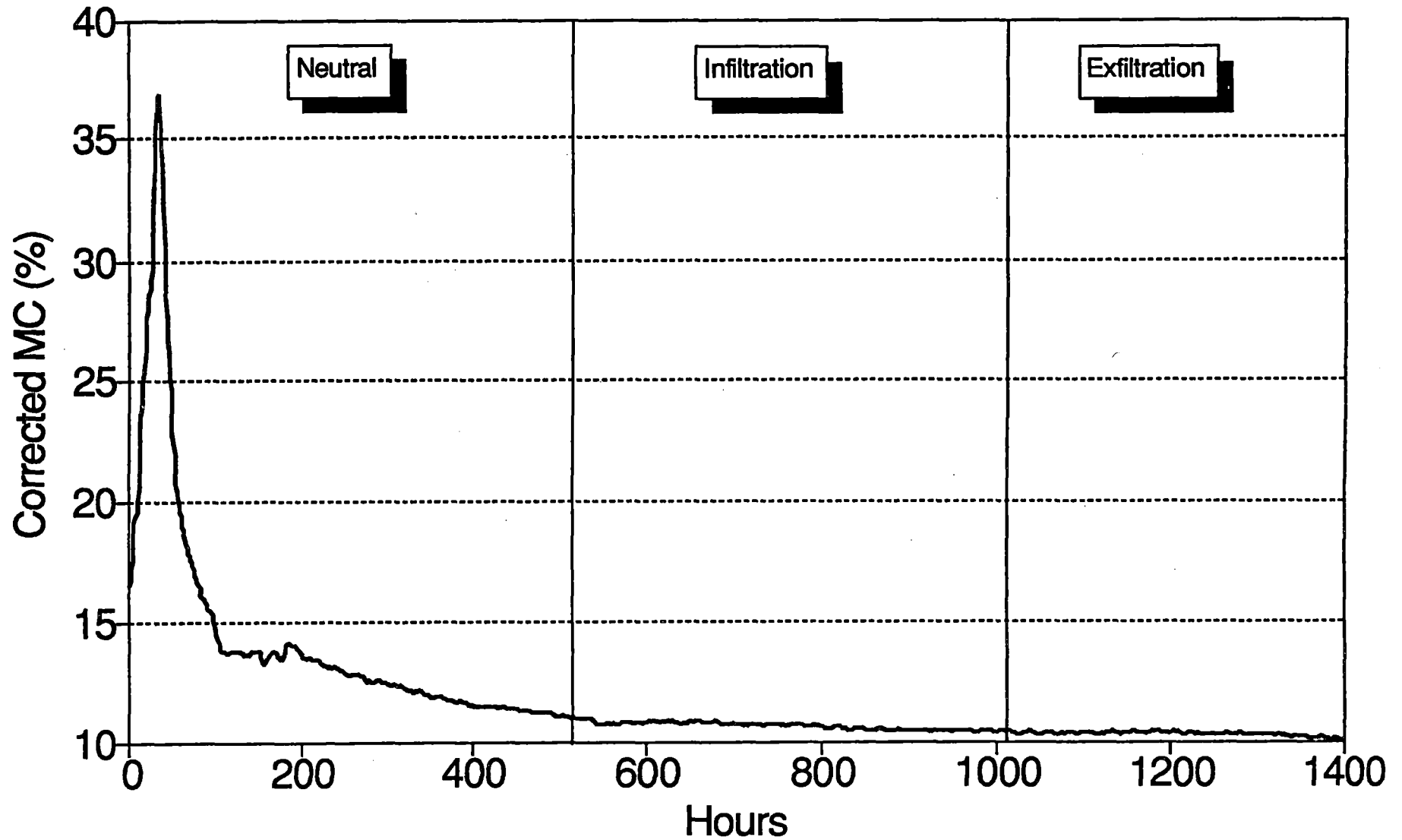
APPENDIX G
Sorption Isotherm Graphs

Sorption Calculations (Spruce, 20C)
Calculated and Measured Data
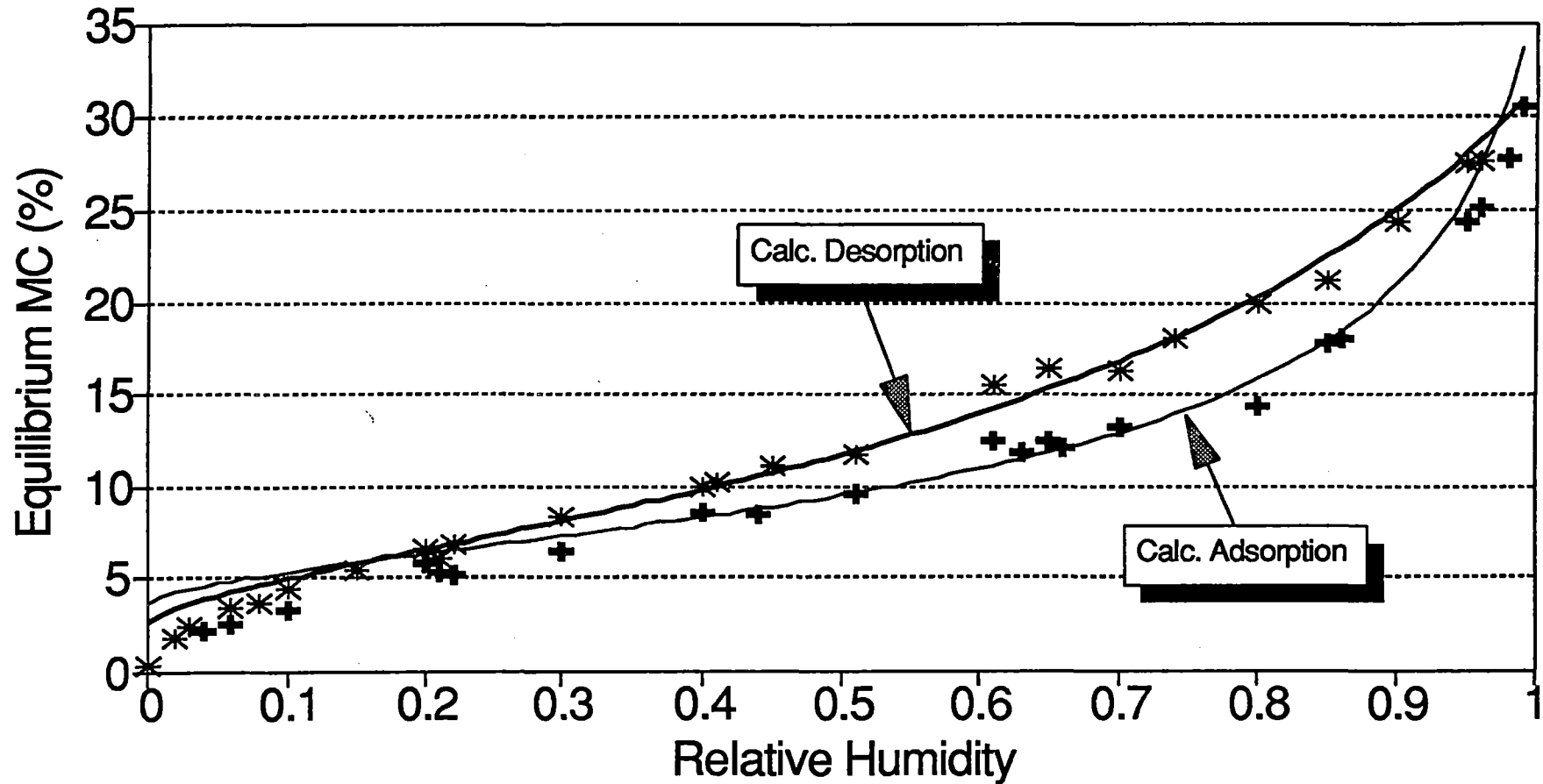
EMC vs Measured MC
WINTER: Panel A, (Sealed/Wood Siding)
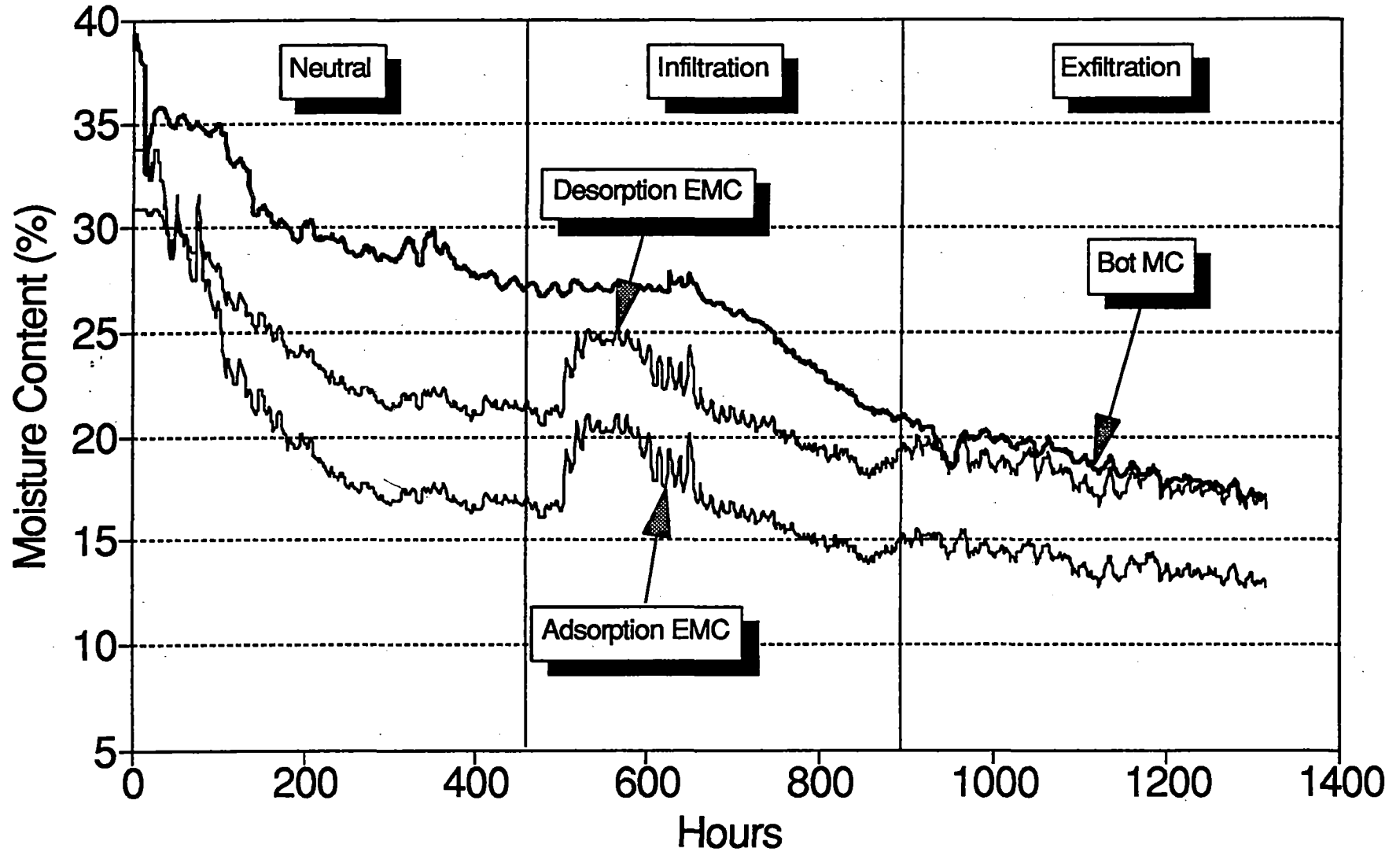
EMC vs Measured MC
WINTER: Panel B, (Vented/Wood Siding)
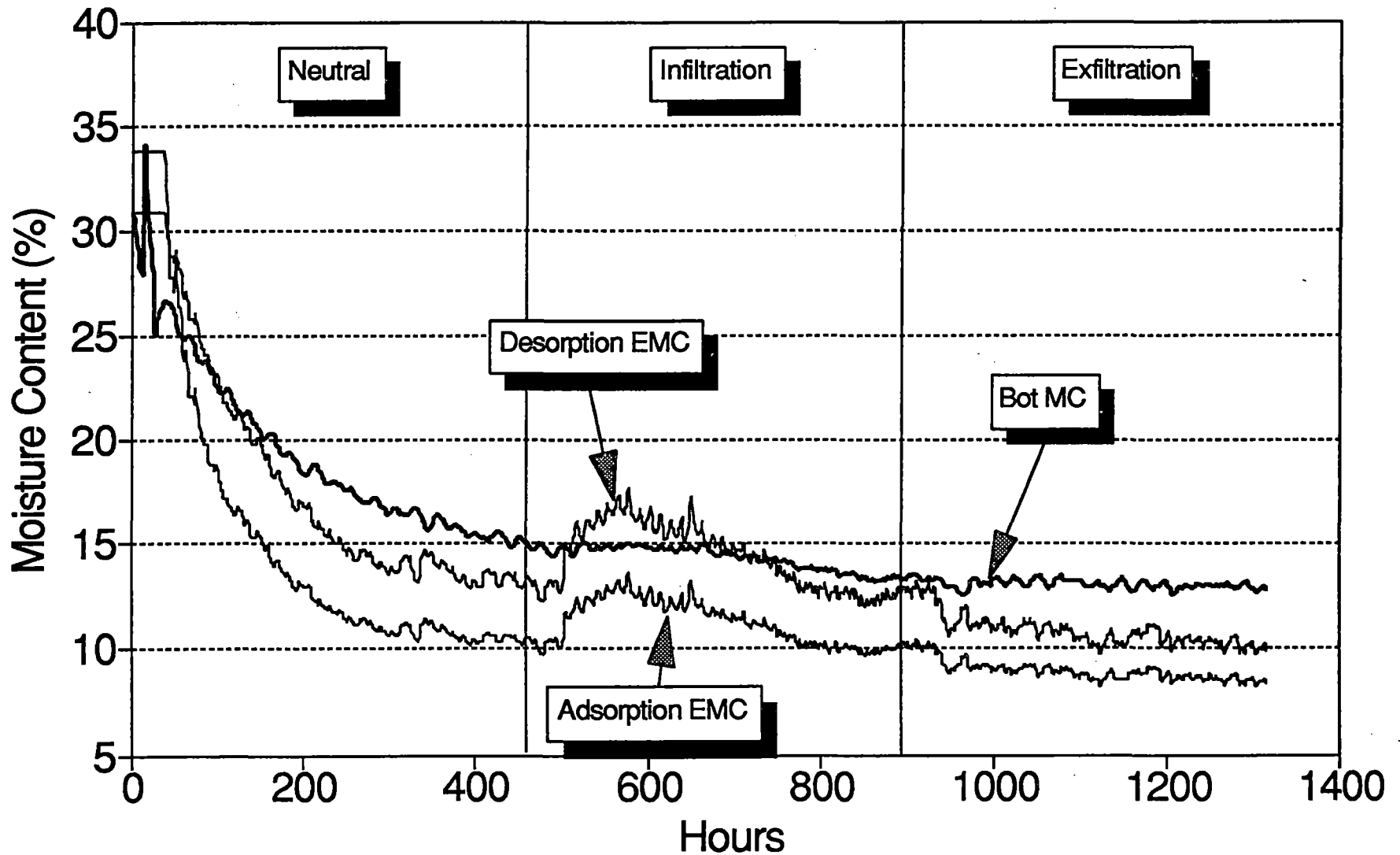
EMC vs Measured MC
SUMMER: Panel A, (Sealed/Wood Siding)
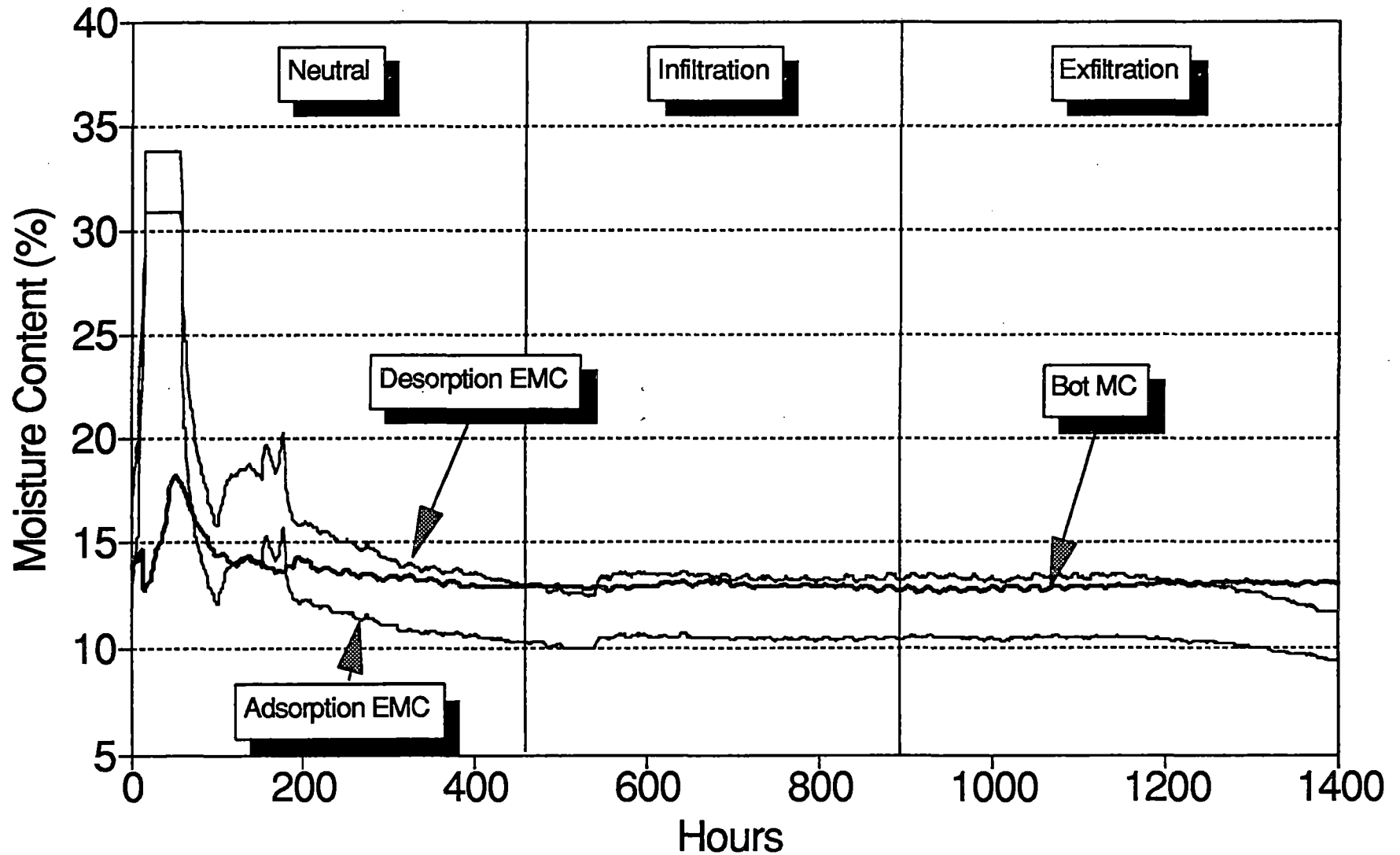
EMC vs Measured MC
SUMMER: Panel B, (Vented/Wood Siding)

Neutral

Infiltration

Exfiltration

Bot MC

Desorption EMC

Adsorption EMC

Moisture Content (%)

Hours
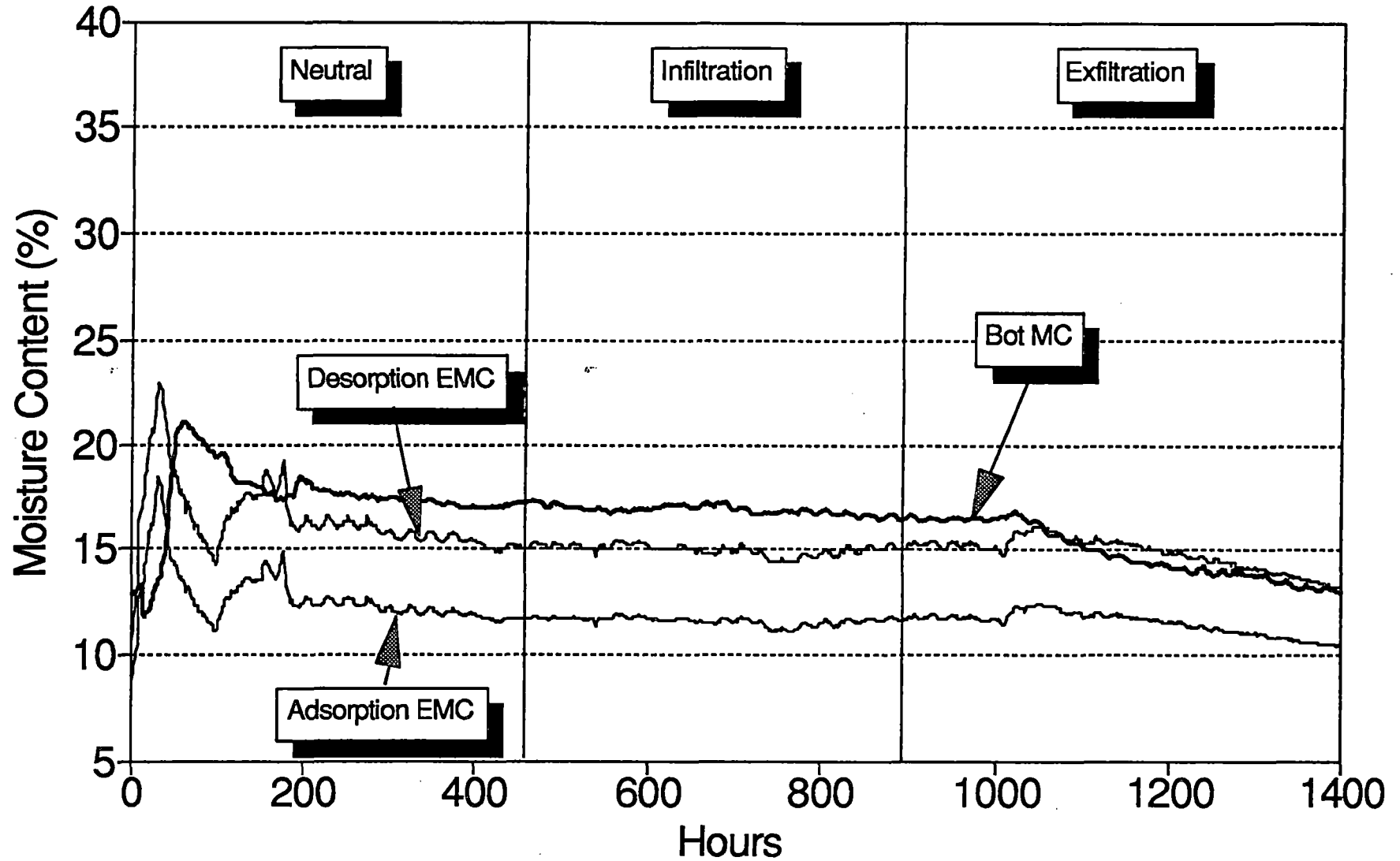
APPENDIX H
Weight Graphs

Panel Weight
PANEL A: SEALED, Wood Siding
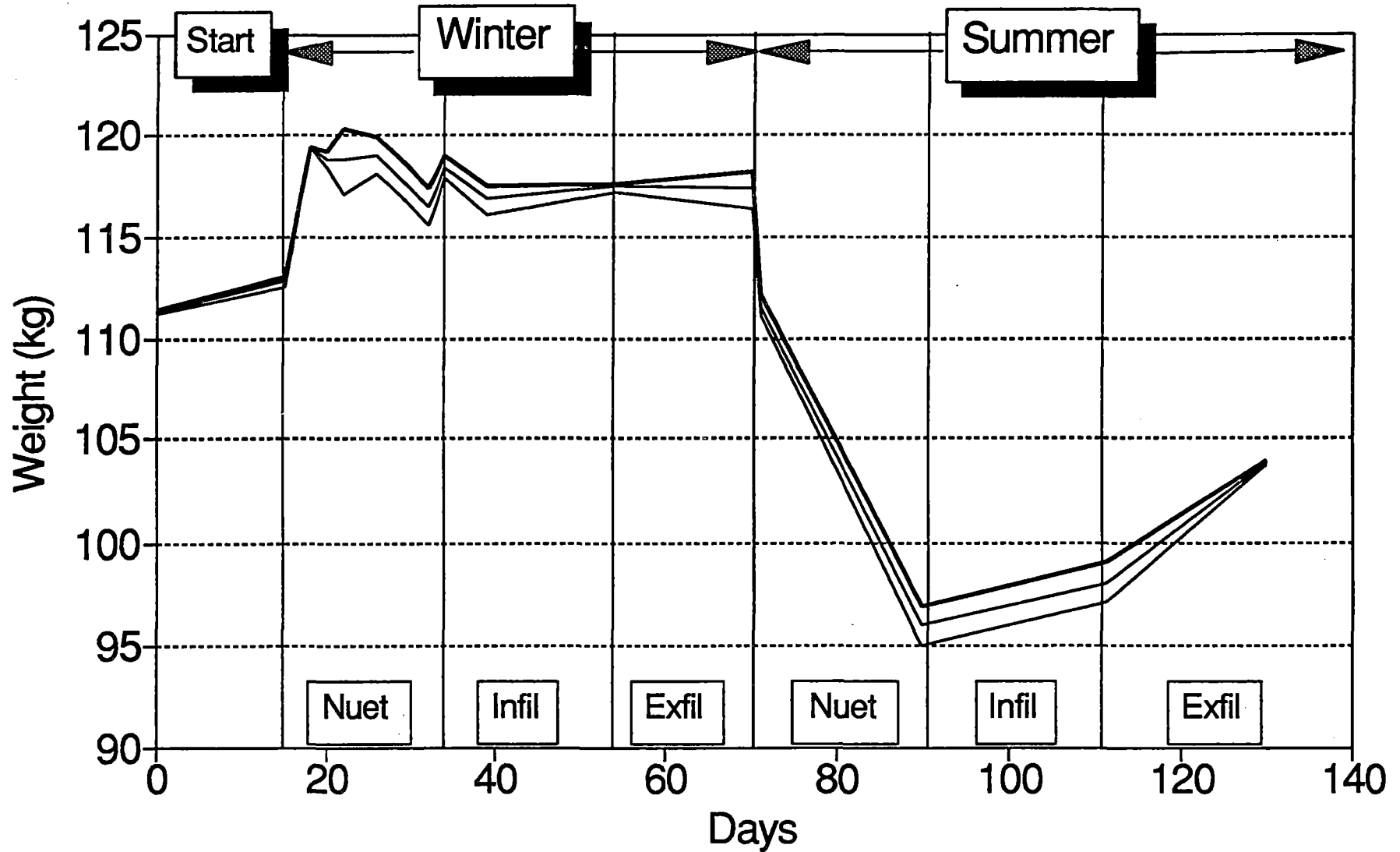
Chart Illustrates High, Low, and Median Measurements

Panel Weight
PANEL B: VENTED, Wood Siding

Start | Winter | Summer

Weight (kg)

125
120
115
110
105
100
95
90

Nuet | Infil | Exfil | Nuet | Infil | Exfil

0   20   40   60   80   100   120   140

Days
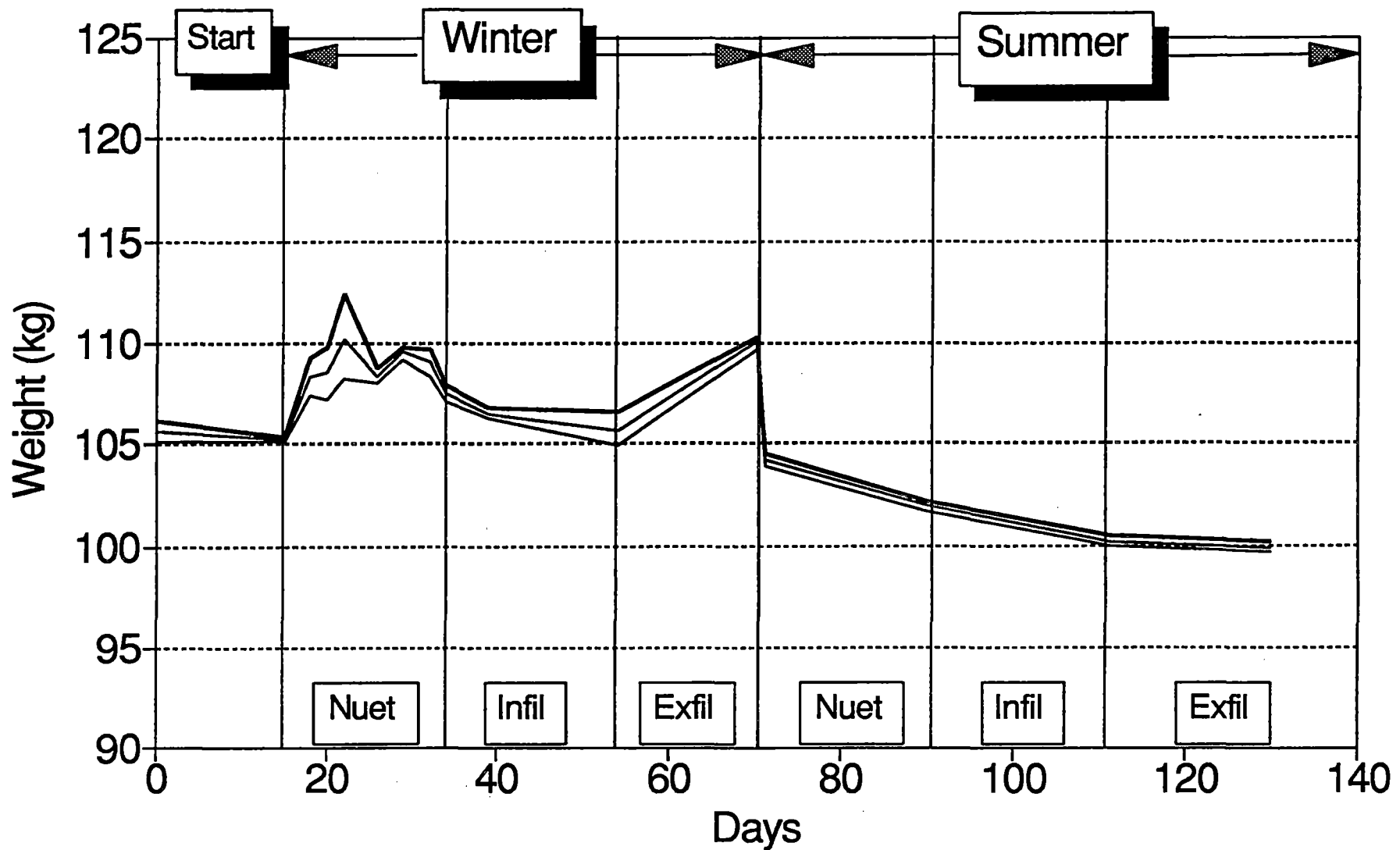
Chart Illustrates High, Low, and Median Measurements

APPENDIX I
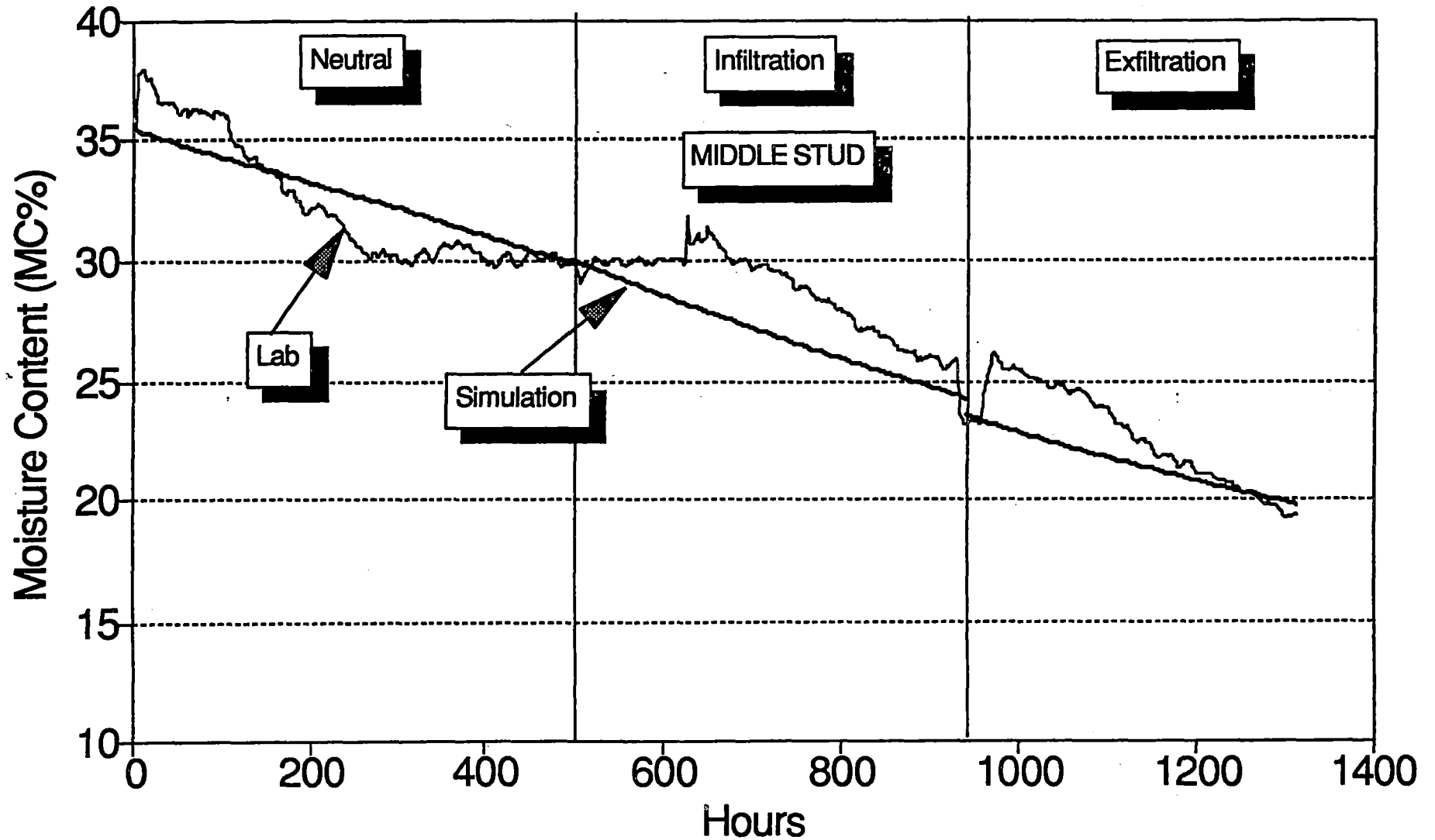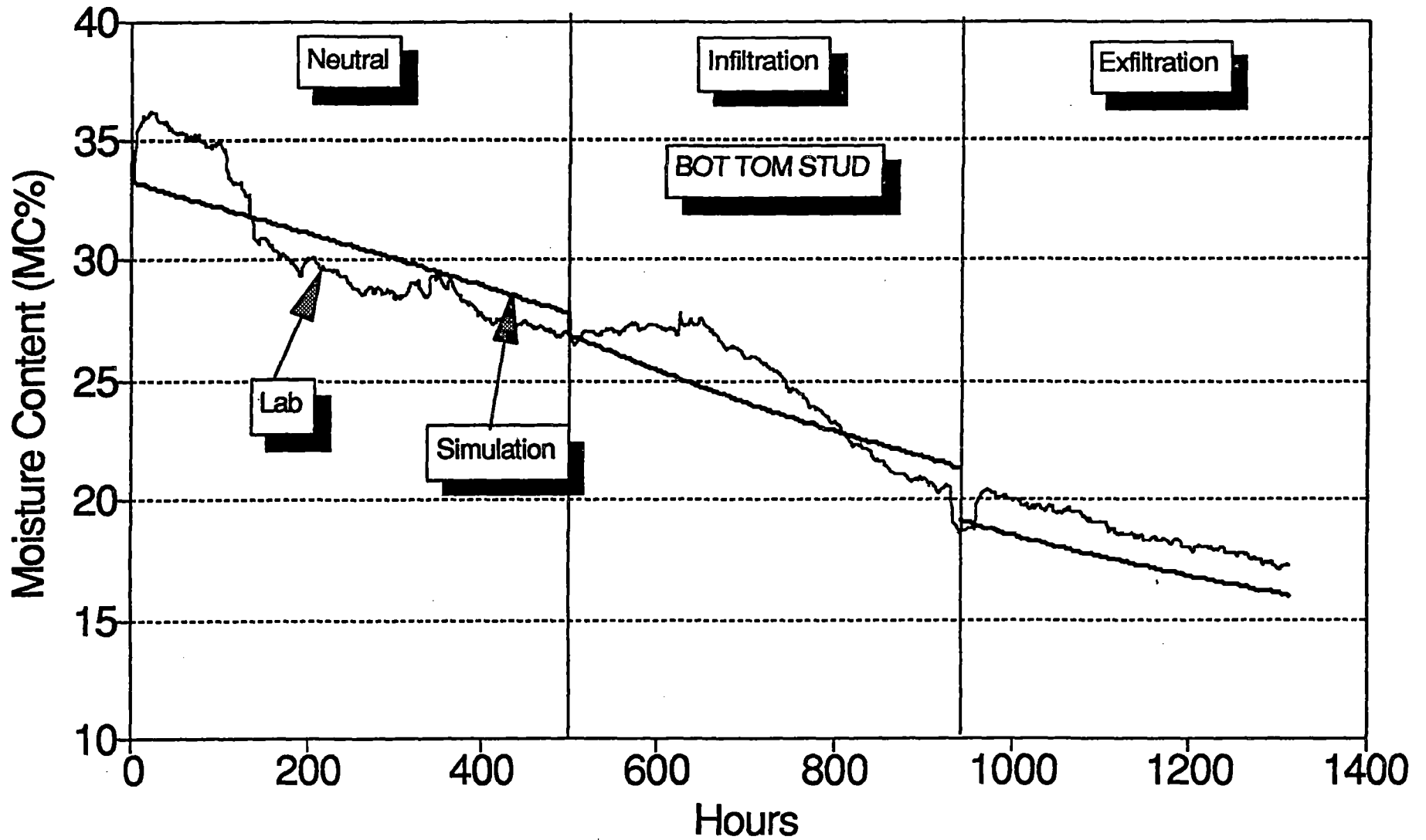## Laboratory/Simulation Comparison Graphs

LAB/SIM MC Comparisons
WINTER: Panel A, (Sealed/Wood Siding)

LAB/SIM MC Comparisons
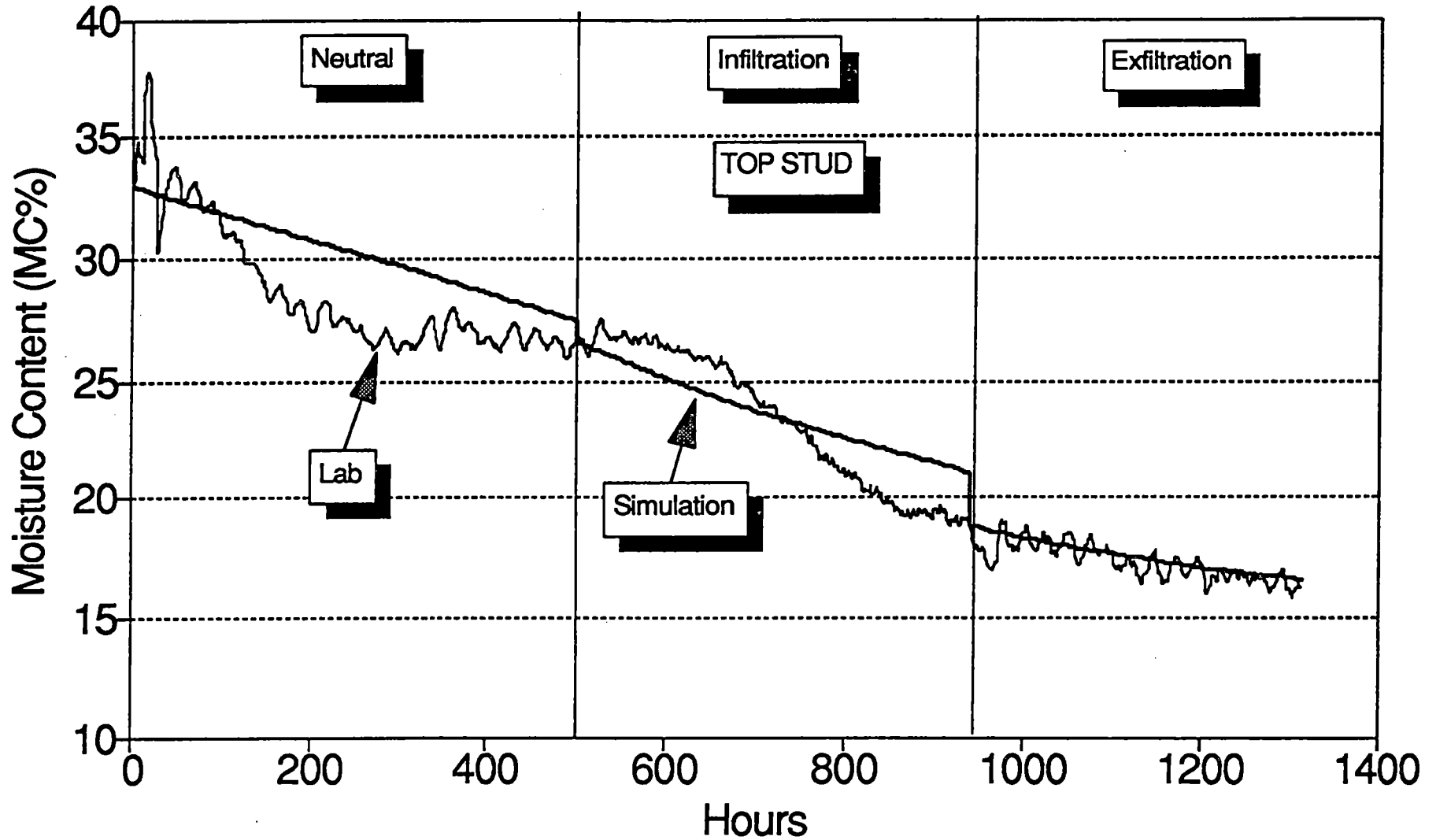WINTER: Panel A, (Sealed/Wood Siding)

LAB/SIM MC Comparisons
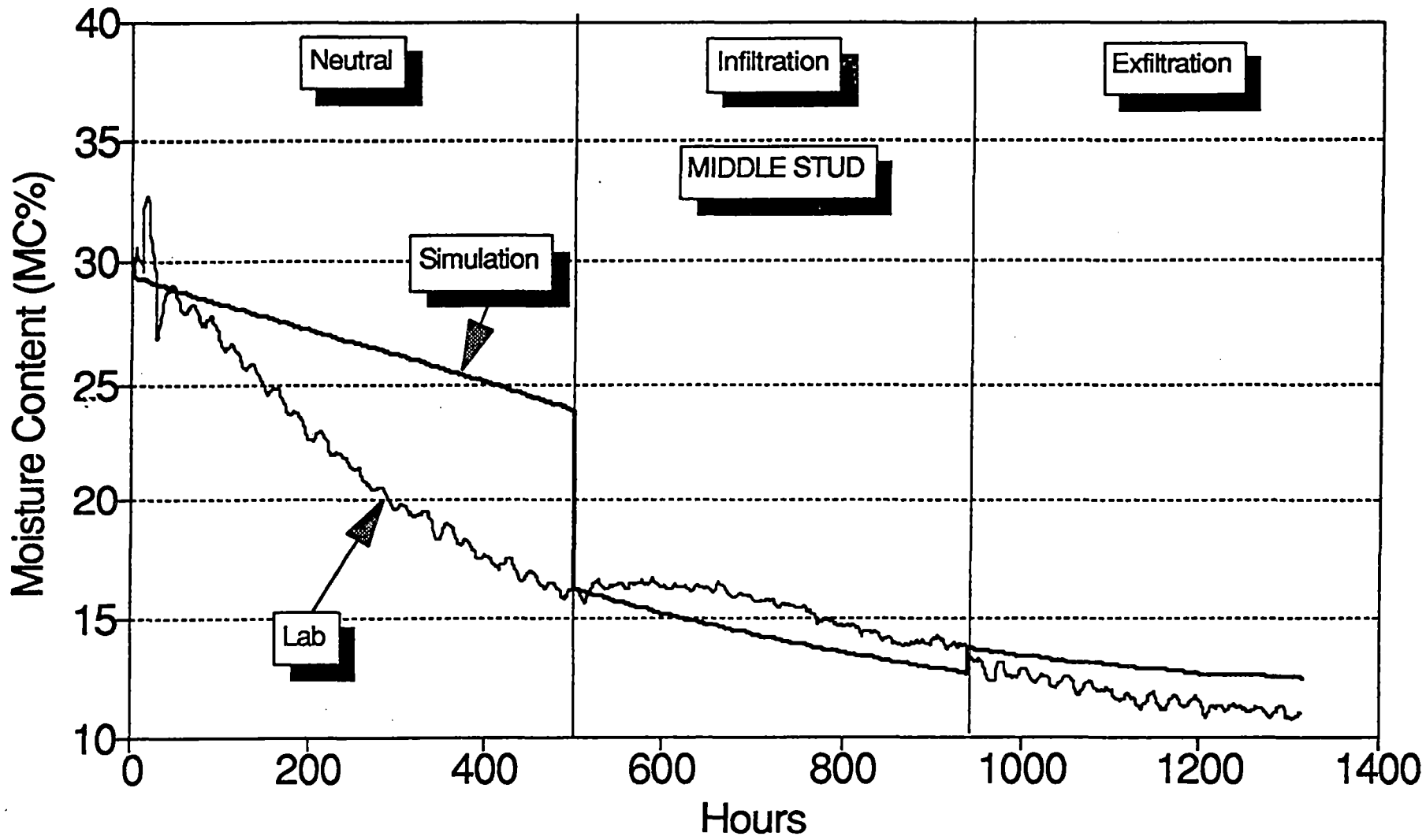## WINTER: Panel A, (Sealed/Wood Siding)

LAB/SIM MC Comparisons
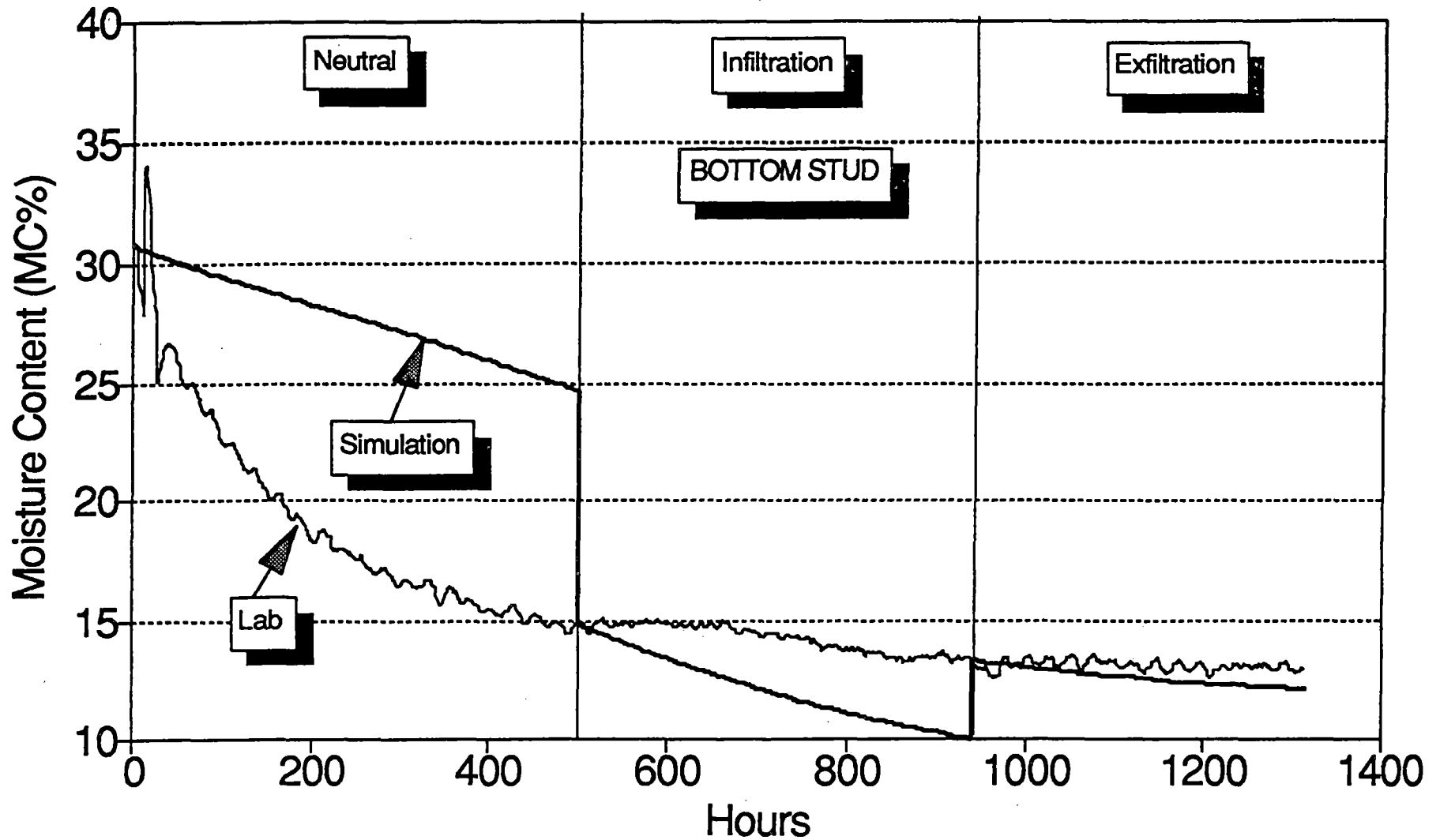## WINTER: Panel B, (Vented/Wood Siding)

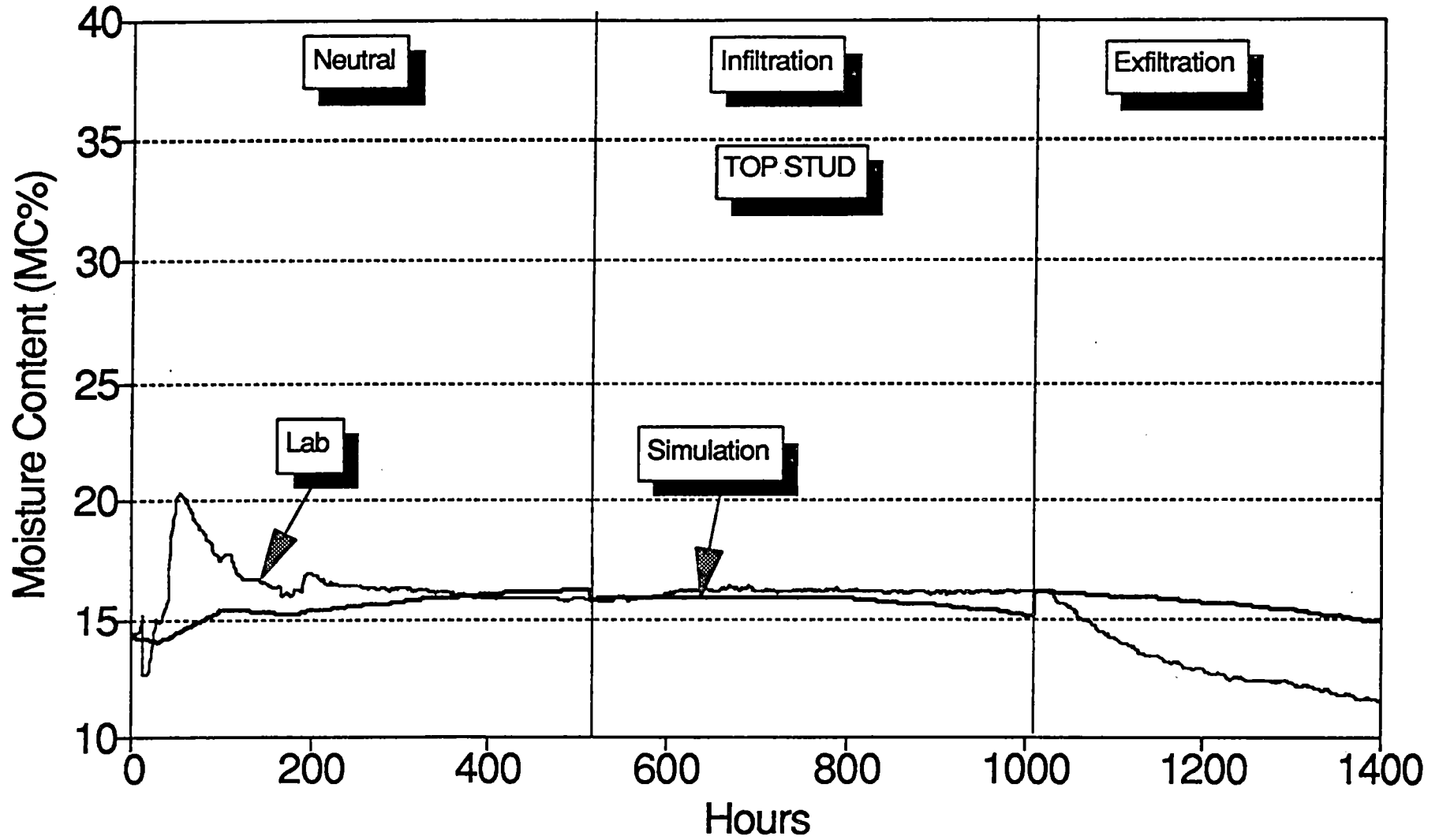# LAB/SIM MC Comparisons
WINTER: Panel B, (Vented/Wood Siding)

LAB/SIM MC Comparisons
WINTER: Panel B, (Vented/Wood Siding)

LAB/SIM MC Comparisons
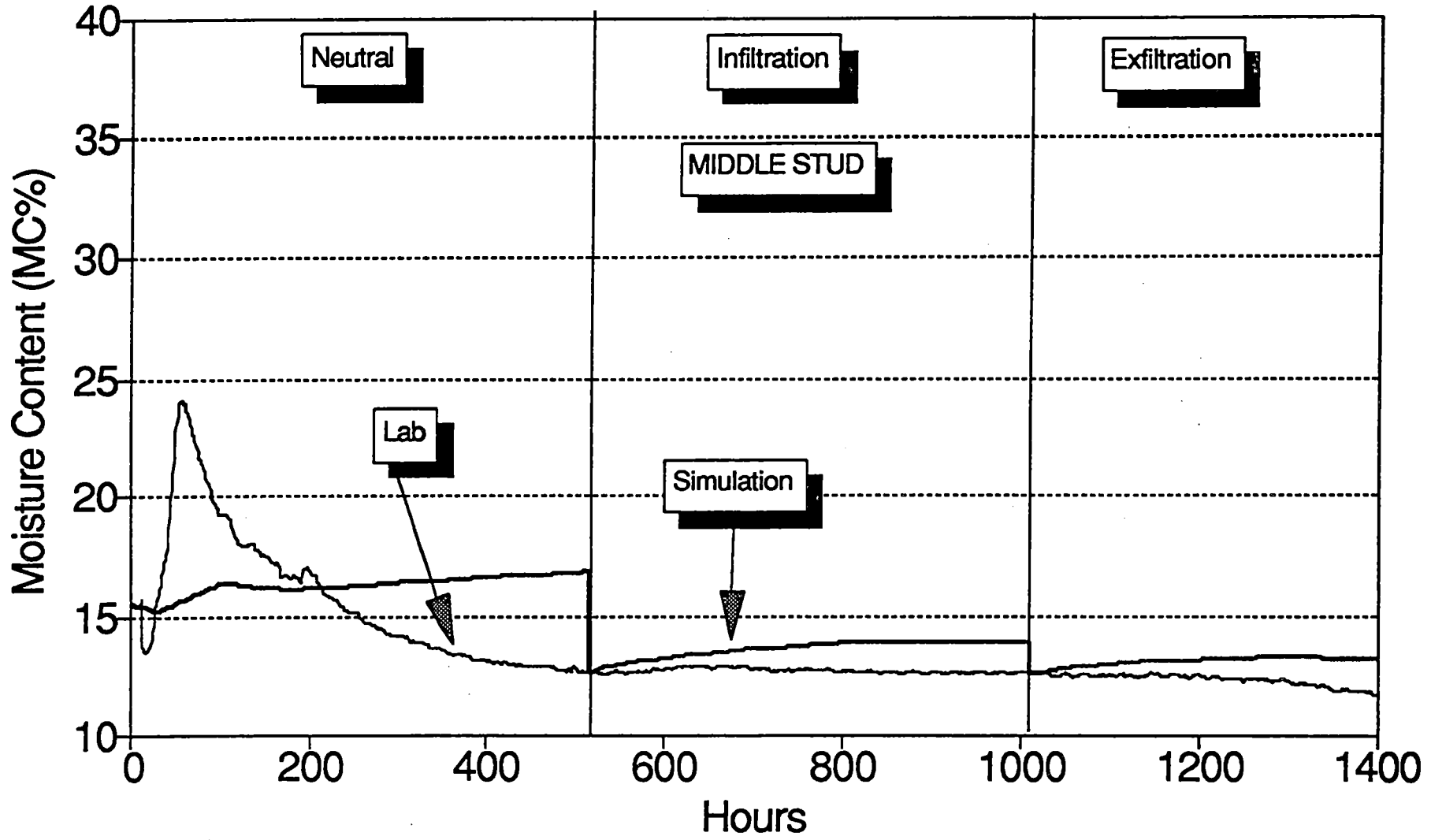SUMMER: Panel A, (Sealed/Wood Siding)

LAB/SIM MC Comparisons
SUMMER: Panel A, (Sealed/Wood Siding)

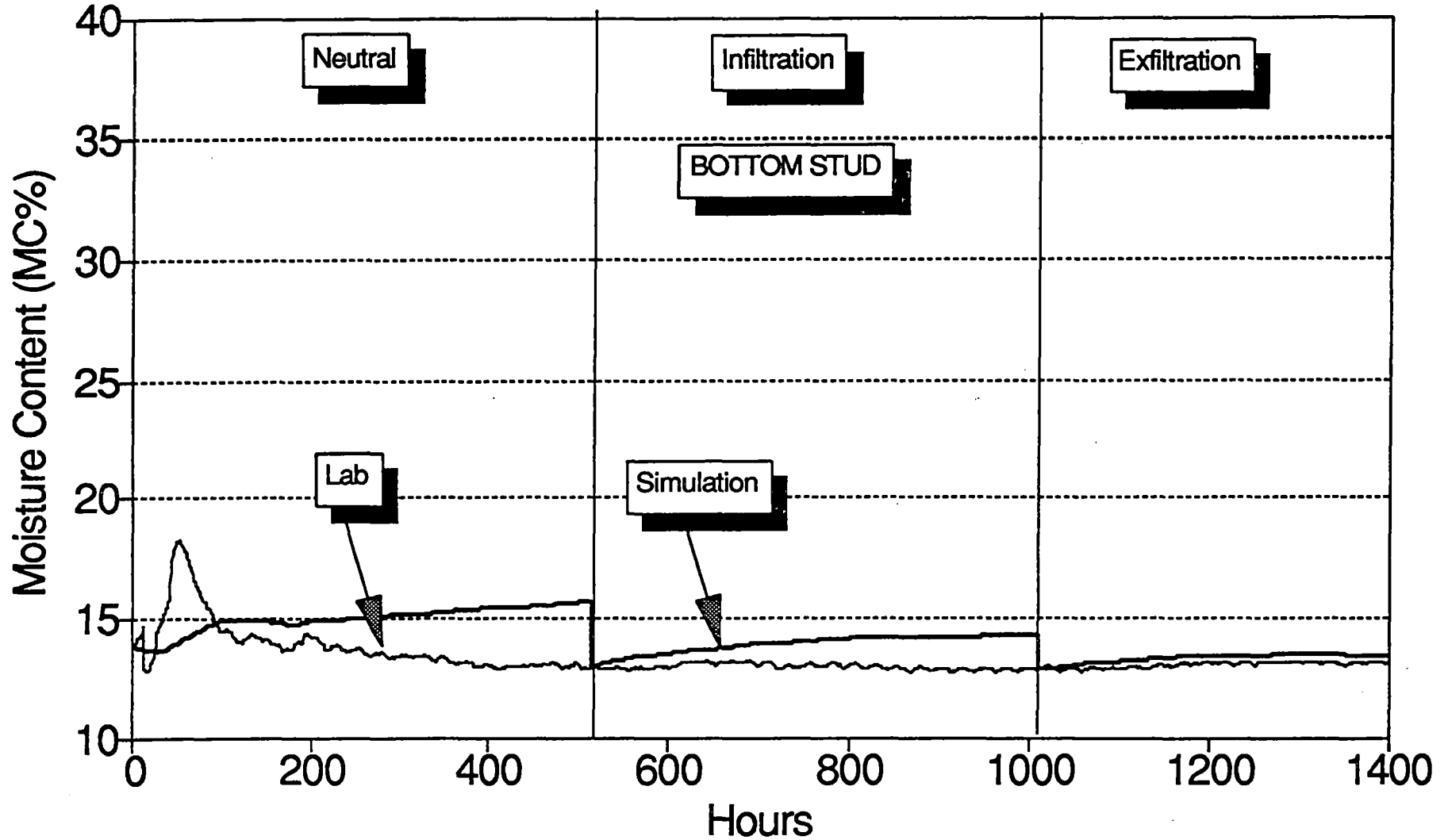## LAB/SIM MC Comparisons
SUMMER: Panel A, (Sealed/Wood Siding)

LAB/SIM MC Comparisons
SUMMER: Panel B, (Vented/Wood Siding)

LAB/SIM MC Comparisons
SUMMER: Panel B, (Vented/Wood Siding)

LAB/SIM MC Comparisons
SUMMER: Panel B, (Vented/Wood Siding)

WALLDRY Air Flow Sensitivity
WINTER: Panel A,(Sealed), Bottom Stud
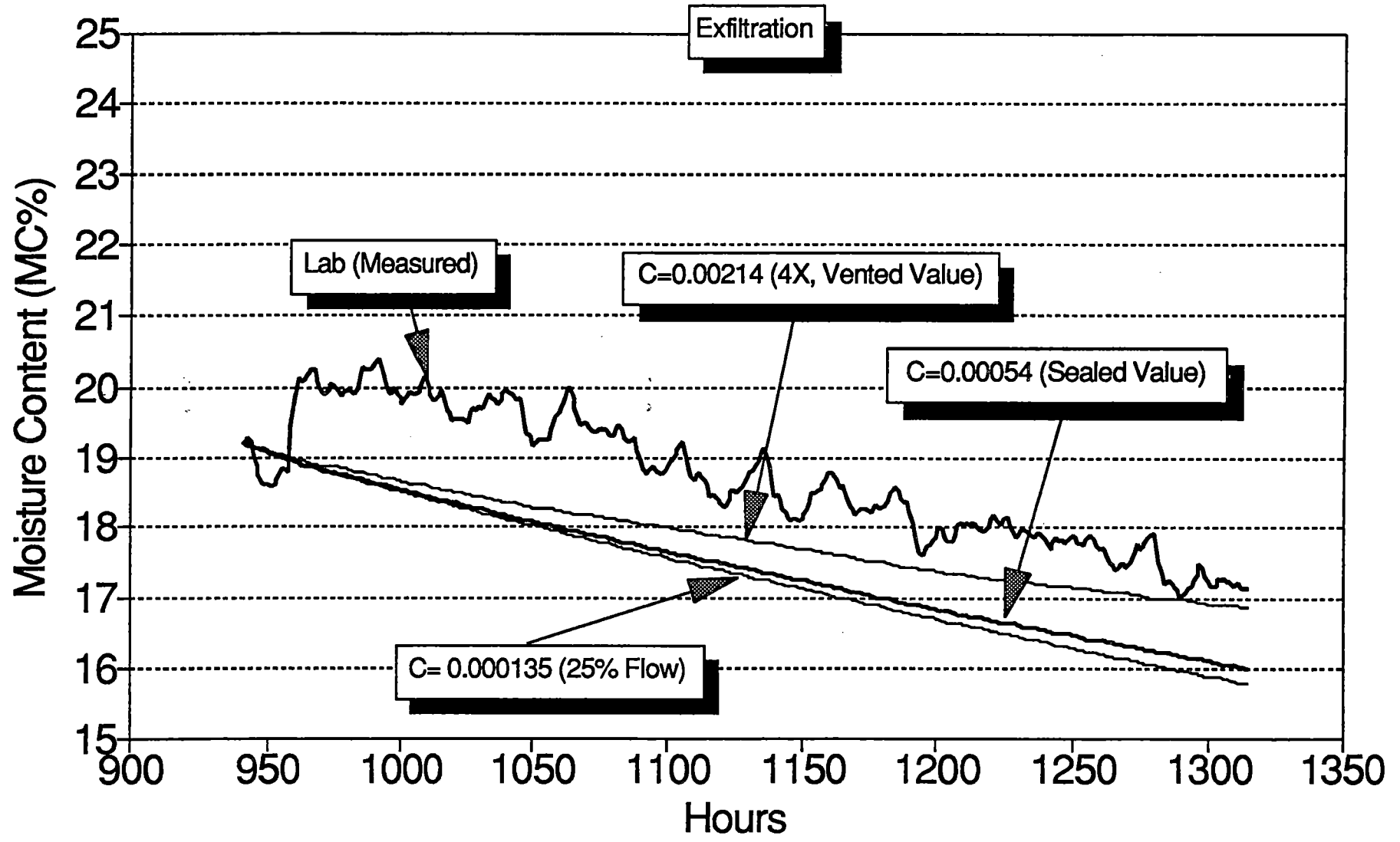
WALLDRY Air Flow Sensitivity
WINTER: Panel B,(Vented), Bottom Stud
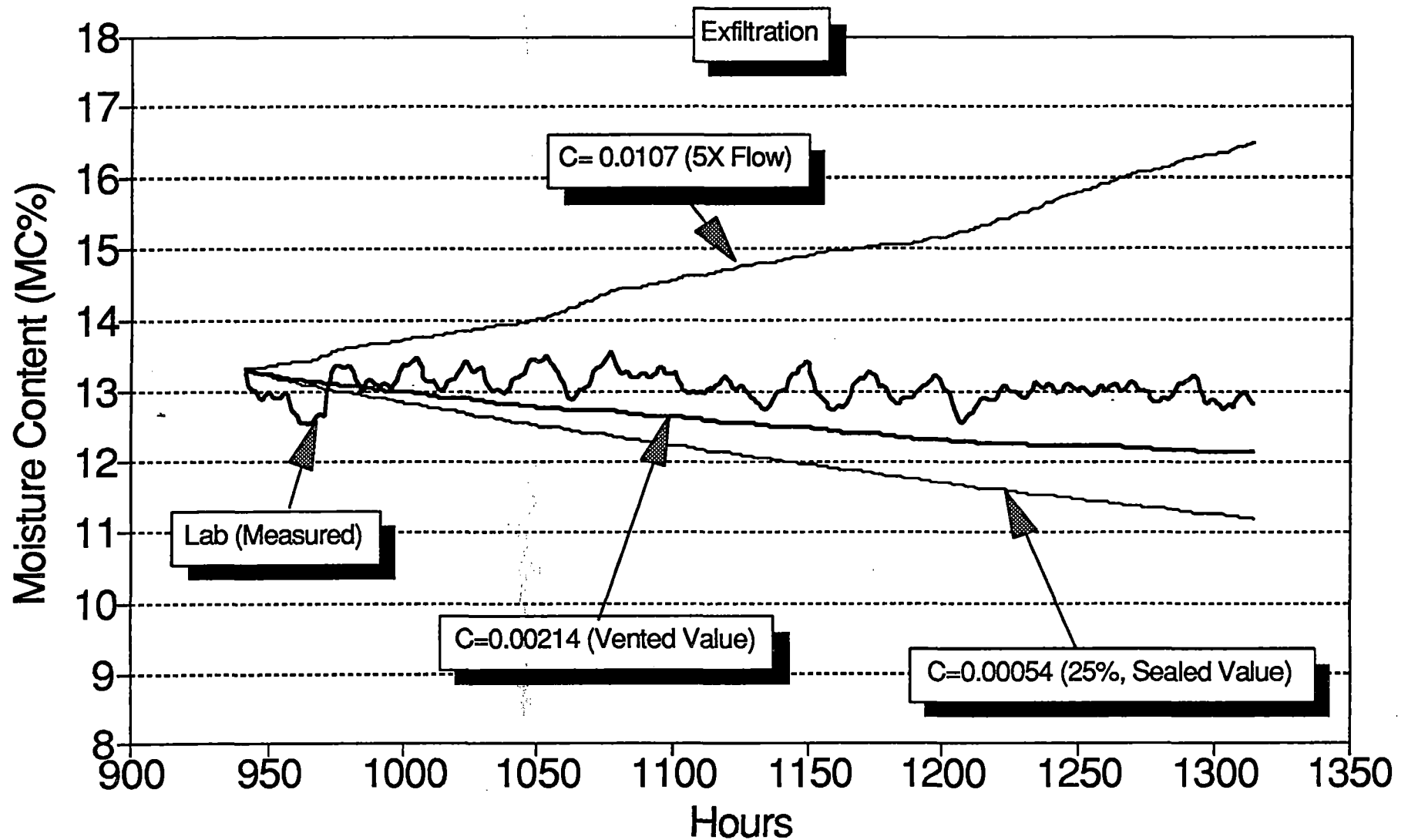
WALLDRY Air Flow Sensitivity
SUMMER: Panel A,(Sealed), Bottom Stud

Exfiltration

C= 0.00054 (Sealed Value)

C= 0.000135 (25% Flow)

Lab (Measured)

C=0.00214 (4X, Vented Value)

Moisture Content (MC%)

Hours
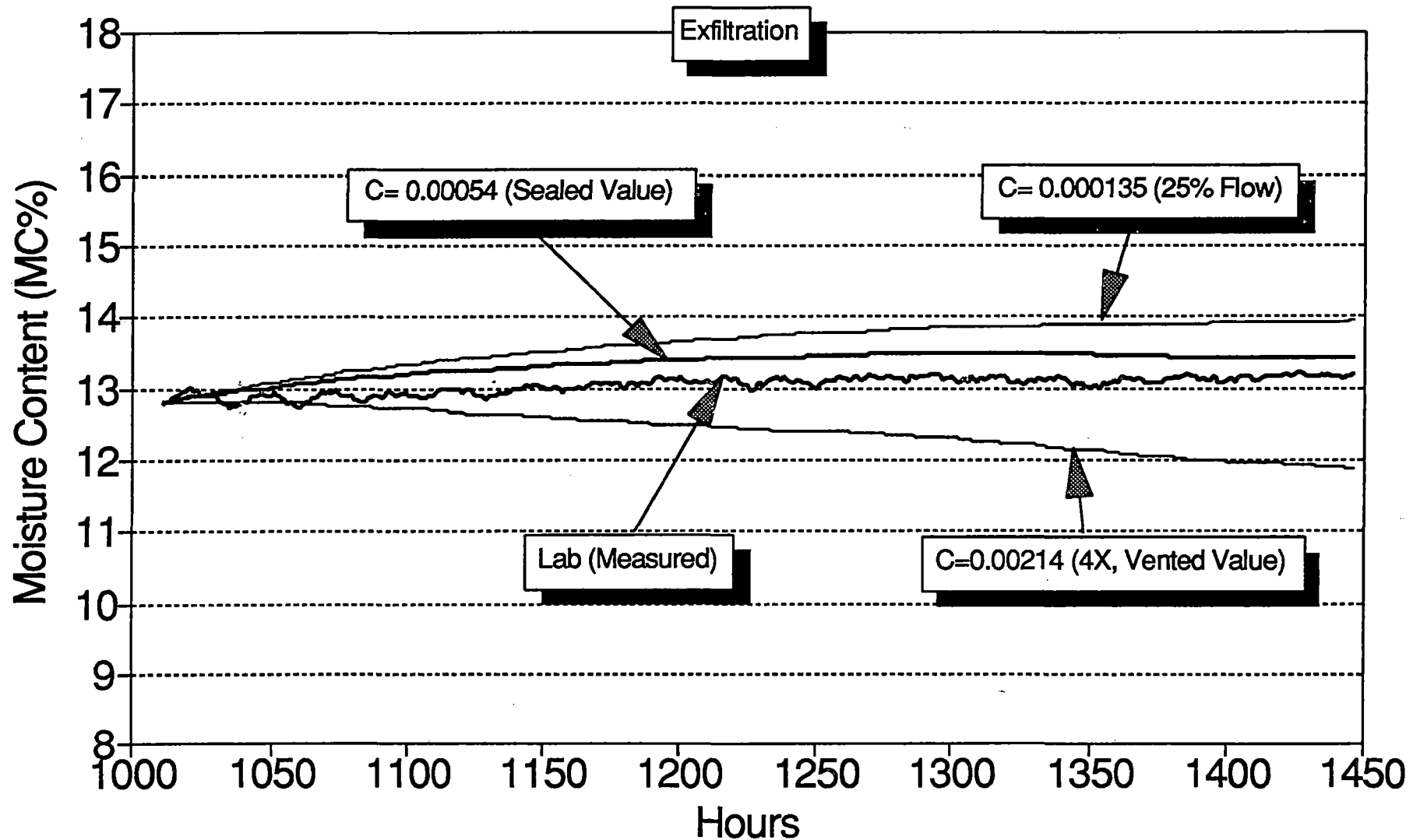
WALLDRY Air Flow Sensitivity
SUMMER: Panel B,(Vented), Bottom Stud
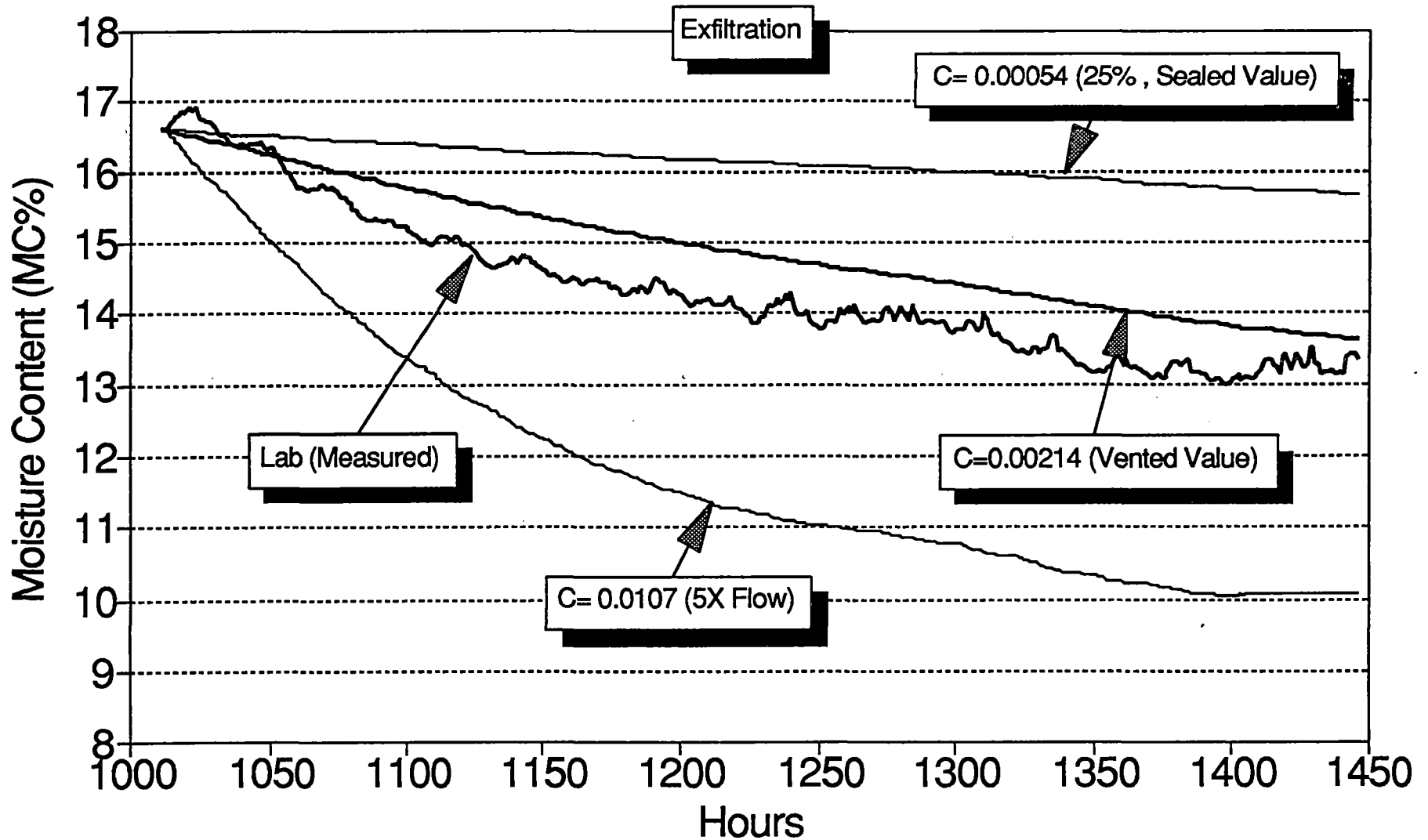
APPENDIX J
Spreadsheet Formats and WALLDRY Instructions

APPENDIX J:
USING THE MODIFIED WALLDRY PROGRAM

User defined exterior and interior temperatures, humidities and differential pressure across the wall is now read from an ASCII file created by printing a master spreadsheet to disk. WALLDRY input screens remain the same, though some inputs are no longer relevant to this version of WALLDRY. (Specifically: Screens 1.1.5, "Indoor Conditions"; 1.1.7, "Initial Wall MC"; 1.2, "Weather Data File Selection"; 1.3, "Time Controls").

1) From A: type Install to run WALLDRY, telling the program which sub-directories will contain the files as requested.

2) Copy files to hard disk, exit WALLDRY

3) Among the files copied to disk is one called LABINPUT.WK1, which is the master spreadsheet containing the headers necessary to input outdoor and indoor information. Load this file into a spreadsheet program. Fill in the information by overwriting the cells, do not change the rows or columns in the file. The air flow coefficient, "C", can be zero, so can the leak influence coefficient. Leak influence coefficient value can be zero, one, fractional, or greater than one.

4) Use the print command and print the whole sheet to disk (insure the default printer is an ASCII printer, without page breaks). Save the file under a name other than "Labinput.wk1"!

5) Run WALLDRY.

6) Create the *.DRY file as before and save.

7) When running the program, you will be asked for the name of the input file (the ASCII print file) created above just before the simulation begins. When WALLDRY is complete, input the resulting *.PRN file into MASTER.WK1 for graphing and analysis.

APPENDIX J
EXAMPLE OF LABINPUT.WK1 FILE
****

WINTER: NEUTRAL: Panel A (SEALED/Wood siding)

Initial Stud Moisture Contents (J = 1 to 9)
  32.62 33.33 34.04 34.75 35.46 35.63 35.80 35.97 36.14

Leakage Characteristic: C & n (for the formula Q = C dP^n), C is in (L/s
0.00054 0.75

Condensation Efficiency & Infilt/Exfilt Heat Transfer Efficiency
  100   100

Field of Influence of Air Leakage (J = 1 to 9) - Exfiltration & Infiltra
    1   1   1   1   1   1   1   1   1
    1   1   1   1   1   1   1   1   1

Number of Hours, 499

Hour	To	Ti	RHo	RHi	Press Diff (infilt +)
1	23.05	21.48	34.21	43.14	2.50
2	3.90	21.88	35.70	41.94	0.24
3	-3.10	22.00	37.56	41.41	0.94
4	-5.85	21.33	37.93	43.39	0.90
5	-8.05	21.25	38.08	45.27	0.90
6	-9.45	22.45	38.12	45.19	1.10
7	-10.65	21.85	37.93	44.94	0.94
8	-12.25	21.88	37.33	44.45	1.20
9	-13.40	20.78	37.22	44.34	1.00
10	-14.20	20.30	37.35	44.50	1.00
11	-14.80	20.45	37.38	44.57	0.90
12	-15.60	20.55	44.84	44.34	0.84
13	-11.50	21.13	44.98	44.26	0.40
14	-15.20	20.50	44.36	43.93	0.74
15	-15.95	21.50	44.03	43.85	1.14
16	-16.30	21.00	44.14	44.00	1.04
17	-16.50	21.63	44.26	44.23	1.04
18	-16.40	21.38	44.59	44.56	1.04
19	-16.10	21.95	44.91	45.05	0.70
20	-15.90	21.10	45.34	45.13	1.14
21	-15.45	20.53	45.63	44.89	1.00
22	-15.25	20.53	46.02	45.14	1.24
23	-14.75	21.38	46.31	45.07	1.14
24	-14.65	21.88	51.38	45.23	1.00
25	-10.10	21.08	51.62	44.49	0.84

APPENDIX J
EXAMPLE OF MASTER.WK1, Spreadsheet for WALLDRY output

CONT...

	A	B	C	D	E	F	G	H	I	J	K
1	File:			MAS 91.08.31			25-Sep-91				
2	(Place curser in box B7, and import the '.PRN' file: /FIN)										
3							SHEATHING		OUTER STUD		
4	DAY	HOUR	TEMP(C	RH			INNER	OUTER	TOP	TOP-MH	MID
5	FROM START		OUT	OUT			(11,5)	(13,5)	(21,9)	(21,8)	(21,5)
6											
7	0.04 0.00	1	23.1	34	0	0	10.00	10.02	42.03	41.81	41.15

CONT...

L	M	N	O	P	Q	R	S	T	U	V
OUTER STUD		INNER STUD			SHEATHING FILM THICKN			AIR SPACE VELOCITY(m/s)		
BOT-MH	BOT	TOP	MID	BOT						
(21,2)	(21,1)	(22,8)	(22,5)	(22,2)	(11,1)	(11,5)	(11,9)	(7,1)	(7,5)	(7,9)
38.56	37.70	41.83	41.17	38.58	0.00	0.00	0.00	-0.00	-0.00	-0.00

APPENDIX K
Program Algorithm Listings

WALLDRY WALLCALC SUBROUTINE: GetWeather

```
SUB GetWeather STATIC
'     WEATHER DATA


'    GET #1, Hr, RECORD


'*Lab Routine

     INPUT #1, Hr, Tdb, Tindoor, RHo, RHindoor, Whead

'*Lab Routine

'    Vwindkph = RECORD.Wind
'    WinDir = RECORD.DIR
'    Tdb = RECORD.Temp
'    RHo = RECORD.RH
```

WALLDRY WALLCALC SUBROUTINE: OpenWeather

SUB OpenWeather STATIC

```
'*Lab Routine
    CLS

    INPUT "Enter the lab conditions ASCII file; e.g. TEST1.LAB: "; WeatherFile$

    OPEN WeatherFile$ FOR INPUT AS #1

    LINE INPUT #1, dum$
    LINE INPUT #1, dum$
    LINE INPUT #1, dum$
    FOR J% = 1 TO 9
        INPUT #1, MC(21, J%)
        MVAP(21, J%) = Mass(21) * MC(21, J%) / 100!
        MC(22, J%) = MC(21, J%)
        MVAP(22, J%) = Mass(22) * MC(22, J%) / 100!
    NEXT


    LINE INPUT #1, dum$
    LINE INPUT #1, dum$
    INPUT #1, FlowCoef(1), FlowExp(1)
    LINE INPUT #1, dum$
    LINE INPUT #1, dum$
    INPUT #1, FlowCoef(2), FlowCoef(3)
    LINE INPUT #1, dum$

    LINE INPUT #1, dum$
    FOR J = 1 TO 9
        INPUT #1, JLeakExf(J)
        JLeakExf(10) = JLeakExf(10) + JLeakExf(J)
    NEXT
    FOR J = 1 TO 9
        INPUT #1, JLeakInf(J)
        JLeakInf(10) = JLeakInf(10) + JLeakInf(J)
    NEXT
    LINE INPUT #1, dum$

    IHrStart = 1
    INPUT #1, dum$, IHrFin
    LINE INPUT #1, dum$
'*End Lab Routine
```

WALLDRY WALLCALC SUBROUTINE: UpdateMoisture

SUB UpdateMoisture (J) STATIC

'   UPDATING THE MOISUTE CONTENT OF THE KEY ELEMENTS

```
IF ITER >= NITER THEN
   MVAP(3, J) = MVAP(3, J) - DRY(3, J) + DRY4O + MSOURCE(3, J)
   MVAP(4, J) = MVAP(4, J) - DRY(4, J) + MSOURCE(4, J)
   MVAP(IOUT, J) = MVAP(IOUT, J) - DRY(IOUT, J) + DRY4I + MSOURCE(IOUT, J)
   MVAP(IIN, J) = MVAP(IIN, J) - DRY(IIN, J) + DRY(IIN1, J) + MSOURCE(IIN, J)

   IF NSHEATH <> 2 THEN
      MVAP(IIN1, J) = MVAP(IIN1, J) - DRY(IIN1, J) + DRY(IIN2, J) + MSOURCE(IIN1, J)
      MVAP(IIN2, J) = MVAP(IIN2, J) - DRY(IIN2, J) + DRY(NE, J) + DRY(NEP1, J) +
               MSOURCE(IIN2, J)

   ELSE

      MVAP(IIN1, J) = MVAP(IIN1, J) - DRY(IIN1, J) + DRY(NE, J) + DRY(NEP1, J) +
               MSOURCE(IIN1, J)

   END IF

      MVAP(NEP1, J) = MVAP(NEP1, J) - DRY(NEP1, J) + DRY(NEP2, J) +
               MSOURCE(NEP1, J)
      MVAP(NEP2, J) = MVAP(NEP2, J) - DRY(NEP2, J) + MSOURCE(NEP2, J)
```

WALLDRY WALLCALC SUBROUTINE: HeatEffects

```
SUB HeatEffects (J) STATIC
'
'   LATENT AND SENSIBLE HEAT EFFECTS FOR ITERATIONS > 1
'
  IF ITER >= 2 THEN
    FOR I = 2 TO NE1
      IF T(I, J) < .001 THEN QVAP1 = QVAP * 1.15 ELSE QVAP1 = QVAP
      QLAT = (DRY(I, J) - MSOURCE(I, J)) * QVAP1 / C16
      IF Hr = IHrStart THEN TOLD(I, J) = T(I, J)
      QSENS1 = -Mcp(I) / C16
      QSENS2 = -Mcp(I) * TOLD(I, J) / C16
      IF Itype(I) = 1 THEN QSENS1 = 0: QSENS2 = 0
      VB#(I) = VB#(I) + QSENS1
      VR#(I) = VR#(I) + QLAT + QSENS2
    NEXT


'*Lab

  IF Whead < 0 THEN

'exfiltration

      IF JLeakExf(J) = 0 THEN GOTO endlab1
      Tdiff = (T(NE, J) - T(15, J))
      ROWLEAK = ROAIR(NE, J)
      VR#(15) = VR#(15) - (FlowCoef(3) / 100) * (Area * 9 * (JLeakExf(J) /
          (JLeakExf(10) + .0000001)) * FlowCoef(1) * (ABS(Whead) ^ FlowExp(1)) / 1000) *
          ROWLEAK * CPAIR * Tdiff


  ELSE

'infiltration

      IF JLeakInf(J) = 0 THEN GOTO endlab1
      Tdiff = (T(1, J) - T(15, J))
      ROWLEAK = ROAIR(NE, J)
      VR#(15) = VR#(15) - (FlowCoef(3) / 100) * (Area * 9 * (JLeakInf(J) /
          (JLeakInf(10) + .0000001)) * FlowCoef(1) * (ABS(Whead) ^ FlowExp(1)) / 1000) *
          ROWLEAK * CPAIR * Tdiff


  END IF

endlab1:

'*Lab
```

WALLDRY WALLCALC SUBROUTINE: NetMoisture

```
SUB NetMoisture (J) STATIC
'   CALCULATING NET MOISTURE FLOW OUT OF WOOD LAYERS

'*Lab

  IF Whead < 0 THEN

'exfiltration

    IF JLeakExf(J) = 0 THEN MSOURCE(NEP1, J) = 0

    MSOURCE(IIN2, J) = 0
    GOTO endlab2
    Rowdiff = (ROVAP(NE, J) - ROVAP(15, J))

    MSOURCE(NEP1, J) = C16 * (FlowCoef(2) / 100) * (Astud / (Astud + Area)) *
            (Area * 9 * (JLeakExf(J) / (JLeakExf(10) + .0000001)) *
            FlowCoef(1) * (ABS(Whead) ^ FlowExp(1)) / 1000) * Rowdiff

    MSOURCE(IIN2, J) = C16 * (FlowCoef(2) / 100) * (Area / (Astud + Area)) *
            (Area * 9 * (JLeakExf(J) / (JLeakExf(10) + .0000001)) *
            FlowCoef(1) * (ABS(Whead) ^ FlowExp(1)) / 1000) * Rowdiff


  ELSE

'infiltration

    IF JLeakInf(J) = 0 THEN MSOURCE(NEP1, J) = 0

    MSOURCE(IIN2, J) = 0: GOTO endlab2
    Rowdiff = (ROVAP(1, J) - ROVAP(15, J))

    MSOURCE(NEP1, J) = C16 * (FlowCoef(2) / 100) * (Astud / (Astud + Area)) *
            (Area * 9 * (JLeakInf(J) / (JLeakInf(10) + .0000001)) *
            FlowCoef(1) * (ABS(Whead) ^ FlowExp(1)) / 1000) * Rowdiff

    MSOURCE(IIN2, J) = C16 * (FlowCoef(2) / 100) * (Area / (Astud + Area)) *
            (Area * 9 * (JLeakInf(J) / (JLeakInf(10) + .0000001)) *
            FlowCoef(1) * (ABS(Whead) ^ FlowExp(1)) / 1000) * Rowdiff


  END IF

endlab2:

'*Lab
```
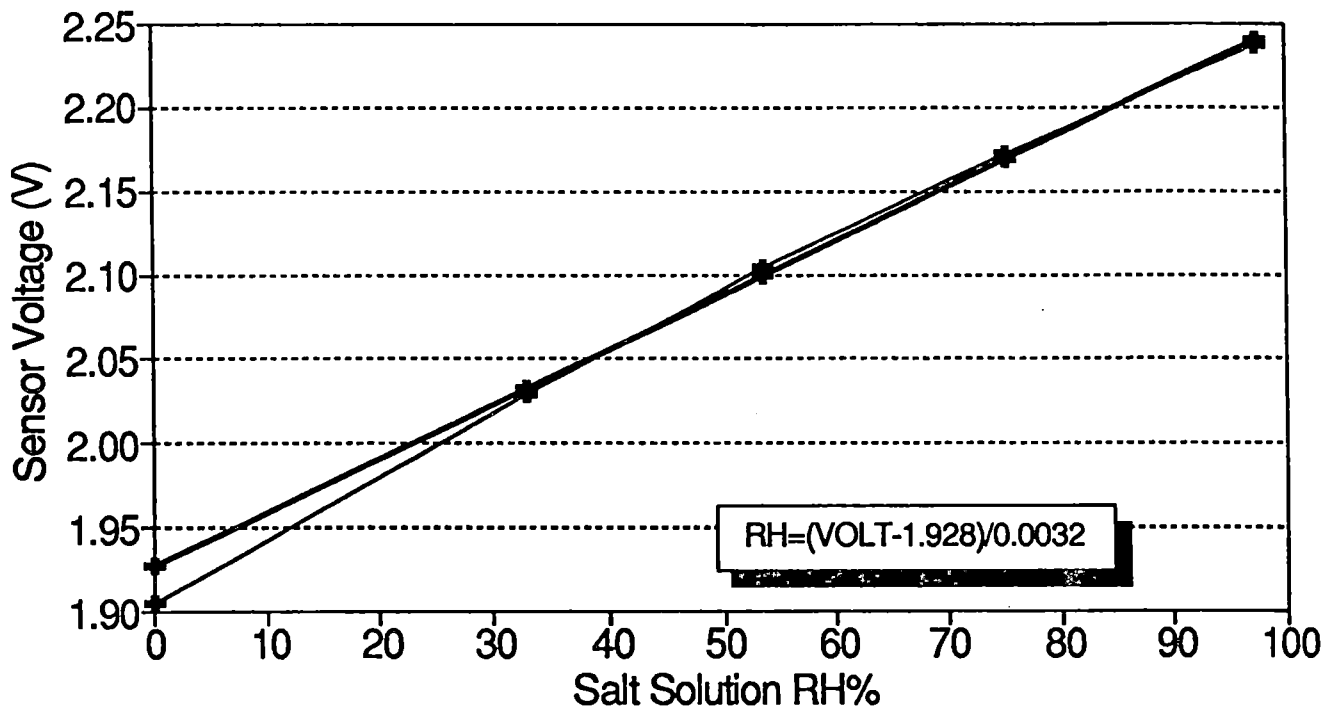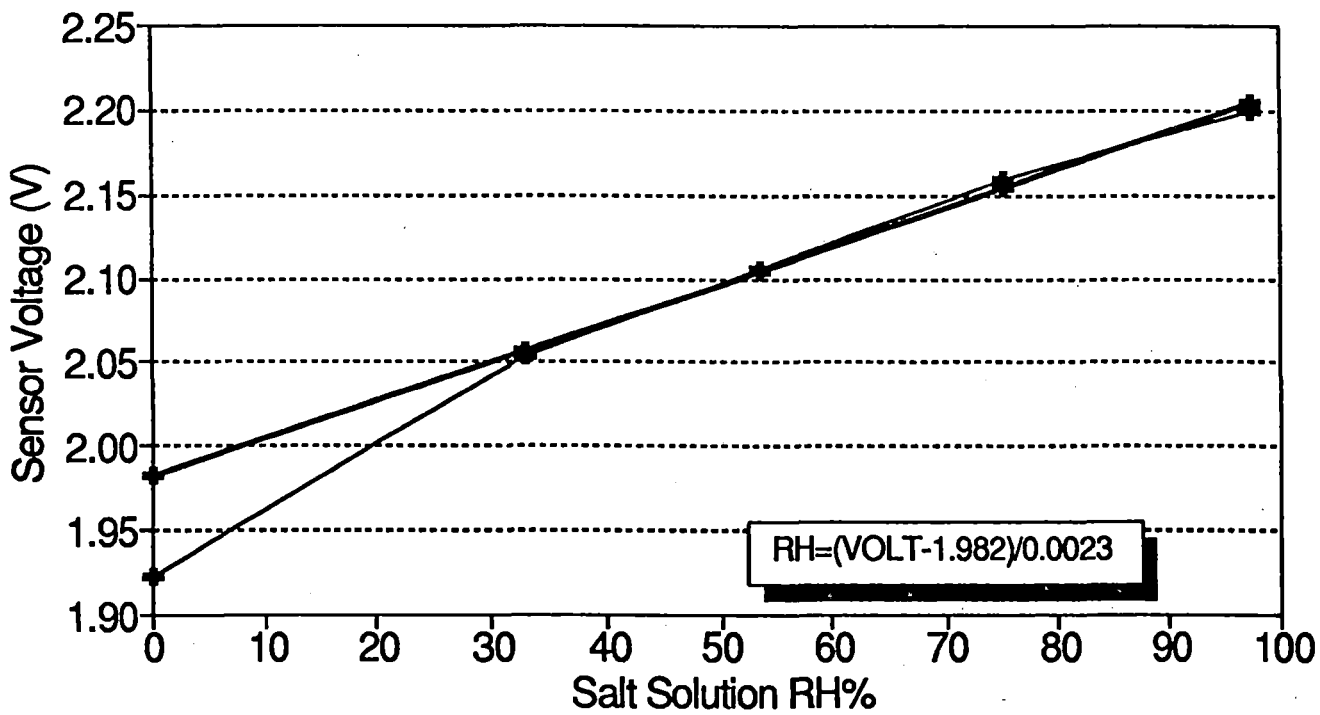
APPENDIX L
RH Sensor Calibrations
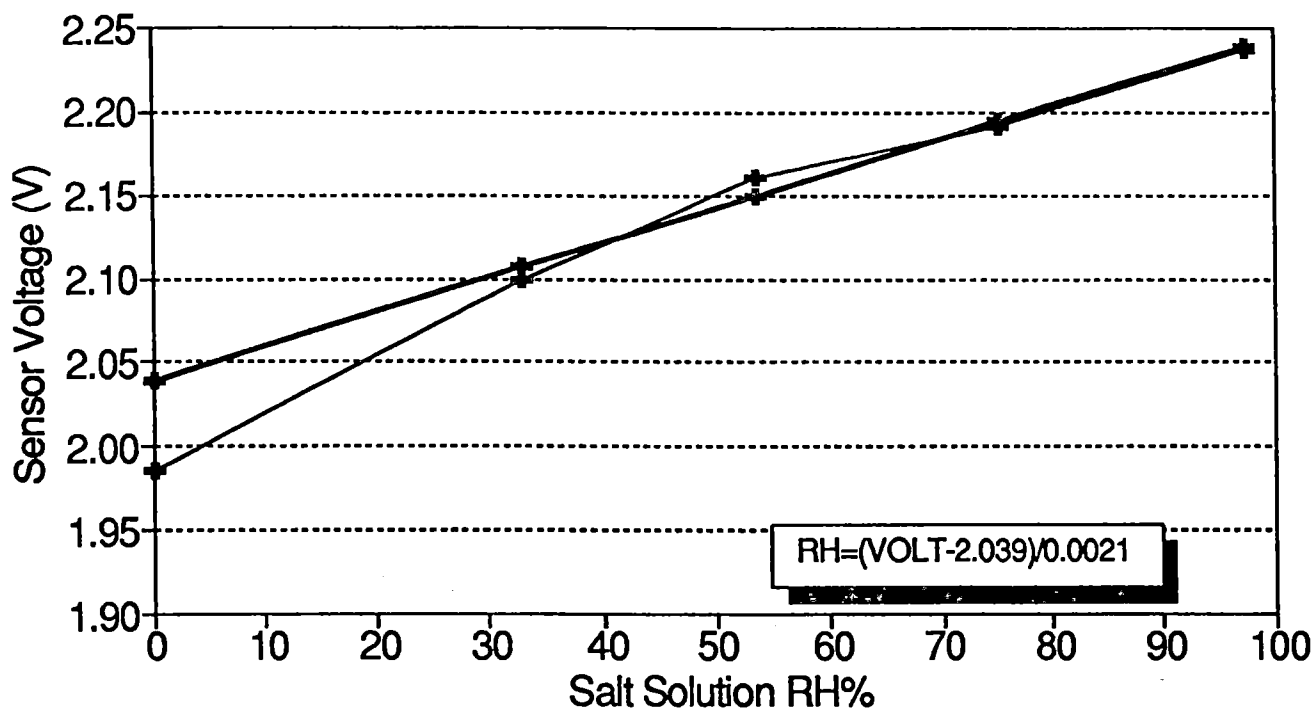
RH SENSOR CALIBRATION
PANEL A

RH=(VOLT-1.928)/0.0032

Sensor Voltage (V)

Salt Solution RH%

—■— Calculated —■— Measured

RH SENSOR CALIBRATION
PANEL B

RH=(VOLT-1.982)/0.0023

Sensor Voltage (V) vs Salt Solution RH%

—+— Calculated —+— Measured

RH SENSOR CALIBRATION
PANEL C

RH=(VOLT-2.039)/0.0021

Sensor Voltage (V) vs Salt Solution RH%

Legend: Calculated — Measured

RH SENSOR CALIBRATION
PANEL D

RH=(VOLT-1.984)/0.0021

Sensor Voltage (V) vs Salt Solution RH%

Legend: Calculated — Measured

RH SENSOR CALIBRATION
PANEL E

RH=(VOLT-2.007)/0.0023

RH SENSOR CALIBRATION
PANEL F

RH=(VOLT-1.978)/0.0021